Doctoral Theses at NTNU 2004:43

Bernt Brønmo Johnsen

Adhesive bonding of aluminium

NTNU
Norwegian University of
Science and Technology
Doctoral thesis
for the degree of doktor ingeniør
Faculty of Engineering Science and Technology
Department of Machine Design and Materials
Technology

NTNU

Adhesive bonding of aluminium

by

Bernt Brønmo Johnsen

Thesis submitted in partial fulfilment of the requirements for the degree

Doktor Ingeniør

Norwegian University of Science and Technology
Department of Machine Design and Materials Technology

December 2003

ISBN 82-471-6294-6 (printed ver.)
ISBN 82-471-6293-8 (electronic ver.)
ISSN 1503-8181

Preface

This work was funded by Hydro Aluminium Structures, SINTEF Materials Technology and The Research Council of Norway. It was performed in the period August 1999 to January 2003. The experimental part was performed at Department of Polymers and Composites, SINTEF Materials Technology, beginning in July 2000.

Firstly, I would like to gratefully acknowledge my supervisor Professor Aage Stori for his excellent guidance, encouragement and exclusively constructive criticism throughout the work with this thesis. I would also take the opportunity to thank my co-supervisor Kristin Vinje, who unfortunately left SINTEF Materials Technology in the Spring of 2002. Another person who deserves a special thank is Kjell Olafsen (also at SINTEF Materials Technology) for his help with all kinds of practical arrangements, cleaver ideas related to the work, and for his presence as a discussion partner.

I wish to express my gratitude to the enthusiastic Tomas Luksepp at Hydro Aluminium Structures. His input and suggestions have been of invaluable importance to the work. Håkon Leth-Olsen at Hydro Research Centre has also been very helpful.

During parts of this work I was connected to the Strategic Institute Program called 'Surface Engineering' at SINTEF Materials Technology. All the staff at this project has my sincere gratitude - especially the project manager Keith Redford, Fabrice Lapique and Bente Gilbu Tilset, but also Astrid Bjørgum, Christian Simensen, John Walmsley and Otto Lunder. They have all been excellent discussion partners coming up with ideas and useful information.

Several other people have also in one way or another contributed to the outcome of this thesis and must be acknowledged. I would like to thank Harry Vogt and Rolf Kalland for their help with specimen preparation, Jens-Anton Horst for help with SEM and EPMA, and Bjørn Steinar Tanem for performing the TEM work. Also, a thank to all

other personnel at SINTEF Materials Technology in Oslo which contributed in making my stay there so fine.

Finally, I would like to thank all my family and friends, who have supported me in these years.

London, December 2003 Bernt B. Johnsen

Contents

Preface iii

Contents v

Summary xi

List of papers xiii

1. Introduction 1
- 1.1 Background 1
- 1.2 Outline of the thesis 2

2. Adhesive bonding 5
- 2.1 Definitions 5
  - 2.1.1 Adhesion mechanisms 5
  - 2.1.2 Advantages and disadvantages of adhesive bonding 6
  - 2.1.3 Adhesive bonding of load bearing aluminium structures 7
- 2.2 Epoxy adhesives 9
- 2.3 Mechanical tests of adhesive bond performance 11
  - 2.3.1 Lap shear tests 11
  - 2.3.2 Wedge test 12
  - 2.3.3 Fatigue testing 13

3. Review of literature 17
- 3.1 Surface pretreatment of aluminium 17
  - 3.1.1 Anodising and aerospace pretreatments 17
    - 3.1.1.1 Alternatives to hexavalent chromium processes 20
  - 3.1.2 Mechanical pretreatments 21
  - 3.1.3 Boiling water pretreatment 22
  - 3.1.4 Silane coupling agents 22
    - 3.1.4.1 Treatment with GPS 24
- 3.2 Chemical interactions 25
  - 3.2.1 Compositional variation at the interphase 27
- 3.3 Effect of water 28
  - 3.3.1 Hydration of the aluminium surface 29
  - 3.3.2 Degradation of adhesive bonds 30
  - 3.3.3 Strength recovery 32

3.3.4 Effect of saline solutions 33

4. Experimental 39
4.1 Materials 39
4.2 Wedge test 39
4.3 Analytical techniques 42
4.3.1 Infrared spectroscopy 42
4.3.1.1 Reflection-absorption infrared spectroscopy 45
4.3.2 Scanning electron microscopy 47
4.3.3 Transmission electron microscopy 48
4.3.4 White-light interferometry 48
4.3.5 X-ray photoelectron spectroscopy 49
4.3.6 Electron microprobe analysis 51
4.3.7 Secondary ion-mass spectrometry 52
4.3.8 Contact angle measurements 53

5. Summary of papers 57
5.1 Paper I, II and III 57
5.2 Paper IV 60
5.3 Paper V and VI 62

6. Silanisation of adhesively bonded aluminium alloy AA6060 with γ-glycidoxy-propyltrimethoxysilane. I. Durability investigation 65
Abstract 65
6.1 Introduction 66
6.2 Experimental 68
6.2.1 Materials 68
6.2.2 Surface pretreatment procedures 68
6.2.3 Bond preparation and environmental testing 68
6.2.4 Surface characterisation 71
6.3 Results and discussion 71
6.3.1 Environmental testing of RDCB wedge test specimens 71
6.3.2 Effect of treatment with GPS 81
6.3.3 General considerations 82
6.4 Conclusion 84
Acknowledgements 85
References 85

7. Reflection-absorption FT-IR studies of the specific interaction of amines and an epoxy adhesive with GPS treated aluminium surfaces 87
Abstract 87

7.1 Introduction 88
7.2 Experimental 90
7.2.1 Materials 90
7.2.2 Specimen preparation and surface treatment 90
7.2.3 Reflection-absorption infrared spectroscopy 92
7.3 Results 92
7.4 Discussion 95
7.4.1 Effect of amine treatments 96
7.4.2 Treatment with DICY and epoxy adhesive 100
7.5 Conclusion 105
Acknowledgements 105
References 106

8. **The role of covalent bonding in silane pretreatment of adhesively bonded aluminium 109**
Abstract 109
8.1 Introduction 110
8.2 Experimental 112
8.2.1 Materials 112
8.2.2 Surface pretreatment procedures 113
8.2.3 Contact angle measurements 114
8.2.4 Bond preparation and environmental testing 114
8.2.5 Reflection-absorption infrared spectroscopy 115
8.3 Results 116
8.3.1 Environmental durability 116
8.3.2 Contact angle measurements 118
8.3.3 Infrared spectroscopy 121
8.4 Discussion 127
8.5 Conclusion 129
Acknowledgements 130
References 130

9. **Silanisation of adhesively bonded aluminium alloy AA6060 with γ-glycidoxy-propyltrimethoxysilane. II. Stability in degrading environments 133**
Abstract 133
9.1 Introduction 134
9.2 Experimental 137
9.2.1 Materials 137
9.2.2 Surface pretreatment procedures 137
9.2.3 Bond preparation and environmental testing 138
9.2.4 Stability of GPS films on aluminium 140

9.3 Results and discussion 140
9.3.1 Environmental effects on GPS films 140
9.3.2 Exposure of RDCB wedge test specimens to acidic and alkaline environments 147
9.4 Conclusion 150
Acknowledgements 151
References 151

10. The durability of bonded aluminium joints: A comparison of AC and DC anodising pretreatments 155
Abstract 155
10.1 Introduction 156
10.2 Experimental 157
10.2.1 Materials 157
10.2.2 Surface pretreatment procedures 158
10.2.3 Bond preparation and environmental testing 158
10.2.4 FT-IR spectroscopy 159
10.3 Results and discussion 159
10.3.1 Environmental durability 159
10.3.2 FT-IR spectroscopy 164
10.3.3 Effect of sealing 170
10.4 Conclusion 173
Acknowledgements 174
References 174

11. The effect of pre-bond moisture on epoxy-bonded sulphuric acid anodised aluminium 177
Abstract 177
11.1 Introduction 178
11.2 Experimental 179
11.2.1 Materials 179
11.2.2 Surface pretreatment procedures 180
11.2.3 Bond preparation and environmental testing 180
11.2.4 FT-IR spectroscopy 182
11.2.5 Transmission electron microscopy (TEM) 182
11.3 Results 182
11.3.1 Environmental testing 182
11.3.2 FT-IR spectroscopy 185
11.3.3 Transmission electron microscopy (TEM) 185
11.4 Discussion 188
11.5 Conclusion 193

Acknowledgements 193
References 193

12. Conclusions 195

Appendix 199

Summary

In order to get approval of adhesive bonding as a reliable joining method in the automotive industry, a better understanding of the interfacial interactions between aluminium surfaces and adhesives is important. It is also important to get a better understanding of the degradation mechanisms of the bonded systems in humid environments, as humidity is known to have a detrimental effect. This work has been focused on an aluminium alloy and a one-component epoxy adhesive that are of particular interest to the automotive industry.

Pretreatment of the aluminium substrates before adhesive bonding is essential. However, the most successful pretreatment processes involve the use of hexavalent chromium, which will be banned from use within few years due to environmental considerations. Alternative pretreatments need to be developed. A literature study identified silanisation with GPS as a pretreatment method with the potential to obtain good durability. On the basis of research performed by SINTEF Materials Technology, AC anodising in hot phosphoric and sulphuric acid solutions were also identified as interesting pretreatment methods.

A modified version of the Boeing wedge test was used to determine the durability of adhesively bonded joints tested in hydrothermal environments. The joints were made of AA6060-T6 aluminium alloy and Betamate XD4600 epoxy adhesive. Both silane films and anodic oxides were investigated using reflection-absorption FT-IR spectroscopy. Other techniques of surface analysis were also used (SEM, TEM, WLI, XPS, ToF-SIMS and contact angle measurements).

The environmental durability of pretreated AA6060-T6 substrates was significantly improved after silanisation with GPS. The grit-blasting + GPS pretreatment process resulted in considerable higher durability than the chromic-sulphuric acid FPL-etch. The general understanding is that silanisation improves the durability through the formation of strong, covalent bonds between the aluminium surface and the adhesive. FT-IR

spectroscopy strongly indicated that a chemical reaction took place between GPS films and amine curing agents. Particularly interesting was the reaction with dicyandiamide, which is a common curing agent in one-component epoxy adhesives. The amines also catalysed the condensation of SiOH groups, resulting in higher degree of SiOSi crosslink density in the siloxane films. However, chemical reaction is not necessary for improved durability. The hydrophobicity of the bonded surface is also an important factor. This effect has not been studied extensively earlier.

Exposure of GPS films to degrading environments showed that the silane desorbed from the surface in acidic solutions, but it was stable in alkaline solutions. The durability of adhesive joints was also reduced in acidic environments. Two models for the degradation of the silanised aluminium surface in acidic environments were proposed: hydrolysis of the siloxane network and corrosion of the underlying aluminium surface.

The environmental durability of substrates that were AC anodised in hot phosphoric and sulphuric acid solutions was good, almost as good as the well-established FPL + PAA pretreatment. DC anodising in sulphuric acid gave inferior durability. FT-IR spectroscopy showed that the anodic films formed in sulphuric acid contain significant amounts of sulphate. This can have a significant negative effect on the long-term properties of bonded joints. The anodic films released water during curing of the adhesive. The observations suggested that a transformation from the hydroxide to the oxide state took place.

Adhesive bonding in wet environment of substrates that were anodised in sulphuric acid had a negative effect on durability. The effect was more pronounced for DC anodised, than for AC anodised substrates. Bonding in wet environment also resulted in changed adhesive properties close to the oxide surface. Very little thixotropic agent was present in a ~200 nm wide region in the adhesive. This was explained by desorption of water from the oxide during curing of the adhesive.

List of papers

I. Silanisation of adhesively bonded aluminium alloy AA6060 with γ-glycidoxy-propyltrimethoxysilane. I. Durability investigation
B.B. Johnsen[a], K. Olafsen[b], A. Stori[b] and K. Vinje[b], *Journal of Adhesion Science and Technology* **16**, 1931-1948 (2002)

II. Reflection-absorption FT-IR studies of the specific interaction of amines and an epoxy adhesive with GPS treated aluminium surfaces
B.B. Johnsen[a], K. Olafsen[b] and A. Stori[b], *International Journal of Adhesion and Adhesives* **23**, 155-163 (2003)

III. The role of covalent bonding in silane pretreatment of adhesively bonded aluminium
B.B. Johnsen[a], K. Olafsen[b] and A. Stori[b], *Journal of Adhesion*, submitted.

IV. Silanisation of adhesively bonded aluminium alloy AA6060 with γ-glycidoxy-propyltrimethoxysilane. II. Stability in degrading environments
B.B. Johnsen[a], K. Olafsen[b], A. Stori[b] and K. Vinje[b], *Journal of Adhesion Science and Technology* **17**, 1283-1298 (2003)

V. The durability of bonded aluminium joints: A comparison of AC and DC anodising pretreatments
B.B. Johnsen[a], F. Lapique[b] and A. Bjørgum[c], *International Journal of Adhesion and Adhesives* **24**, 153-161 (2004)

VI. The effect of pre-bond moisture on epoxy-bonded sulphuric acid anodised aluminium
B.B. Johnsen[a], F. Lapique[b], A. Bjørgum[c], J. Walmsley[d], B.S. Tanem[d] and T. Luksepp[e], *International Journal of Adhesion and Adhesives* **24**, 183-191 (2004)

Affiliations

[a]Department of Machine Design and Materials Technology, Norwegian University of Science and Technology, Trondheim, Norway
[b]Department of Polymers and Composites, SINTEF Materials Technology, Oslo, Norway
[c]Department of Corrosion, Joining and Surface Technology, SINTEF Materials Technology, Trondheim, Norway
[d]Department of Applied Physics, SINTEF Materials Technology, Trondheim, Norway
[e]Hydro Aluminium Structures, Raufoss, Norway

Chapter 1
Introduction

1.1 Background

As a result of the desire to reduce polluting fuel consumption, there is an increasing demand for lightweight aluminium structures in the transportation industry. Adhesive bonding is in many cases an alternative to other joining methods, such as, e.g., bolting and welding, since these methods often introduce locally weaker points.

The main purpose of this study was to obtain a better understanding of the chemical interactions between aluminium surfaces and adhesives. In order to get approval of adhesive bonding as a reliable joining method in the automotive industry, a better understanding of the interfacial interactions is important. It is also important to get a better understanding of the degrading mechanisms of the bonded systems in hostile environments. Most of the literature on adhesive bonding of aluminium focuses on alloy AA2024-T3. This is the preferred aluminium alloy in the aerospace industry, and pretreatment and adhesive bonding of the material has been extensively studied. The present work has been focused on aluminium alloy AA6060-T6 and the one-component epoxy adhesive Betamate XD4600, since these materials are of particular interest to the automotive industry. They are both used by Hydro Aluminium Structures in the production of space frames for the sports car Lotus Elise.

One major disadvantage of adhesive bonding is the need for expensive pretreatment processes of the bonded substrates. The most successful pretreatment processes contain hexavalent chromium (Cr^{VI}). However, due to the toxicity of Cr^{VI}, it will be banned from use in the European automotive industry in July 2007. Alternative pretreatments need to be developed. One of the main goals of this work was to study different non-toxic pretreatment systems and their effect on adhesion, the degradation in hostile environments, and the interactions in the aluminium-adhesive interface. Investigation of corrosion of adhesively bonded aluminium was beyond the scope of this study.

The thesis can be divided into two major parts. One is dealing with silanisation of aluminium surfaces (Chapters 6 to 9), and another is dealing with anodised surfaces (Chapters 10 to 11). The initial part of the experimental work was focused on silanisation with GPS. However, since these systems give excellent durability properties, but rather poor corrosion protection, they may be unsuitable as pretreatment systems for, e.g., space frames. They may have a greater potential as repair systems for damaged automotive parts. Therefore, the remaining part of the experimental work was focused on anodising pretreatments, which have a greater potential as the sole pretreatment system. Both silanised and anodised systems were investigated with the same experimental techniques.

1.2 Outline of the thesis

The thesis is organised in chapters where Chapters 6 to 11 are written with the intention of being published as papers in international journals. These chapters are displayed as the papers were in their final accepted or submitted form. As a consequence, some literature reviews and experimental methods are inevitably repeated several times.

A short introduction to adhesive bonding, including definitions of common technical terms, is given in Chapter 2, while an extensive review of the literature on adhesive bonding is given in Chapter 3. The experimental methods used in this study are described in Chapter 4. Particularly the wedge test, used for determination of environmental durability, and FT-IR spectroscopy are thoroughly described. These two techniques are a very central part of the performed work.

The major findings in the papers (as seen in Chapters 6 to 11) are summarised in Chapter 5. Chapters 6 and 7 are dealing with aluminium surfaces silanised with GPS and bonded with an epoxy adhesive. In Chapter 6, the environmental durability of the silanised surfaces is determined. Durability is improved after silanisation. In Chapter 7, the improved durability is explained in terms of covalent bonding between the silane film and the curing agent in the epoxy adhesive. GPS is compared with other silanes in

Chapter 8. The results indicate that the hydrophobicity of the surface has an effect on durability. In Chapter 9, the stability of the silane films and the durability in degrading environments are investigated.

Chapters 10 to 11 are dealing with anodised aluminium surfaces bonded with an epoxy adhesive. In Chapter 10, DC and AC anodising in phosphoric and sulphuric acid solutions are compared. AC anodising is a promising pretreatment method. In Chapter 11, the sulphuric acid anodised substrates are bonded in wet and dry environments. Differences in durability and interphasial properties were observed.

Chapter 12 gives concluding remarks and some suggestions for further work.

Chapter 2
Adhesive bonding

2.1 Definitions

An *adhesive* can be defined as a material that can join materials together and resist separation. The phenomenon which allows the adhesive to transfer a load from the bonded material to the adhesive is called *adhesion*, and *adhesive bonding* is the method by which materials can be joined with adhesives to generate assemblies [1-3]. The assembly made by the use of an adhesive is called an *adhesive joint* or *adhesive bond*. The solid materials in the adhesive joint other than the adhesive are known as the *adherends* or *substrates*. The boundary between the substrate surface and the adhesive is called the *interface*, or in the case of a transition region, the *interphase*. Failure in this region is referred to as *interfacial* or *adhesive failure*. *Cohesion* refers to adhesion or attraction within the adhesive bulk phase, and failure occurring within the adhesive is referred to as *cohesive failure*. The ability of an adhesive joint to resist the effects of a degrading environment, such as high humidity at elevated temperature, is referred to as the *environmental durability* of the joint.

2.1.1 Adhesion mechanisms

Both primary and secondary bonds are important in adhesion, depending on the interfacial structure [3]. The most common forces in the adhesive/substrate interface are van der Waals forces, which are referred to as secondary bonds. Hydrogen bonds also fall into this category. The van der Waals forces diminish rapidly with distance. Appreciable attractions are obtained only when the distance of intermolecular separation is on the order of 5Å. Under the category of primary bonds are ionic and covalent bonds.

Table 1
Bond types and typical bond energies [4]

Type of bond	Bond energy (kJ/mol)
Ionic	590-1050
Covalent	63-710
Metallic	113-347
Permanent dipole-dipole interactions	4-42
Dipole-induced dipole	<2
Dispersion (London) forces	0.08-42

In addition to the formation of primary and secondary bonds, mechanical interlocking can also take place. A 'lock and key' effect between the substrate and the cured adhesive can occur, depending on the roughness of the substrate.

The adhesion mechanisms between epoxy adhesives and aluminium surfaces are much more thoroughly described in Chapter 3.2.

2.1.2 Advantages and disadvantages of adhesive bonding

There are several advantages and disadvantages with the use of adhesive bonding compared to more traditional methods of joining, such as bolting, brazing, welding etc. [1,2]. When a substrate is pierced by a mechanical fastener, a hole is created in the substrate. At the edges of the hole, the material may experience large stress concentrations which may cause a decrease in the mechanical properties of the adherend. Adhesive bonding, on the other hand, does not exhibit large stress concentrations, but adhesive joints require a much larger area of contact between the adherends. Other advantages of adhesive bonding are: the ability to join dissimilar materials, the ability to join thin-sheet material efficiently, an increase in design flexibility, an improvement in the appearance, and an improvement in corrosion resistance. However, there are some disadvantages: surface pretreatment for the substrates to be bonded is required to attain a long service life of the joints, the upper-service temperatures that polymeric adhesives can withstand is limited, adhesives are not typically used for joining thick metallic components, and non-destructive test methods for adhesive joints are relatively limited.

2.1.3 Adhesive bonding of load bearing aluminium structures

Adhesives have been used for many years in aerospace applications, where high durability bonded aluminium structures are obtained by using adhesives based on phenolic or epoxy resins [5]. One of the biggest concerns with respect to adhesive bonding is confidence in their durability. However, the ability of an adhesive to retain its properties over long periods of time has been demonstrated [6]. Joints from the top wing of a 30 year old Nimrod aircraft, bonded with Redux phenolic based adhesive, were analysed. The mechanical properties were retained and durability tests on the old adhesive gave similar strength retention compared to modern adhesives. Therefore, both the adhesive and the chromic acid anodising treatment used to prepare the aluminium surface gave high performance joints that lasted 30 years.

Adhesives are currently also used in many areas in the manufacture of automobiles, but so far the use of adhesives in load bearing structures has been limited. However, there are exceptions: Hydro Aluminium manufacture lightweight spaceframes for the low volume production of Lotus Elise and Opel Speedster sports cars. The spaceframes are made of extruded aluminium profiles that are sulphuric acid anodised prior to assembly by adhesive bonding.

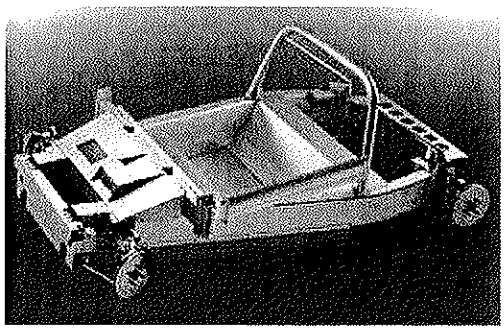

Figure 1. The spaceframe of the Lotus Elise.

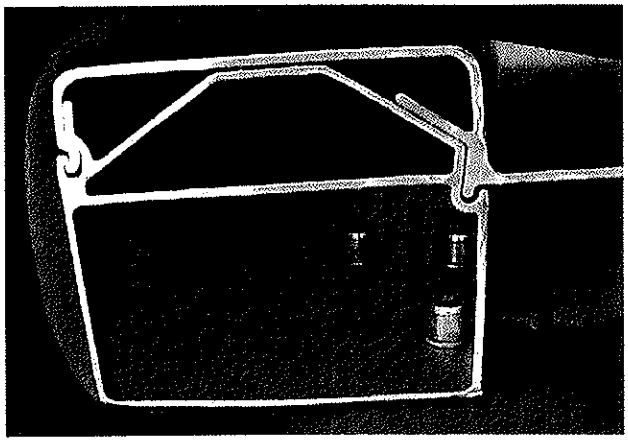

Figure 2. Cross-section of a part of the adhesively bonded spaceframe of the Lotus Elise.

A major reason for the limited use of adhesives in structural automotive applications is, as for aerospace applications, concern about the fatigue and durability behaviour of these components. The adhesive joints must perform satisfactorily under service conditions that include dynamically applied loads and exposure to hostile environments, such as water and road salt. Unfortunately, water is one of the most hostile environments for adhesive joints, and the use of surface pretreatment processes for the substrates being joined is therefore required. Despite these disadvantages adhesive bonding gives flexibility in design that is more difficult to achieve with other joining methods. This also includes the use of thinner sheet materials and more lightweight structures. The bonded over-lap joint covers a much larger area than other joining methods and gives a better distribution of stresses that may ultimately cause failure. Adhesive bonding also provides the possibility of joining of dissimilar materials, e.g., aluminium-steel joints, where the adhesive bondline prevents contact between the metals and thus can minimise the effect of corrosion.

2.2 Epoxy adhesives

Epoxy adhesives are usually the preferred choice in adhesive bonding of load bearing aluminium structures. One of the reasons is that epoxy adhesives are far easier to work with than the phenolic adhesives [7].

It is resins with an oxirane ring as their reactive group that are known as epoxy resins [2]. Epoxy resins form the largest variety of structural adhesives currently available. Many epoxy resins are based upon the reaction of phenols with epichlorohydrin. Reaction of Bisphenol A with epichlorohydrin leads to the most common epoxy resin, the diglycidyl ether of Bisphenol A (DGEBA). DGEBA can be further reacted with Bisphenol A to generate higher molecular weight resins which can be either epoxy or phenol terminated. Bisphenol F can also be reacted with epichlorohydrin to generate resins analogous to the DGEBA-based resins. Bisphenol F-based resins have the important attribute of lower viscosity than the DGEBA resins. Another major chemical class of epoxy resin is the epoxidised phenolic resin.

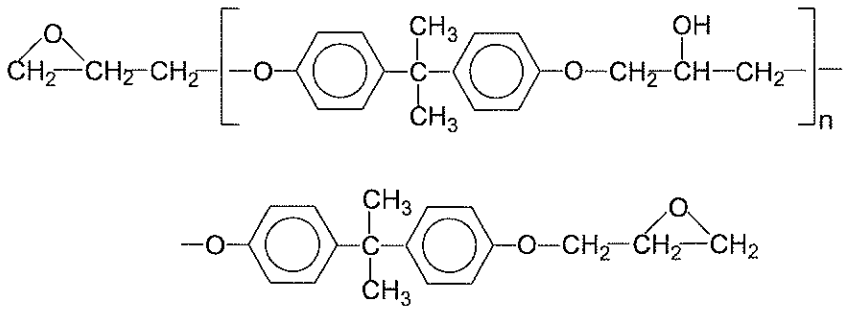

Figure 3. General formula of DGEBA resins. When n = 0 the molecular weight is 340, when n = 10 the molecular weight is 3000. Commercial resins seldom have average molecular weights exceeding 4000 [8].

Part of the reason for the wide use of epoxy resins in structural adhesives is the substantial number of crosslinking reactions to which oxirane groups are sensitive. Epoxy resins can react with alcohols, mercaptans and anhydrides (not frequently used in

adhesives). Lewis acids act as catalysts for the cationic polymerisation of oxirane-based resins, and epoxy resins can also be polymerised anionically.

The most common curing agents used with epoxy resins are based upon amines. Primary amines react with epoxy resins at room temperature without the presence of a catalyst. Aromatic amines react with epoxy resins slowly at room temperature, but rapidly at elevated temperatures. For room temperature cure of epoxy resins, the most common curing agent is based upon the primary aliphatic amine, such as e.g. diethylenetriamine. Room temperature curing epoxy adhesives are delivered as two-component pastes.

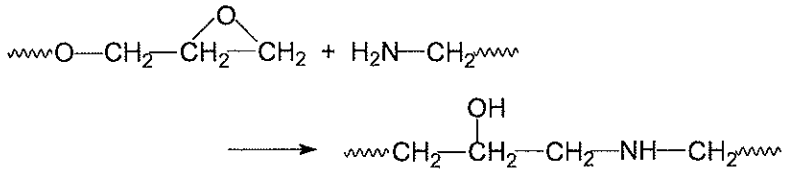

Figure 4. Reaction of the glycidyl group with a primary amine.

The most common agent for high temperature cure of epoxy resins is dicyandiamide. This molecule may in theory have the potential for a five-fold crosslink, but it has been claimed that the functionality is in fact closer to three [9]. A substantial number of elevated temperature curing epoxy resins use dicyandiamide as the sole curing agent or in combination with other curing agents. Tertiary amines are often used as catalysts. The tertiary amine opens up the epoxy ring which reacts further with other epoxy rings or hydroxyl groups in a complicated overall reaction mechanism [8]. High temperature curing epoxy resins are available as one-component pastes (e.g. Betamate XD4600) or as film adhesives (e.g. FM-73).

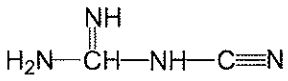

Figure 5. The chemical structure of dicyandiamide.

Thermosetting adhesives are amorphous, highly cross-linked materials after curing [1]. This microstructure results in useful properties, such as high modulus and fracture strength, low creep and good performance at elevated temperatures. However, thermosetting polymers are also relatively brittle materials having a poor resistance to crack initiation and growth. A method of modifying the microstructure of thermosetting polymers to greatly increase their toughness, but without being significantly impairing the other desirable properties, is to incorporate a second phase of dispersed rubber particles into the polymer. Two mechanisms that enable the presence of rubber particles to increase the toughness of the polymer are of major importance: (a) localised shear yielding in the epoxy polymer which occurs between the rubber particles, and (b) plastic hole, or void, growth in the epoxy polymer which is initiated by cavitation or debonding of the rubber particles. Due to the large number of particles involved, the total irreversible energy dissipation may be considerable.

2.3 Mechanical tests of adhesive bond performance

The tests used to study the physical properties of adhesives and adhesive bonds can be broadly separated into four categories: tensile, shear, cleavage and peel. In the literature dealing with adhesive bonding of structural aluminium specimens, a selection of three different tests are normally used to determine the bond performance. These three tests are briefly described in the following sections.

2.3.1 Lap shear tests

The standard test method for evaluating the shear strength of adhesive bonds is described in ASTM D1002 [10]. The lap shear test is possibly the most common test method for the evaluation of adhesive bonds. After cure, the over-lap specimen is placed in a tensile testing machine and loaded to failure. The lap shear bond may also be placed in an adverse environment (such as exposure to elevated temperatures, solvents, or high humidity) before testing to failure. When applied logically and realistically the lap shear test can be used as a reasonable and easy comparison of the strength of adhesives. It can also be used as a quality control method when testing for consistency

of adhesive bond strength. Despite the stress state of the adhesive in the specimen and despite its lack of realism, the lap shear specimen has been used to evaluate essentially every adhesive.

The following refs. have used the lap shear test in order to evaluate the performance of epoxy adhesive/aluminium systems [5,11-22].

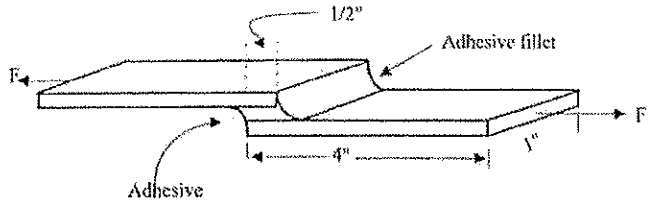

Figure 6. Diagram of the ASTM D1002 lap shear specimen [2].

2.3.2 Wedge test

The wedge test is described in ASTM D3762 [23]. A wedge is inserted into the bondline of a bonded aluminium specimen, thereby creating a tensile stress in the region of the crack tip. The specimen is exposed to an appropriate environment, and the resulting crack growth and failure modes are evaluated. In principle may any test conditions be used.

Since it is the interfacial regions in which environmental failure initiates, a joint design which has a relatively high stress concentration at, or near, the interface will tend to reveal durability effects more readily [4]. The wedge test has greater sensitivity towards environmental attack than, e.g., the conventional lap joint. The wedge test has been found to be particularly useful as a quick and convenient quality control technique for assessing the adherend surface pretreatment with respect to joint durability.

Boeing Corporation has shown that there is a strong correlation between the in-service durability of adhesive bonds and the extent of crack growth in the wedge test specimen [2]. In addition, the mode of failure can be an indicator of environmental durability. Thus, if one carries out a wedge test and the failure mode is apparently interfacial and the crack growth is long, the prediction is that the bond will not be durable in service. In contrast, a failure mode where the failure is cohesive in the adhesive and the crack growth is short is considered to be a predictor of good in-service durability.

The wedge test has been used thoroughly in order to determine the performance of adhesively bonded aluminium [14,17,20,24-33]. A schematic drawing of the wedge test specimen used in this study is shown in Chapter 4.2.

2.3.3 Fatigue testing

A test may be accelerated by increasing the temperature, load or humidity, or by a combination of these factors. However, only moderate increases above the likely maximum should be used. It is especially important to avoid a shift above the glass transition temperature, T_g, of the adhesive because the mechanical properties will undergo large changes and the uptake of water will increase markedly [34]. Thus, it is important to ensure that accelerated tests are selected that do give the same outcome as would be seen in real life, the aim being to accelerate the mechanisms of environmental attack and not to produce mechanisms different to those seen in real life.

The methods of fracture mechanics are ideally suited to study the cyclic fatigue behaviour of adhesive joints at realistic temperatures and humidities [1]. It is also possible to use data generated from the relatively short-term cyclic fatigue tests, to predict quantitatively the lifetime of bonded joints and components that are subjected to cyclic fatigue loads while in service.

In case of metallic substrates, either the double-cantilever beam (DCB), the reinforced double-cantilever beam (RDCB), or the tapered double-cantilever beam (TDCB) may be employed. The TDCB test specimen has been used to obtain the values of the rate of

crack growth rate per cycle, da/dN, as a function of maximum strain energy release rate, G_{max}, applied in the fatigue cycle.

Examples of practical use of cyclic fatigue tests are given in refs. [35-38], and in an ASTM standard [39]. The dramatic effects an aggressive, hostile environment may have upon the mechanical performance of the joint have been revealed. The fatigue tests performed in wet environments were greatly inferior to those performed in dry environment. XPS studies of chromic acid etched joints investigated in ref. [35] revealed that the locus of failure after testing in dry environment was completely cohesive in the adhesive layer, while the locus of failure after testing in wet environment was mainly through the aluminium oxide layer [40].

References

[1] A.J. Kinloch, *Proc. Inst. Mech. Eng.* **211(H)**, 307-335 (1997)

[2] A.V. Pocius, Adhesion and Adhesives Technology, Carl Hanser Verlag, Munich, 1997.

[3] S. Wu, Polymer Interface and Adhesion, Marcel Dekker, New York, 1982.

[4] A.J. Kinloch, Durability of Structural Adhesives, Elsevier Applied Science Publishers, London, 1983.

[5] M. Brémont and W. Brockmann, *J. Adhesion* **58**, 69-99 (1996)

[6] S.B. Dunkerton and C. Vlattas, *Int. J. Mater. Prod. Tec.* **13**, 105-121 (1998)

[7] L.J. Hart-Smith and G. Strindberg, *Proc. Inst. Mech. Eng.* **211(G)**, 133-156, (1997)

[8] J.A. Brydson, Plastics Materials, Butterworth & Co, London, 1975.

[9] S.A. Zahir, *Adv. Org. Coat. Sci. Tech.* 4, 83-102 (1982)

[10] ASTM D1002, American Society for Testing and Materials, Philadelphia, PA.

[11] W.P. De Wilde, G. Van Vickenroy, L. Tirry and A.H Cardon, *J. Adhesion Sci. Technol.* **9**, 149-158 (1995)

[12] D.M. Brewis, J. Comyn, A.K. Raval and A.J. Kinloch, *Int. J. Adhesion Adhesives* **10**, 247-253 (1990)

[13] M.R. Bowditch, *Int. J. Adhesion and Adhesives* **16**, 73-79 (1996)

[14] C.L. Ong, W.Y. Shu and S.B. Shen, *Int. J. Adhesion Adhesives* **12**, 79-84 (1991)

[15] B.M. Parker, *Int. J. Adhesion Adhesives* **13**, 47-51 (1993)

[16] D.J. Arrowsmith, D.A. Moth and S.P. Rose, *Int. J. Adhesion Adhesives* **12**, 67-72 (1992)

[17] T.J. Smith, *J. Adhesion* **14**, 145-174 (1982)

[18] H. Woo, P.J Reucroft and R.J. Jacob, *J. Adhesion Sci. Technol.* **7**, 681-697 (1993)

[19] A.F. Harris and A. Beevers, *Int. J. Adhesion Adhesives* **19**, 445-452 (1999)

[20] W. Thiedman, F.C. Tolan, P.J. Pearce and C.E.M. Morris, *J. Adhesion* **22**, 197-210 (1987)

[21] J. Wang and D. Feldman, *J. Adhesion Sci. Technol.* **7**, 565-576 (1991)

[22] O. Lunder, B. Olsen and K. Nisancioglu, *Int. J. Adhesion Adhesives* **22**, 143-150 (2002)

[23] ASTM D3762, American Society for Testing and Materials, Philadelphia, PA.

[24] A.N. Rider, D.R. Arnott, A.R. Wilson and O. Vargas, *Mater. Sci. Forum* **189/190**, 235-240 (1995)

[25] A.N. Rider and D.R. Arnott, *Surf. Interface Anal.* **24**, 583-590 (1995)

[26] D.R Arnott, A.R. Wilson, A.N. Rider, L.T. Lambriandis and N.G Farr, *Appl. Surface Sci.* **70/71**, 109-113 (1993)

[27] R.A. Crook, J.W. Sinclair, L.W. Poulter and K.J. Schulte, *J. Adhesion* **69**, 315-329 (1998)

[28] K.B. Armstrong, *Int. J. Adhesion Adhesives* **17**, 89-105 (1997)

[29] A.N Rider, C.L. Olsson-Jacques and D.R. Arnott, *Surf. Interface Anal.* **27**, 1055-1063 (1999)

[30] X. Zhou, G.E. Thompson and G. Potts, *Trans. IMF* **78**, 210-214 (2000)

[31] A.N. Rider and D.R. Arnott, *Int. J. Adhesion Adhesives* **20**, 209-220 (2000)

[32] C.M Bertelsen and F.J. Boerio, *Prog. Org. Coat.* **41**, 239-246 (2001)

[33] A.N. Rider and D.R. Arnott, *J. Adhesion* **75**, 203-228 (2001)

[34] D.M. Brewis, in: A.J. Kinloch (Ed.), Durability of Structural Adhesives, Elsevier Applied Science Publishers, London, 1983. p. 215-254.

[35] J.K. Jethwa and A.J. Kinloch, *J. Adhesion* **61**, 71-95 (1997)

[36] M. Fernando, W.W. Harjoprayitno and A.J. Kinloch, *Int. J. Adhesion Adhesives* **16**, 113-119 (1996)

[37] R. Joseph, J.P. Bell, A.J. McEvily and J.L. Liang, *J. Adhesion* **41**, 169-187 (1993)

[38] A.J. Kinloch, M.S.G. Little and J.F. Watts, *Acta. Mater.* **48**, 4543-4553 (2000)

[39] ASTM D3433, American Society for Testing and Materials, Philadelphia, PA.

[40] R.A. Dickie, L.P. Haack, J.K. Jethwa, S.J. Kinloch and J.F. Watts, *J. Adhesion* **66**, 1-37 (1998)

Chapter 3
Review of literature

3.1 Surface pretreatment of aluminium

The pretreatment of aluminium in order to enhance adhesion has been subject to much research, and has been extensively reviewed by Critchlow and Brewis [1]. In this review a wide range of mechanical, chemical, electrochemical or other treatments designed to modify the surface of aluminium to enhance bond durability were identified. These may be combined with a range of chemical 'add-ons', such as primers, coupling agents or hydration inhibitors to stabilise the surface during storage or to further enhance bond durability. Furthermore, a diverse range of surface analytical techniques were also identified, these range from simple wettability or optical inspection methods to more complex and costly ultra high vacuum based techniques. These techniques provide useful data in adhesion studies, for example, in studying surface chemistry and topography or in failure analysis. Armstrong [2] and Venables [3] have also given reviews on pretreatment of aluminium.

3.1.1 Anodising and aerospace pretreatments

Adhesives have been used for many years in aerospace applications, where high durability bonded aluminium structures are obtained by using adhesives based on epoxy or phenolic resins [4]. Surface preparation techniques of aluminium for adhesive bonding in aerospace applications have been reviewed by Kozma and Olefjord [5]. It has been realised for years that proper chemical pretreatment of aluminium prior to epoxy bonding is essential for developing bond strengths necessary for high performance aircraft applications [6]. Particularly three different pretreatments have been used by the aerospace industry: chromic acid etching (CAE) - particularly the FPL-process in which aluminium is etched in an aqueous dichromate-sulphuric acid solution - and phosphoric and chromic acid anodising (PAA and CAA, respectively), in which an anodising potential is applied to the metal while it is immersed in the acidic electrolyte. Detailed description of the processes can be found for the FPL-etch [7,8],

PAA [7,9] and CAA [7,10], and also for the sulphuric acid anodising (SAA) process [7], which is of greater importance in the automotive industry.

According to Armstrong [2] anodising seems to have a number of advantages over other methods of pretreatment; the porosity of the oxide layer produced on the aluminium surface provide for mechanical interlocking of the adhesive, the oxide is not electrically conductive and therefore cuts off the flow of electrons necessary to produce corrosion, and chemical bonding between the adhesive and the oxide layer is possible.

PAA is currently the preferred treatment of the American aerospace industry, and it is widely considered to give the most durable joints [1,11]. Venables and co-workers showed that the pore structure formed by the PAA pretreatment significantly increased the durability compared with the FPL etch [3,6]. If the PAA surface is bonded with an adhesive with viscosity low enough to fill the pores of the oxide, then several beneficial effects will occur [12]: (1) A crack that propagates in the adhesive/aluminium interface have to take detours into the adhesive. The adhesive plastically deforms, and energy is

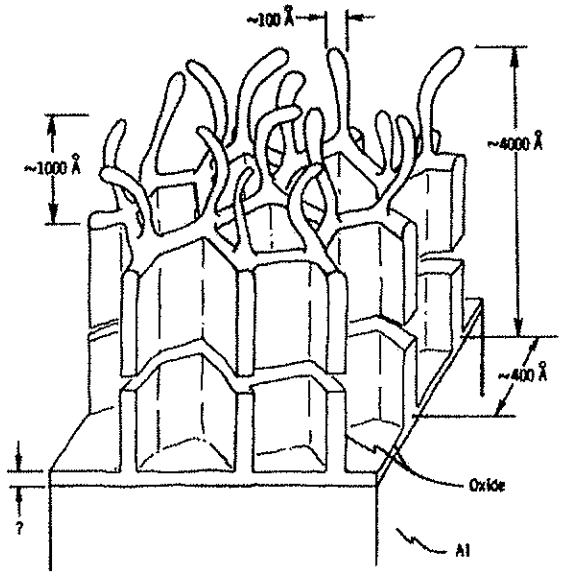

Figure 1. Drawing of the oxide morphology produced on an aluminium surface by PAA treatment (50.000×) [6].

consumed. (2) The filled pores on the surface provide for mechanical interlocking of the adhesive. A 'lock and key' effect occurs, and the solid adhesive cannot move from the pore without plastically deforming. (3) The increased surface roughness also increases the contact area. The total energy of the surface interaction increases by an amount proportional to the surface area.

The anodic oxide produced by the PAA process has the advantage of being hydration resistant, due to an outer layer of aluminium phosphate. Phosphate ions are known to form stable oxide layers and to inhibit hydration reactions in wet environments [13-15]. However, treatment of aluminium surfaces with phosphonate hydration inhibitors may still reduce durability due to poor coupling with the epoxy adhesive [14].

CAA is currently the preferred pretreatment process of European aeroplane manufacturers [1]. The surface oxide produced is thick, porous and highly structured, and the oxide is resistant to attack by moisture. Prior treatment with a chromic acid etch is beneficial to the long-term durability. Bonded joints made of CAA surfaces usually give much better durability than FPL-etched surfaces, although poorer durability have also been observed [16].

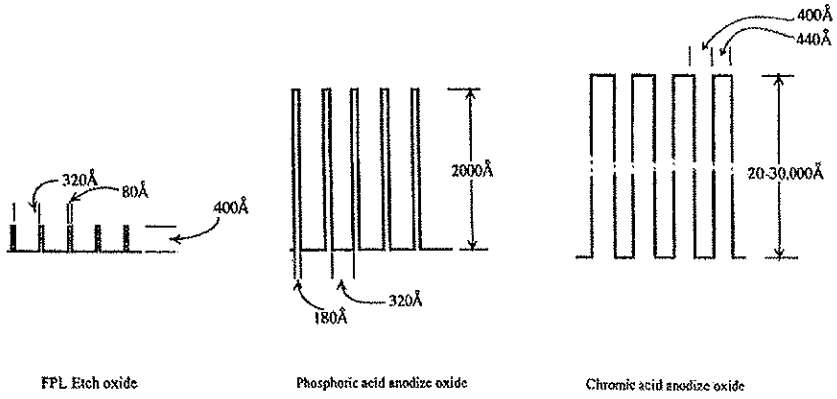

Figure 2. Schematic diagram of oxide films generated on aluminium by: FPL-etching, PAA and CAA. Even though the oxide films are shown in two dimensions, they are three-dimensional [12].

The topography produced by the FPL-etch has been reported to be highly microrough with a well-defined matrix of fibrils extending from the surface, but with a relatively thin oxide layer beneath this structure [1]. FPL-etched surfaces are consistently out-performed by those which have been anodised. Inconsistent results make it unsuitable as a stand-alone treatment for the bonding of primary structures.

Digby and Packham [17] examined the durability of aluminium-epoxy joints by the means of the Boeing wedge test. The FPL-etch produced a scalloped surface with a network of shallow pores and protrusions on top of a thin barrier layer. The anodising treatments produced the classic open pore structure of the PAA surfaces and a much finer pore structure on the SAA surface. The SAA treatment gave poor durability. There appeared to be little penetration of the surface by the adhesive, possibly due to the finer pores of the SAA film. This reduced the area available for chemical bonding and reduced the degree of mechanical interlocking. Visual inspection and XPS analysis indicated that the failure was close to interfacial.

The importance of properly wetting of the oxide surface by the adhesive has been investigated [15-16]. Arrowsmith *et al.* [15] determined the initial joint strength and durability of lap shear joints of SAA surfaces bonded with adhesives of different viscosity. After immersion in water the joints bonded with a low-viscous acrylic adhesive retained their joint strength, whereas there was a marked fall in strength of the joints bonded with epoxy adhesives. The reason for this loss of strength was thought to be due to the difficulty of wetting the surface with the epoxides, which led to the presence of voids due to entrapment of air in the epoxy joints. Subsequent migration of water into these voids during immersion in water led to the loss of strength.

3.1.1.1 Alternatives to hexavalent chromium processes

Hexavalent chromium compounds are a fundamental part of the three most successful surface treatments used to optimise the structural bonding of aluminium and its alloys: CAE, PAA and CAA. However, hexavalent chromium is reported to be toxic to most living species [18]. Environmental factors together with stricter legislation has therefore led researchers to look for alternative, more environmentally friendly, pretreatment

processes. Critchlow [11] has written a short review of chromate-free alternatives to hexavalent chromium processes. The alternatives mentioned are: grit-blasting, laser ablation, plasma-spray, the P2 etch (a sulphuric acid-ferric sulphate based pretreatment), STAB 1, 2 and 3 (STAB 3 comprises a dip in concentrated NaOH solution [19]), and conversion coatings. Critchlow [11] also showed that two chromate-free conversion coatings, Bonderite 777 and EP2472, were at least as effective as a chromate-containing process, Bonderite 705. Grit-blasting was out-performed by the conversion coating treatments.

3.1.2 Mechanical pretreatments

Rider *et al.* [20] conducted durability tests on AA2024-T3 aluminium alloy bonded with FM-73 epoxy adhesive. Three pretreatment sequences were followed; abrasion with Scotchbrite followed by cleaning in methyl-ethyl-ketone (MEK) or water, or grit-blasting with alumina powder. The grit-blast pretreatment offered substantially better durability than the Scotchbrite/MEK treatment, but only marginally better than the Scotchbrite/water treatment. XPS analysis indicated that the failure in the Scotchbrite/MEK treated specimens had occurred in very close proximity to the aluminium oxide/adhesive interface. For the grit-blasted and Scotchbrite/water treated specimens it was indicated that the fracture path had occurred predominantly in the aluminium oxide. The difference in durability of Scotchbrite/MEK and Scotchbrite/water treatments was related to the distribution contaminant. It was proposed that the MEK wipe distributed hydrocarbon contaminant approaching a thin uniform layer whereas the water wipe distributes contaminant approaching irregular islands. The irregular islands should lead to a greater density of available bonding sites on the oxide than the uniform layer. The combination of low hydrocarbon concentration and random surface roughness for the grit-blasted treatment relative to the Scotchbrite treatments led to higher bond durability. However, there is no obvious relation between fine and coarse grits with respect to difference in adhesion strength [21].

Still, the macroroughness can have a significant influence on the adhesion strength. Rider *et al.* [22-23] investigated aluminium surfaces which were ultramilled to base angles of 60°, 120° and 180° (in decreasing order of roughness). The results showed that

the difference in surface area was only 1.5 fold, but that increased surface roughness improved the fracture toughness by two orders of magnitude. The authors proposed that a rough surface would lead to higher stress intensity at the surface peaks than in the hollows, and that the density of micro-cavities (where diffusion of water can take place) may then be significant only in the region of the peaks of a roughened surface [22].

3.1.3 Boiling water pretreatment

The aluminium-water system has been extensively reviewed by Alwitt [24]. The immersion of aluminium in boiling water produces an oxyhydroxide film with a flake-like structure [25]. The boiling pretreatment has been found to improve bond durability between epoxy adhesives and aluminium [26-27]. For immersion times greater than 60 min, a decrease in bond durability was observed [26]. This decrease was explained by a decrease in both the film porosity and the surface area at extended treatment times, resulting in a decrease in the number of adhesive-oxide bonds. The reduction of adhesive diffusion into the oxide structure would also reduce the opportunity for mechanical interlocking between the adhesive and the oxide film.

Strålin and Hjertberg [28-31] have also examined the adhesion of ethylene copolymers to aluminium pretreated by immersion in boiling water. They suggested that an improvement in adhesion was due to stronger acid-base interactions, increased contact surface and mechanical keying into the porous oxide surface [29].

3.1.4 Silane coupling agents

Organofunctional silanes are widely used as coupling agents to enhance the durability of adhesive joints [32]. A review of the silane coupling agent literature has been given by Rosen [33]. The general understanding is that silanisation improves adhesion through the formation of strong, covalent bonds between the aluminium surface and the adhesive. The silanes generally have a hydrolysable group (e.g. $-OCH_3$) and an organofunctional group (e.g. an epoxy group) usually selected to be chemically reactive with a given adhesive. After hydrolysis, the silane can enable the formation of strong Al-O-Si bonds between the hydroxyl groups on the metal surface and the hydrolysed groups of the silane. A silane coupling agent is said to perform two functions in order to

improve the environmental durability of a bonded joint [34]. Firstly, it will increase the density of strong bonds between the oxide and the adhesive. Secondly, it will improve the hydrolytic stability of the aluminium oxide. The formation of a weak hydrated layer on the aluminium surface is significantly hindered by the formation of a cross-linked multilayer film [14,35-36].

A wide range of silanes has been developed for improved adhesion or protection of the metal surface [37-40]. A common silane used to obtain improved adhesion of aluminium surfaces bonded with epoxy adhesives is γ-aminopropyltriethoxysilane (APS). The durability of such systems have been shown to be very dependent on the pH of the silane solution – the natural pH 10.4 solution was inferior to a pH 8 solution adjusted by HCl [41]. Two particular problems when using APS have been noted: (1) The primary amino group may form bicarbonate salts with CO_2 [42], and (2) An "upside-down" interaction may occur, where interfacial bonding is through the amino group rather than the hydrolysed ethoxy groups at Si [43]. Another important silane pretreatment is the two-step BTSE[1] + APS treatment. The first layer of BTSE provides the required corrosion protection and metal adhesion, while the second layer of APS provides the necessary adhesion at the silane/polymer interface [38,44].

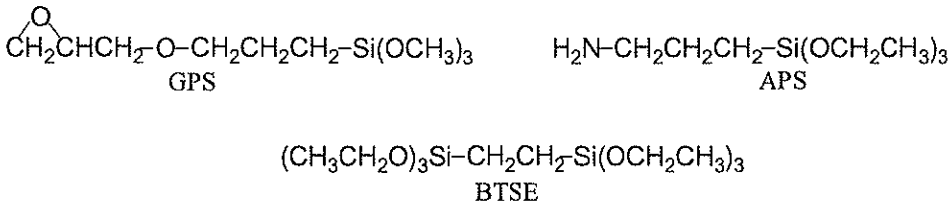

Figure 3. The chemical structures of GPS, APS and BTSE.

[1]BTSE = Bis-1,2-(triethoxysilyl)ethane

3.1.4.1 Treatment with GPS

One of the most commonly used silanes is γ-glycidoxypropyltrimethoxysilane (GPS). The treatment of aluminium surfaces with aqueous solutions of GPS before adhesive bonding has been shown to improve bond durability [14,27,36,41,45], and the deposition of GPS and the films formed by GPS on aluminium surfaces have been investigated with a variety of techniques, including FT-IR, XPS and ToF-SIMS [36,43,46-55].

Abel *et al.* [50] used ToF-SIMS to show that the strong Al-O-Si bond is formed between hydrolysed GPS and aluminium surfaces, while the existence of a covalent bond between a GPS film on aluminium and an epoxy adhesive was shown by Rattana *et al.* [56]. Rattana *et al.* [56] showed that the amine curing agent interacted covalently with the epoxy ring of the GPS molecule and the DGEBA resin, forming a network of covalent bonds from the aluminium surface through to the bulk of the adhesive. Thus, it is possible for an amine-cured epoxy adhesive system to interact covalently with a GPS film on aluminium. XPS and ToF-SIMS studies showed that diethanolamine (DEA) deposited onto GPS coated aluminium undergoes two types of interactions: the formation of covalent bonds with nucleophilic addition or a Brønsted type of interaction between the nitrogen of DEA and the silanol functionality of hydrolysed GPS [57].

It has also been reported that other phenomena besides covalent bonding in the silane/adhesive interface have effect on the adhesion. The existence of an interpenetrating network in the silane film/polymer interphase can have effect on bond properties. This effect can occur if contact is made between a polymer and uncrosslinked silanols which still have some degree of solubility [37,58].

3.2 Chemical interactions

The chemical interactions between aluminium surfaces and adhesives have been investigated using advanced surface analysis, often by using model molecules imitating amine-cured epoxy adhesives [57,59-66]. The detailed mechanism of interaction between a model compound and an aluminium surface is complex and strongly dependent on the surface chemical state.

Barthés-Labrousse [60] presented a critical discussion of the adhesion mechanism at amine-cured epoxy/aluminium interfaces. Adsorption of model molecules showed the formation of an alkoxide Al-O-R species. The formation of this alkoxide species is a result of the reaction between alcoholic hydroxyl hydrogen (R-**OH**) of the model molecule and hydroxyl groups (Al-**OH**) on the aluminium surface. Because OH species are always present on 'real world' surfaces, the formation of alkoxide species is possible. A polar interaction of the alcohol group of the molecule with both hydroxyl and oxide sites at a PAA surface was also indicated. Bonding with oxidised Al is via oxygen lone-pairs of the alcohol termination of the molecule co-ordinated to hard acidic aluminium ions (Lewis-like reaction).

Not only the interaction of the adhesive hydroxyl group, but also the interaction of the amino functionality with the aluminium surface is the subject of much controversy. Due to the complexity of the surface chemical state, both Lewis and Brønsted acid sites are likely to be present on 'real world' surfaces, leading to the coexistence of both these types of binding mechanisms. Bonding with clean (oxide free) aluminium occurs via nitrogen lone-pairs co-ordinated to soft acidic aluminium atoms (Lewis-like acid-base reaction).

Marsh *et al.* [59] used XPS to show that while a high purity aluminium surface produced no firm evidence of any chemisorptive interaction with 2,3-epoxy-propylphenyl ether, the aluminium strongly absorbed three aminous/hydroxylaminous molecules. The interaction was apparently via a primary mechanism involving Lewis

bonding of the nitrogen atoms to the cationic surface sites, with some protonation of nitrogen atoms as a secondary mechanism. No evidence of reaction between molecular and surface hydroxyl groups to form Al-O-C alkoxide bonds could be observed in this study.

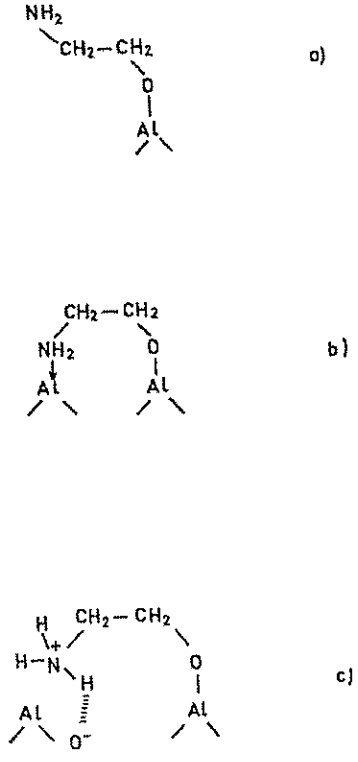

Figure 4. Possible modes of interaction of the amino functionality with aluminium 'real world' surfaces: a) free amino groups; b) NH_2 groups co-ordinated to an aluminium ion; and c) amine protonation effect [60].

Nakamae *et al.* [67] attributed the localisation of an amine curing agent in a cured epoxy resin/4,4′-diaminodiphenylmethane (DDM) curing agent system at the cured epoxy/oxidised aluminium interface to acid-base interactions formed between the amino groups in DDM and the acidic sites on the oxidised aluminium surface. The oxidised aluminium has many anionic charges and few cationic charges in the presence of a basic

substance like DDM. Accordingly, electron exchange between the oxidised aluminium surface and DDM can easily occur, and acid-base interactions of the type $N^{+}H_3$---$O^{-}Al$ form between the amino groups of DDM and acidic sites on the oxidised aluminium.

The interaction of larger molecules, such as the adduct of DGEBA and diethylamine, with oxidised/hydroxylated aluminium has also been examined. Bolouri *et al.* [61] concluded that the adduct bonded to aluminium oxide/hydroxide surfaces via a chelating mechanism, with Lewis-type bonding of the hydroxyl and amino functionalities to an aluminium ion. Affrossman *et al.* [62] suggest that while Lewis bonding of the amino functionality occurs, the hydroxyl functionality binds to the surface via the formation of an alkoxide unit.

3.2.1 Compositional variation at the interphase

Several authors have investigated the region between the aluminium substrate and the homogenous polymer, referred to as the interphase [68-71]. There is general agreement that interphases exists, but debate evolves around the characteristic length scale of the interphase and its composition and structure. Arayasantiparb *et al.* [70] examined the size and composition of the epoxy-aluminium interphase using spatially resolved EELS in a STEM instrument. Large concentration gradients were observed close to the PAA aluminium surface in the epoxy/amine systems; a gradual compositional change from 25 vol% curing agent in the bulk epoxy to 80 vol% at the epoxy/oxide interface. The interphase extended 90±15 nm from the oxide surface into the bulk. These chemical segregations may have important implications on the properties and performance of epoxy-aluminium adhesive joints. Bentadjine *et al.* [72] proposed a formation mechanism of the interphase region of epoxy-diamine resins on metallic substrates investigated by NMR and FT-IR. Partial dissolution of the oxide/hydroxide was observed. The metallic ions diffuse within the liquid mixture and react with the amine groups of the curing agent to form metallo-organic complexes. These metallo-organic complexes react with the DGEBA epoxy monomer to form a new epoxy network with quite different properties to the polymer bulk ones [73].

Fondeur and Koenig [68] used FT-IR to investigate thin epoxy adhesive films on anodised and untreated aluminium surfaces. An epoxy resin was cured with dicyandiamide. The curing agent segregated preferentially on the untreated aluminium surface, but the epoxy was preferred on the anodised aluminium surface. The large amount of excess dicyandiamide on its salt form near the untreated surface promoted complete cure at the surface. In the case of the anodised aluminium surface, it was expected that a large number of Al-OH groups could be involved in hydrogen bonding with the nitrogen atom in the curing agent. However, no spectroscopic evidence for this interaction was observed. The only effect seen was the lesser amount of dicyandiamide and a relatively large number of unreacted epoxy groups at the surface. Fondeur and Koenig [74] also showed the existence of uncured regions close to the anodised surface using NMRI. On the other hand, the images of epoxy between untreated aluminium surfaces were characterised by large amounts of inhomogenities finely distributed in the sample.

3.3 Effect of water

Water can affect both the physical and mechanical properties of the adhesive itself and also the nature of the interface or interphase that exists between it and the substrate. The effects of water on adhesive joints are described by Bowditch [75]. The degradation of adhesive, substrate and chemical bonds across the interface as a result of interaction with water, are all possible. After water has gained access via diffusion through the adhesive or wicking along the interface, joints may be weakened in a variety of ways. Water is absorbed and plasticises all organic adhesives. Although the effect of plasticisation is commonly to weaken, low concentrations of water may have the net effect of strengthening some joints. A second, more important degradation mechanism is 'displacement' of adhesive by water, which is likely wherever the adhesion is primarily due to the operation of van der Waal's forces. Hydrolysis of covalently bonded interfaces may occur, depending on the nature of the chemical moieties and the temperatures involved. Attack by water of the oxide substrate has been invoked as the

reason for the poor durability of adhesive joints to metallic substrates with hydrolysable oxides.

The ageing effects of DGEBA/dicyandiamide systems due to exposure to relatively high temperature and high humidity have been studied [76-77]. De Nève and Shanahan [76] found that water uptake is significant at 70°C and 100% relative humidity. The glass transition temperature, T_g, and the elastic modulus corresponding to the rubbery state both decreased with water uptake. Xiao *et al.* [77] examined the irreversible interactions between water and the model epoxy resin. The results showed that the epoxy backbone chains can be cut and segments leach out during hygrothermal ageing at 90°C. It was believed that water breaks the crosslink chains by hydrolysis reactions. Tertiary amine groups were postulated as the weakest points in the cured resin.

3.3.1 Hydration of the aluminium surface

Pethrick *et al.* [78] used dielectric measurements to investigate the hydration of aluminium oxide. The aluminium oxides produced by most surface pretreatments are not thermodynamically stable in moist environments and give a complex range of oxide-hydroxides on addition of water: boehmite (AlOOH), bayerite ($Al(OH)_2$) and gibbsite ($Al(OH)_3$). The aluminium-water system has been reviewed by Alwitt [24]. The following reactions may occur in humid environments:

$$Al_2O_3 + H_2O \rightarrow 2AlOOH$$

$$AlOOH + H_2O \rightarrow Al(OH)_3$$

A non-porous form of γ-Al_2O_3 was shown to absorb water very rapidly during the first hour, then uptake increased more slowly reaching ca. 0.5 mole H_2O per Al_2O_3 in one day, after which the absorption increased very slowly [78]. The initial absorption process corresponds to the very fast uptake of a monolayer of water. Dry alumina absorbs water to give a monolayer of hydroxyl groups and the new surface will have high affinity for water and can react to give surface oxide-hydroxide. Further absorption

requires build-up of water on the surface and/or conversion of subsurface oxide to oxide-hydroxide. This conversion requires diffusion of water through the surface oxide and it expands the outer layer. This process will be slow, giving a build-up of hydrated surface structure which will contain loosely bound water. Water in these systems exists in a number of forms: trapped in the oxide as a hydrate, reacted with the oxide to form a hydroxide, in the hydrated surface layers, trapped in capillaries or voids, and condensed on to the surface.

Hydration of an aluminium oxide surface under an adhesive film can occur [20,79]. In a bonded aluminium joint, the local strength of the bond would have been reduced and the growth of hydration products would generate stresses that would result in crack growth. Thus, one mechanism that induces crack propagation in moist environment is subadhesive hydration of the aluminium substrate.

3.3.2 Degradation of adhesive bonds

Rider *et al.* [14,22,34] presented a stress based bond degradation model to explain how water degrades an adhesive bond. According to this model, the process of degradation involves: the migration of water ahead of the crack tip, the decoupling of the adhesive or coupling agent from the oxide, and the hydration of oxide at the unprotected sites on the oxide surface. The rate at which these three steps proceed in a particular system will determine the fracture path. The generalised model assumes that stress applied to the specimen will lead to greater deformation of the polymer at the interface than in the bulk adhesive. The density of bonds between the polymer and the substrate will determine the size of micro-cavities generated at the stressed interface near the crack tip. The size of micro-cavities and their degree of inter-connection will determine the rate of diffusion and local concentration of moisture ahead of the crack tip. The rate of degradation depends on the moisture concentration, the density of unprotected hydration sites and the rate of decoupling of polymer bonds protecting hydration sites on the substrate.

Arslanov and Kalashnikova [80] claimed that the processes resulting in failure of an adhesive system are: diffusion of water to the interface, hydrolysis of interfacial bonds

and hydration of aluminium oxide. Water transport into the interfacial region is a necessary condition of its failure, since the separation of the adhesive from the substrate occurs due to hydrolysis of interfacial bonds and/or hydration of aluminium oxide.

Yu and Spelt [81] observed that water-filled blisters were formed during accelerated ageing experiments. The blisters grew with time, originated both in the adhesive and at the epoxy-aluminium interface, and were found only at 100% relative humidity at both 65°C and 85°C; blisters were never observed at 85% relative humidity or lower. It was proposed that the blisters grew under the influence of osmosis, originating in water clusters at microscopic voids. The existence of a blistering threshold has important implications for the selection of appropriate accelerated ageing conditions, i.e., blistering may never be encountered under actual service conditions at less than 100% relative humidity, and would be a misleading failure mechanism in accelerated testing at such high relative humidities. The possibility of a critical relative humidity in bonded joints has been investigated [82].

Brockmann *et al.* [7] proposed two models for the failure of adhesively bonded aluminium joints under the influence of moisture: one with and one without corrosion. The models differ principally by the pH value in the bondline during degradation. One degradation mechanism is the *bondline corrosion* where acidic hydrogen's attacks the area around a weakly corroded zone, and causes failure in the oxide. The bondline corrosion is dependent on the presence of bimetallic primary corrosion. The other degradation mechanism is more interesting from a practical point of view when amine-cured epoxy adhesive systems are utilised. The *alkaline failure mechanism* occurs if ammonia and low molecular weight amines set free from curing of the epoxy adhesive systems, diffuses into the oxide/polymer boundary area. If water then penetrates into the bondline an alkaline medium is produced:

$$NR_3 + H_2O \rightarrow NR_3H^+ + OH^-$$

Low molecular weight amines and ammonia can also be produced by degradation reactions in the polymer. The above-mentioned hydrolysis produces a pH greater than 8, in which aluminium oxides are unstable. Consequently, the aluminium oxide is destabilised and subject to a transformation reaction according to the dissolution:

$$Al_2O_3 + 3H_2O + 2OH^- \rightarrow 2Al(OH)_4^-$$

It has been shown that the presence of Mg oxides on the aluminium alloy surface improves the durability of joints made with dicyandiamide-cured epoxy adhesives [4,83]. The presence of Mg oxide in the aluminium oxide film is expected to improve the stability in alkaline environment due to the fact that Mg oxides are thermodynamically passive at high pH [83]. The durability properties of bonded lap shear joints made of degreased $AlMg_3$ hardly showed any signs of strength loss after storage in water at 70°C and the joints showed very good hydrolytic stability [4]. Degreased $AlMg_3$ contains approximately equal amounts of aluminium and magnesium on its surface (Al/Mg ratio 0.83). On the other hand, the aluminium oxides present on the surface of clad-$AlCuMg_2$ (Al/Mg ratio 24.1) were not stable against hydration and bonded joints exposed to water ultimately failed in the layer of hydrated aluminium oxides.

3.3.3 Strength recovery

Arslanov and co-workers [80,84-86] have observed the strength recovery of epoxy-aluminium adhesive joints exposed to water. At the initial stage of exposure to water, failure of the adhesive system occurs. The most probable failure mechanism was the hydrolysis of Al-O-C bonds and the destruction of hydrogen bonds. However, longer exposure times resulted in strength recovery of the adhesive joints. The strength recovery was explained by complete curing of the epoxy polymer at the surface and the formation of a composite region that strengthens the system. The composite consisted of epoxy polymer filled with hydroxide particles. Diffusion of metal to fairly large distances is possible during the curing of the polymers at the aluminium surfaces. This

can explain a rather large content of hydroxide in the polymer phase. The diffusion of metal ions have been suggested elsewhere [72].

3.3.4 Effect of saline solutions

Salt solutions have been shown to be much more detrimental to the performance of bonded aluminium joints than water alone [4,87-88]. So *et al.* [87] tested adhesive joints under cyclic loading in distilled water and 3 wt% NaCl solution (simulation of sea water) with temperatures from 5°C to 45°C. The fatigue tests results for joints in NaCl solution showed that the fatigue performance was greatly reduced by replacing distilled water with NaCl solution. This indicated that NaCl solution was a more aggressive reagent than water under cyclic load. Tensile testing of lap shear joints also showed that the strength was reduced after immersion in a solution of NaCl [88]. Corrosion enhanced the deterioration of these joints. The adherends were corroded around and underneath the adhesive film. It was specially observed that localised corrosion occurred at the edge of the adhesive zone. This could easily lead to development of cracks in the corroded area and reduce the joint strength.

Brémont and Brockmann [4] observed that lap shear joints exposed in salt chamber exhibited a heavily corroded zone starting from the edges of the bonded joints. Further inside the bonded joint, a bright metallic zone where the adhesive was delaminated and the metal substrate was practically not corroded. Adjacent to the previous zone, a zone where there were no visible sign of the detrimental effects of corrosion, and the failure was cohesive within the adhesive.

References

[1] G.W. Critchlow and D.M. Brewis, *Int. J. Adhesion Adhesives* **16**, 255-275 (1996)

[2] K.B. Armstrong, *Int. J. Adhesion Adhesives* **17**, 89-105 (1997)

[3] J.D. Venables, *J. Mater. Sci.* **19**, 2431-2453 (1984)

[4] M. Brémont and W. Brockmann, *J. Adhesion* **58**, 69-99 (1996)

[5] L. Kozma and I. Olefjord, *Mater. Sci. Tech.* **3**, 860-874 (1987)

[6] J.D. Venables, D.K. McNamara, J.M. Chen, T.S. Sun and R.L. Hopping, *Appl. Surface Sci.* **3**, 88-98 (1979)

[7] W. Brockmann, O.-D. Hennemann, H. Kollek and C. Matz, *Int. J. Adhesion Adhesives* **3**, 115-143 (1986)

[8] ASTM D2651, American Society for Testing and Materials, Philadelphia, PA.

[9] J.A. Marceau, in: Adhesive Bonding of Aluminum Alloys, E.W. Thrall and R.W. Shannon (Eds.), Marcel Dekker, New York, 1985. p. 51-74.

[10] P.F.A. Bijlmer, in: Adhesive Bonding of Aluminum Alloys, E.W. Thrall and R.W. Shannon (Eds.), Marcel Dekker, New York, 1985. p. 21-40.

[11] G.W. Critchlow, *Trans. IMF* **76**, B6-B10 (1998)

[12] A.V. Pocius, Adhesion and Adhesives Technology, Carl Hanser Verlag, Munich, 1997.

[13] W.P. De Wilde, G. Van Vickenroy, L. Tirry and A.H Cardon, *J. Adhesion Sci. Technol.* **9**, 149-158 (1995)

[14] A.N. Rider and D.R. Arnott, *Surf. Interface Anal.* **24**, 583-590 (1995)

[15] D.J. Arrowsmith, D.A. Moth and S.P. Rose, *Int. J. Adhesion Adhesives* **12**, 67-72 (1992)

[16] J.A. Bishopp and G.E. Thompson, *Surf. Interface Anal.* **20**, 485-494 (1993)

[17] R.P. Digby and D.E. Packham, *Int. J. Adhesion Adhesives* **15**, 61-71 (1995)

[18] N.L. Rogers, in: Adhesive Bonding of Aluminum Alloys, E.W. Thrall and R.W. Shannon (Eds.), Marcel Dekker, New York, 1985. p. 41-50.

[19] T.J. Smith, *J. Adhesion* **14**, 145-174 (1982)

[20] F. Fondeur and J.L. Koenig, *J. Adhesion* **43**, 263-271 (1993)

[21] A.F. Harris and A. Beevers, *Int. J. Adhesion Adhesives* **19**, 445-452 (1999)

[22] A.N Rider, C.L. Olsson-Jacques and D.R. Arnott, *Surf. Interface Anal.* **27**, 1055-1063 (1999)

[23] A.N. Rider and D.R. Arnott, *J. Adhesion* **75**, 203-228 (2001)

[24] R.S. Alwitt in: Oxides and Oxide Films, Vol. 4, J.W. Diggle and A.K. Vijh (Eds.), Marcel Dekker, New York, 1976. p. 169-254.

[25] A.J. Kinloch, Durability of Structural Adhesives, Elsevier Applied Science Publishers, London, 1983.

[26] A.N. Rider, *J. Adhesion Sci. Technol.* **15**, 395-422 (2001)

[27] A.N. Rider and D.R. Arnott, *Int. J. Adhesion Adhesives* **20**, 209-220 (2000)

[28] A. Strålin and T. Hjertberg, *J. Adhesion Sci. Technol.* **6**, 1233-1250 (1992)

[29] A. Strålin and T. Hjertberg, *J. Adhesion Sci. Technol.* **7**, 1211-1229 (1993)

[30] A. Strålin and T. Hjertberg, *J. Adhesion* **41**, 51-80 (1993)

[31] A. Strålin and T. Hjertberg, *J. Appl. Polym. Sci.* **49**, 511-521 (1993)

[32] M.R. Horner, F.J. Boerio and H.M. Clearfield, in: K.L. Mittal (Ed.), Silanes and Other Coupling Agents, VSP, Utrecht, 1992. p. 241-262.

[33] M.R. Rosen, *J. Coatings Tech.* **50**, 70-82 (1978)

[34] A.N. Rider, D.R. Arnott, A.R. Wilson and O. Vargas, *Mater. Sci. Forum* **189/190**, 235-240 (1995)

[35] A.J. Kinloch, *Proc. Inst. Mech. Eng.* **211(H)**, 307-335 (1997)

[36] D.R Arnott, A.R. Wilson, A.N. Rider, L.T. Lambriandis and N.G Farr, *Appl. Surface Sci.* **70/71**, 109-113 (1993)

[37] E.W. Plueddeman, Silane Coupling Agents, Plenum Press, New York, 1982.

[38] W.J. van Ooij and T. Child, *Chemtech* **28**, 26-35 (1998)

[39] W. Thiedman, F.C. Tolan, P.J. Pearce and C.E.M. Morris, *J. Adhesion* **22**, 197-210 (1987)

[40] P. Walker, *J. Adhesion Sci. Technol.* **5**, 279-305 (1991)

[41] W. Thiedman, F.C. Tolan, P.J. Pearce and C.E.M. Morris, *J. Adhesion* **22**, 197-210 (1987)

[42] D.J. Ondrus and F.J. Boerio, *J. Colloid Interface Sci.* **124**, 349-357 (1988)

[43] M. Kono, X. Sun, R. Li, K.C. Wong, K.A.R. Mitchell and T. Foster, *Surface Rev. Lett.* **8**, 43-50 (2001)

[44] V. Subramanian and W.J van Ooij, *Surface Eng.* **15**, 168-172 (1999)

[45] R.P. Digby and S.J. Shaw, *Int. J. Adhesion Adhesives* **18**, 261-264 (1998)

[46] P.R. Underhill, G. Goring and D.L. DuQuesnay, *Appl. Surface Sci.* **134**, 247-253 (1998)

[47] P.R. Underhill, G. Goring and D.L. DuQuesnay, *Int. J. Adhesion Adhesives* **18**, 307-311 (1998)

[48] P.R. Underhill, G. Goring and D.L. DuQuesnay, *Int. J. Adhesion Adhesives* **18**, 313-317 (1998)

[49] P.R. Underhill, G. Goring and D.L. DuQuesnay, *Int. J. Adhesion Adhesives* **20**, 195-199 (2000)

[50] M.-L. Abel, J.F. Watts and R.P. Digby, *Int. J. Adhesion Adhesives* **18**, 179-192 (1998)

[51] M.-L. Abel, R.P. Digby, I.W. Fletcher and J.F. Watts, *Surface Interface Anal.* **29**, 115-125 (2000)

[52] M.-L. Abel, A. Rattana and J.F. Watts, *J. Adhesion* **73**, 313-340 (2000)

[53] Y.L. Leung, M.Y Zhou, P.C. Wong and K.A.R. Mitchell, *Appl. Surface Sci.* **59**, 23-29 (1992)

[54] G.A. Woods, S. Haq, N.V. Richardson, S. Shaw, R. Digby and R. Raval, *Surface Sci.* **433-435**, 199-204 (1999)

[55] C.M Bertelsen and F.J. Boerio, *Prog. Org. Coat.* **41**, 239-246 (2001)

[56] A. Rattana, J.D. Hermes, M.-L. Abel and J.F. Watts, *Int. J. Adhesion Adhesives* **22**, 205-218 (2002)

[57] M.-L. Abel, A. Rattana and J.F. Watts, *Langmuir* **16**, 6510-6518 (2000)

[58] P. Walker, in: Silanes and Other Coupling Agents, K.L. Mittal (Ed.), VSP, Utrecht, 1992. p. 21-48.

[59] J. Marsh, L. Minel, M.-G. Barthés-Labrousse and D. Gorse, *Appl. Surface Sci.* **133**, 270-286 (1998)

[60] M.-G. Barthés-Labrousse, *J. Adhesion* **57**, 65-75 (1996)

[61] H. Bolouri, R.A. Pethrick and S. Affrossman, *Appl. Surface Sci.* **17**, 231-240 (1983)

[62] S. Affrossman, N.M.D. Brown, R.A. Pethrick, V.K. Sharma and R.J. Turner, *Appl. Surface Sci.* **16**, 469-473 (1983)

[63] S. Affrossman, R.F. Comrie and S.M. MacDonald, *J. Chem. Soc. Faraday Trans.* **94**, 289-294, (1998)

[64] C. Fauquet, P. Dubot, L. Minel, M.-G. Bartés-Labrousse, M.R. Vilar and M. Villatte, *Appl. Surface Sci.* **81**, 435-441 (1994)

[65] S. Affrossman and S.M. MacDonald, *Langmuir* **12**, 2090-2095 (1996)

[66] S. Affrossman and S.M. MacDonald, *Langmuir* **10**, 2257-2261 (1994)

[67] K. Nakamae, T. Nishino, X. Airu and S. Asaoka, *Int. J. Adhesion Adhesives* **15**, 15-20 (1995)

[68] F. Fondeur and J.L. Koenig, *Appl. Spectrosc.* **47**, 1-6 (1993)

[69] S.-H. Hong and J.-S. Tsai, *Macromol. Mater. Eng.* **276/277**, 59-65 (2000)

[70] D. Arayasantiparb, S. McKnight and M. Liberia, *J. Adhesion Sci. Technol.* **15**, 1463-1484 (2001)

[71] R.G. Dillingham and F.J. Boerio, *J. Adhesion* **24**, 315-335 (1987)

[72] S. Bentadjine, R. Petiaud, A.A. Roche and V. Massardier, *Polymer* **42**, 6271-6282 (2001)

[73] A.A. Roche, J. Bouchet and S. Bentadjine, *Int. J. Adhesion Adhesives* **22**, 431-441 (2002)

[74] F. Fondeur and J.L. Koenig, *J. Adhesion* **43**, 289-308 (1993)

[75] M.R. Bowditch, *Int. J. Adhesion and Adhesives* **16**, 73-79 (1996)

[76] B. De Nève and M.E.R. Shanahan, *Int. J. Adhesion Adhesives* **12**, 191-196 (1992)

[77] G.Z. Xiao, M. Delmar and M.E.R. Shanahan, *J. Appl. Polym. Sci.* **65**, 449-458 (1997)

[78] R.A. Pethrick, D. Hayward, K. Jeffrey, S. Affrossman and P. Wilford, *J. Mater. Sci.* **31**, 2623-2629 (1996)

[79] G.D. Davis, P.L. Whisnant and J.D. Venables, *J. Adhesion Sci. Technol.* **9**, 433-442 (1995)

[80] V.V. Arslanov and I.V. Kalashnikova, *Colloid Journal* **58**, 697-706 (1996)

[81] Y. Tu and J.K. Spelt, *J. Adhesion* **72**, 359-372 (2000)

[82] D.M. Brewis, J. Comyn, A.K. Raval and A.J. Kinloch, *Int. J. Adhesion Adhesives* **10**, 247-253 (1990)

[83] O. Lunder, B. Olsen and K. Nisancioglu, *Int. J. Adhesion Adhesives* **22**, 143-150 (2002)

[84] I.V. Kalashnikova, V.V. Matveev and V.V. Arslanov, *Colloid Journal* **58**, 722-729 (1996)

[85] V.V. Arslanov, I.V. Kalashnikova and I.A. Gagina, *Colloid Journal* **61**, 20-25 (1999)

[86] V.V. Arslanov, R.S. Vartapetyan and D.A. Ivanov, *Colloid Journal* **56**, 13-18 (1994)

[87] H.W. So, N.N.S. Chen and P.I.F. Niem, *J. Adhesion* **44**, 245-256 (1994)

[88] N.N.S. Chen, P.I.F. Niem and H.W. So, *J. Adhesion* **39**, 243-260 (1992)

Chapter 4
Experimental

The following sections give a description of the experimental techniques used in this study. A theoretical background for the different techniques is given. It is referred to the papers (see Chapters 6 to 11) for a detailed description of the experimental procedures, such as the surface pretreatment of aluminium and sample preparation.

4.1 Materials

The substrate material used in this study was extruded profiles of aluminium alloy AA6060-T6. The composition of this alloy by weight is 0.46% Mg, 0.40% Si, 0.18% Fe, 0.021% Mn, 0.002% Cu, 0.015% Zn, 0.01% Ti, Al balance [1]. The yield strength of AA6060-T6 is 190 MPa. The material used as reinforcement for the wedge test joints was extruded aluminium alloy AA7021-T1. The yield strength of AA7021-T1 is 310 MPa. Both aluminium materials were supplied by Hydro Aluminium. The adhesive used was a commercial epoxy based structural adhesive, Betamate XD4600 from Dow Automotive. The E-modulus of XD4600 is 3500 MPa.

4.2 Wedge test

The wedge test was used to determine the durability of the adhesively bonded aluminium substrates. The test was performed according to a modified version of ASTM D3762 [2], where a wedge is inserted into the bondline of a bonded aluminium specimen, thereby creating a tensile stress in the region of the crack tip. The specimen is exposed to an appropriate environment, and the resulting crack growth and failure modes are evaluated. In principle may any test conditions be used.

Wedge-style reinforced double cantilever beam (RDCB) specimens were prepared by bonding a 'sandwich' assembly consisting of two AA6060-T6 substrates and two AA7021-T1 reinforcement sheets. The RDCB geometry was chosen in order to prevent

plastic deformation of the substrates after insertion of the wedge. Each 'sandwich' assembly was prepared by bonding two pretreated AA6060-T6 substrates of dimensions 2 × 180 × 110 mm (thickness × length × width) using XD4600. An AA7021-T1 reinforcement with dimensions 6.2 × 180 × 110 mm (thickness × length × width) was bonded with XD4600 at the back of each substrate. Adhesive bonding was carried out within few hours after pretreatment in order to avoid contamination of the surface. The exception was the anodised substrates. These substrates were stored in polyethylene bags and bonded several days after pretreatment. Steel spacers of thickness 0.1 mm were used to control the thickness of the bondline between the AA6060-T6 substrates. One of the spacers was placed at the front of the substrate in order to prevent bonding of this area. This will ease the insertion of the wedge into the RDCB specimen. The substrate/reinforcement bondlines were not controlled in any way, resulting in bondline thickness around 0.05 mm.

The bonded 'sandwich' assembly was cured in an oven at 180°C for 30 min (not including oven heat-up time), held together with a number of paper clips. After curing, the assembly was cut into three RDCB specimens with correct specimen geometry according to ASTM D3762 (16.5 × 152.4 × 25.4 mm). The only exception from the ASTM standard was that specimen thickness was 16.5 mm. The cut edges were polished in order to achieve a shiny surface. A shiny surface is necessary while measuring crack length, making it easier to see the crack between the adhesive and the substrate.

Stainless steel wedges were inserted into the bondline with a tensile testing machine at a constant rate of 10 mm/min. After insertion, the RDCB specimens were stored overnight at room temperature before measurement of initial crack length and exposure to the selected test environment. Normally, a minimum of five specimens were used for each test, and the crack length was measured on both sides of each specimen using a 60× microscope. During environmental exposure the specimens were removed from the test chamber for approximately 15 min at fixed intervals for measurement of crack

length. At the end of the test period, the specimens were forcibly opened and the failure mode was evaluated.

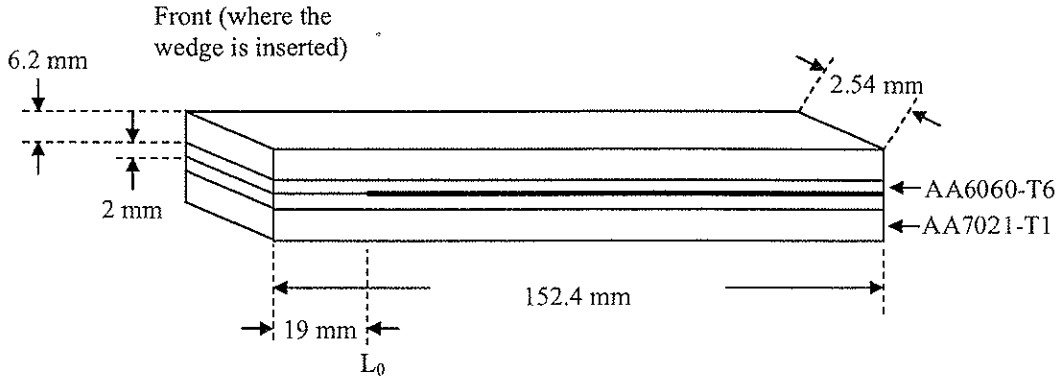

Figure 1. Schematic drawing of a RDCB specimen before insertion of the stainless steel wedge. Geometry according to ASTM D3762, with the exception for specimen thickness. Measurement of crack length starts at point L_0.

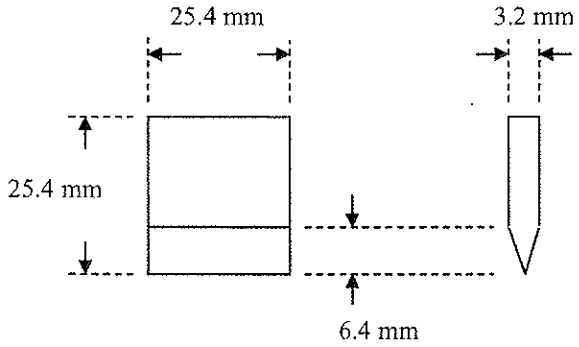

Figure 2. Schematic drawing of a stainless steel wedge.

(A)

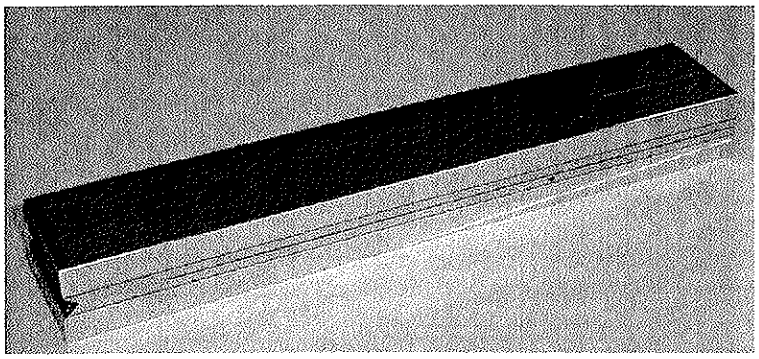

(B)

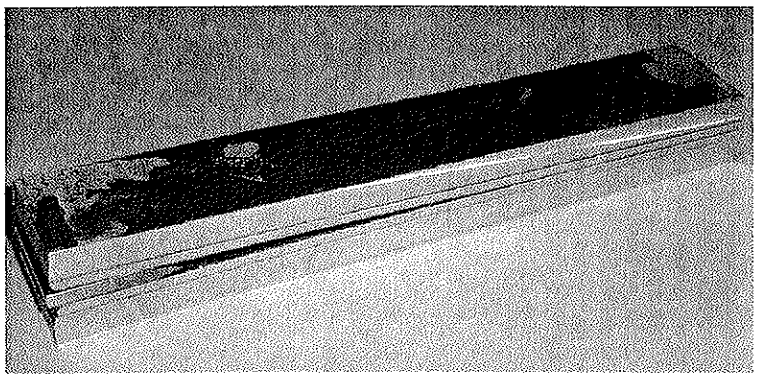

Figure 3. RDCB wedge test specimen: (A) before insertion of the wedge, and (B) after environmental testing.

4.3 Analytical techniques

4.3.1 Infrared spectroscopy

Infrared spectroscopy is an analytical tool for examination of the molecular structure of organic and inorganic compounds [3]. When infrared light is passed through a sample of an organic compound, some of the frequencies are absorbed while other frequencies are transmitted through the sample without being absorbed [4]. If the absorbance or transmittance is plotted against frequency, the result is an infrared spectrum.

Consequently, the infrared spectrum is a set of absorption bands whose intensity and frequency provides information of structure and bonding in the molecule.

The position of an absorption band can be specified in units of frequency, ν (Hz), wavelength, λ (μm), or wavenumber, $\bar{\nu}$ (cm^{-1}). Wavenumber units (cm^{-1}) are normally used. Organic applications of infrared spectroscopy are almost entirely concerned with the range 4000-650 cm^{-1}. The region of frequencies lower than 650 cm^{-1} is called the *far infrared*, and that of frequencies higher than 4000 cm^{-1} is called the *near infrared.* These regions are respectively farther from and nearer to the visible spectrum.

The vibrational frequency of two atoms joined together by a chemical bond can be calculated with reasonable accuracy, using the equation:

$$\nu = \frac{1}{2\pi}\left(\frac{k}{m_1 m_2/(m_1 + m_2)}\right)^{1/2}$$

where ν = frequency; k = the *force constant* of the bond; and m_1, m_2 = masses of the two atoms. The quantity $m_1m_2/(m_1 + m_2)$ is often expressed as μ, the *reduced mass* of the system. The vibrational frequency can be transformed to wavenumber by:

$$\bar{\nu} = \frac{\nu}{c}$$

where c = the velocity of light (3.0×10^8 m/s).

The vibrational frequency of a bond is expected to increase when the bond strength increases, and also when the reduced mass of the system decreases.

The absorbance of a sample at a particular frequency is defined as:

$$A = \log \frac{I_o}{I}$$

where I_o and I are the intensities of the light before and after interaction with the sample, respectively. Absorbance is therefore a logarithmic ratio. The transmittance of a sample is defined as:

$$T = \frac{I}{I_o}$$

For a single methylene group several vibrational modes are available, and any atom joined to two other atoms will undergo comparable vibrations (e.g. any AX_2 system such as CH_2, NH_2, NO_2 etc.). Each of the different modes may (and frequently does) give rise to different absorption bands. The stretching energy of a bond is greater than the bending energy, and stretching absorptions of a bond appear at higher frequencies in the infrared spectrum than the bending absorptions of the same bond.

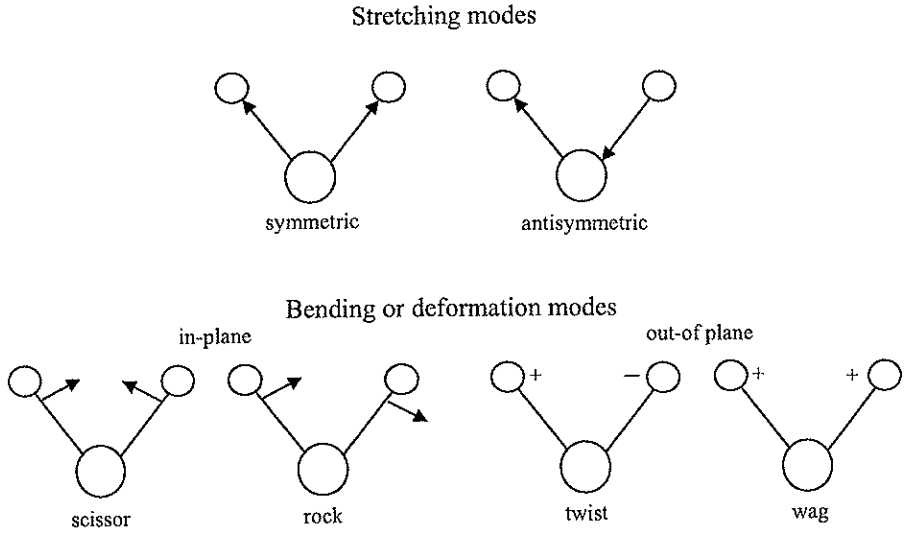

Figure 4. Vibration modes in an AX_2 group (-CH_2, -NH_2, -NO_2 etc. behave analogously).

4.3.1.1 Reflection-absorption infrared spectroscopy

The major disadvantage of infrared spectroscopy in surface analysis was for a long time its low sensitivity compared to high vacuum techniques, but this changed with the development of the Fourier transform infrared (FT-IR) instrumentation [3]. Today FT-IR instruments are suitable for surface analysis such as reflection-absorption infrared (RAIR) spectroscopy. RAIR is a technique for obtaining the infrared spectra of extremely thin films on reflecting substrates. Infrared light impinges at a certain angle on the sample deposited on the metal. The infrared light interacts with the sample and hits the reflective surface followed by a repeated interaction with the sample and reflection. For metallic substrates such as aluminium, the optimum angle of incidence is near grazing incidence. Only the parallel component of the incident infrared light will then be absorbed. Vibrational modes of the molecule which oscillate perpendicular to the surface consequently have greatest probability of absorption. The modes which oscillate parallel to the surface will not be detected.

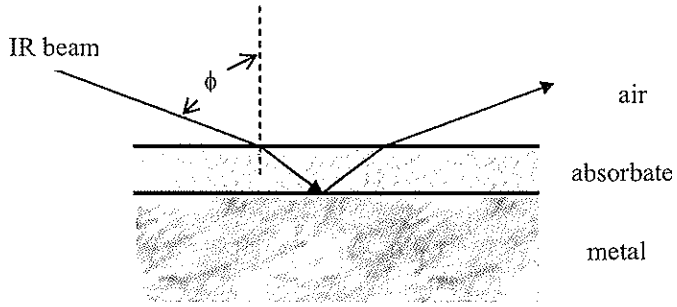

Figure 5. Principle of the reflection-absorption infrared technique. The infrared beam with incidence angle ϕ, is reflected at the metal-absorbate interface.

Aluminium specimens were investigated with reflection-absorption infrared (RAIR) spectroscopy. The analysis was performed with a Perkin Elmer 1725X FT-IR Spectrometer in case of the silane treated specimens, and a Perkin Elmer Spectrum One FT-IR Spectrometer in case of the anodised specimens. The specimens were mounted on a Spectra-Tech Specular Reflectance Model #500 external reflectance accessory, and

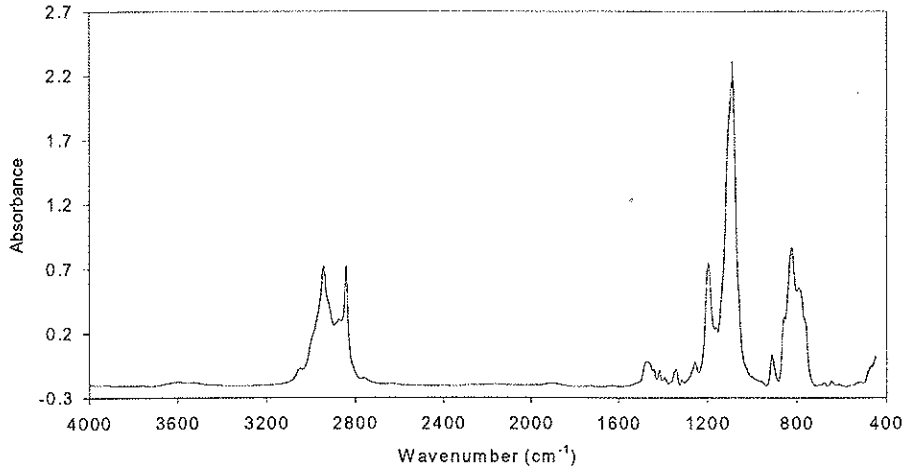

Figure 6. Example of an FT-IR spectrum: the transmission spectrum of GPS deposited on a KBr-pellet.

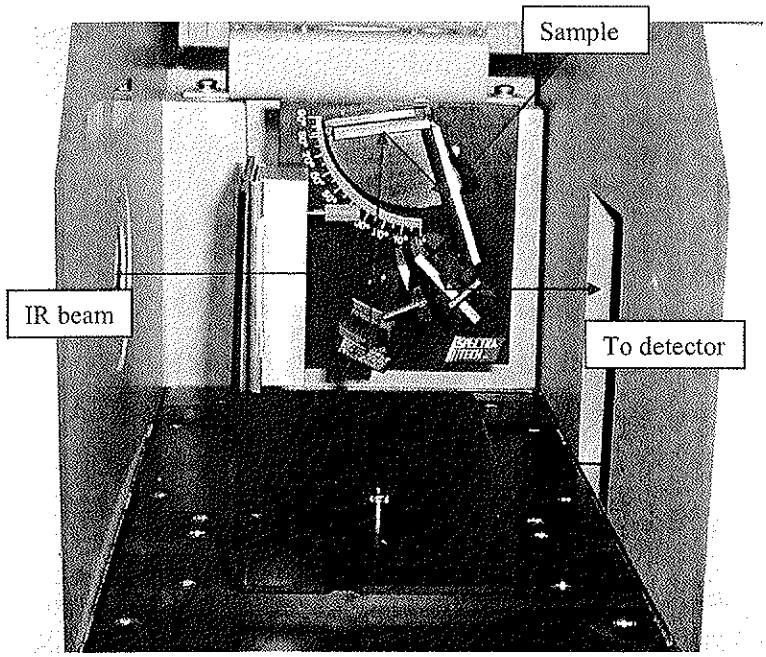

Figure 7. Picture of the external reflectance accessory mounted in the FT-IR instrument.

the spectra were normally recorded as an average of 100 scans with a resolution 4 cm^{-1} in the range 400-4000 cm^{-1} (for the anodised specimens 10 scans were averaged). The angle of the infrared beam to the normal of the specimen surface was 80° for the silane treated specimens and 60° for the anodised specimens. A bare aluminium specimen was used to obtain a background spectrum for the RAIR analysis. Transmission infrared spectra were obtained by deposition of the chemical compound on KBr-pellets. In this case normally 25 scans were averaged.

4.3.2 Scanning electron microscopy

Scanning electron microscopy (SEM) provides morphologic and topographic information about surfaces of solids [5]. The surface of a specimen to be examined is scanned with an electron beam, and the reflected beam of electrons is collected and displayed. The image that appears represents the surface features of the specimen.

The most striking feature of an SEM image is its depth of view, which gives a good topographical impression of the sample. To obtain such an image the Secondary Electron (SE) signal is used. The resolution of a modern SEM instrument is about 40 Å and the maximum useful magnification is about 10.000×. With the Back-Scattered Electron (BSE) signal one can also observe the distribution of the mean atomic number of the sample.

Elemental analysis of all elements down to atomic number 5 (B) in areas down to a few μm wide and deep can be performed with an X-ray spectrometer attached to the instrument. This makes closer investigation of interesting points/areas on the surface possible, e.g., intermetallic particles on aluminium surfaces. There are basically two types of X-ray spectrometers: Energy Dispersive (EDS or EDX) and Wavelength Dispersive (WDS or WDX). EDS is the most versatile and common system, because it allows simultaneous analysis of all elements.

Sample preparation is usually not necessary with SEM. However, electrically insulating samples must be coated with a thin layer of a conducting material in order to avoid electrically charging of the sample. The most common coating for microscopy is gold

applied by sputter coating, while coating with evaporated carbon is the most widely used light element coating.

In this study, a JEOL JSM-59000 LV scanning electron microscope was used.

4.3.3 Transmission electron microscopy

The transmission electron microscope (TEM) is an optical analogue of the ordinary light microscope where an electron beam replaces the light, and magnetic fields replace the glass lenses [6]. The magnetic lenses used in electron microscopes exhibit significant spherical and chromatic aberrations. These lenses are thus operated with very small opening angles, less than 1^{o}, and the point resolution that can be achieved with a high-performance microscope is less than 0.2 nm.

The TEM is an extremely versatile instrument that can be used on virtually any kind of sample, provided it can be made sufficiently thin to allow the electron beam to pass through without any significant energy losses. This condition in general requires samples that are less than a few hundred nanometres thick. Besides providing direct microstructural information down to atomic level at the resolution limit, the TEM is also a diffraction instrument capable of producing diffraction patterns from small well-defined areas of the sample. Furthermore, by equipping the TEM with suitable detectors it is also possible to measure analytical information associated with the various types of excitation that are induced by the incident electron beam. The most commonly used techniques are X-ray fluorescence spectroscopy and energy-loss spectroscopy.

In this study, electron transparent foils for TEM examination were prepared by ultramicrotomy. Foils with thickness ~ 75 nm were put on Cu grids and examined in a Phillips CM 30 TEM operated at 200 keV.

4.3.4 White-light interferometry

The surface topography of pretreated AA6060-T6 substrates was investigated with white-light interferometry (WLI). The common feature of most non-contact profilers is that they use light beams in some form of a microscope to obtain a surface profile [7].

The height sensitivity depends on the particular instrument and can vary from a few nm to less than 0.1 nm. The height resolution of most optical profilers is absolute because heights are measured in fractions of a known wavelength. WLI instruments are suitable for making precise measurements of surface topography [8]. The instruments divide a beam of light into a number of beams that travel unequal paths who when reunited interfere with each other creating regions of high and low intensity. This interference appears as a pattern of light and dark bands called interference fringes.

The instrument used was WYKO NT-2000 from Veeco Instruments. The instrument can be operated in two measurement modes: Vertical scanning interferometry (VSI) and Phase shifting interferometry (PSI). The VSI mode uses white light and is suitable for surfaces with roughness from 3 nm to 500 μm, e.g. aluminium surfaces, while the PSI mode uses red light and is only suitable for very smooth surfaces. The magnification range is 1.3-106.5×.

In this study the instrument was operated at the VSI instrument mode, with a magnification of 106.5×. A measurement is made in few seconds, and a number of data processing options are available for surface analysis. The lateral resolution of the instrument is lower than the resolution of a SEM, but the main advantage of the WYKO is that a good image of topography and topography parameters can be obtained

There is normally no need for sample preparation, but the grit-blasted and the sulphuric acid anodised surfaces investigated in this study were vacuum-coated with a thin layer of gold (15-20 nm) in order to increase the reflectivity of these rough surfaces.

4.3.5 X-ray photoelectron spectroscopy

X-ray photoelectron spectroscopy (XPS) is a non-destructive technique for elemental analysis of, e.g., metal and polymer surfaces. In XPS the surface is bombarded with low energy X-rays, resulting in direct emission of a photoelectron [9]. The binding energy of such a photoelectron is characteristic of the element from which it came and the way in

which that element is chemically bonded. The XPS analysis is done under ultra-high vacuum conditions to assimilate the sensitivity of the technique.

The binding energy of the electron in the solid can be determined by measurement of the kinetic energy of the photoelectron, according to the following equation [9-10]:

$$E_B = h\nu - E_{kin} - \phi$$

where E_B = binding energy of electron level; E_{kin} = kinetic energy of ejected photoelectron; $h\nu$ = characteristic energy of X-ray photon; and ϕ = work function of the spectrometer (constant).

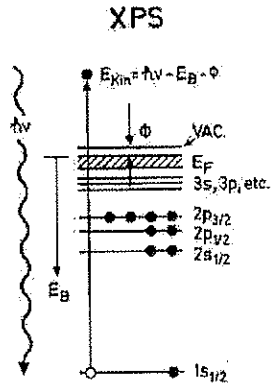

Figure 8. Schematic illustration of photoelectron emission [9].

Modern instruments are equipped with monochromators, and the radiation most commonly used is Al K_α. The main advantage of the monochromator is that the energy resolution of the recorded spectra is increased, which facilitates the interpretation. An alternative X-ray source is Mg K_α.

The main advantage of the XPS-method is possibility to determine chemical state of an element. It can be differentiated between aluminium metal atoms, Al^0, and aluminium

atoms bound to oxygen in oxide, Al^{3+}. Atoms in the Al^{3+} state will emit photoelectrons with higher binding energy than atoms in the Al^0 state. The binding energies of the oxide (metallic) states of Al 2s and Al 2p are 120.5 (118.0) eV and 75.8 (73.0) eV, respectively. The difference between the 2s and 2p binding energies is called the chemical shift.

The in-depth distribution of elements in the surface region can be determined by tilting the surface in such a way that the take-off angle of the photoelectrons is varied. An alternative way to obtain in-depth information is profiling by ion etching. The disadvantage of using this method is that ion etching of alloys may lead to selective sputtering of one of the components and thereby changes the surface composition. Ion etching can also cause phase changes of compounds, e.g., the transformation of $Al(OH)_3$ to Al_2O_3.

X-ray photoelectron spectroscopy (XPS) analysis was performed with a VG Microlab 3 instrument with Mg K_α as radiation source. The take-off angle was set at 45°. The size of the analysed area is about 1 mm^2, and the data obtained are thus the average composition in the analysed region.

4.3.6 Electron microprobe analysis

Electron microprobe analysis (EPMA) is a fully qualitative and quantitative method of non-destructive analysis of μm-size volumes at the surface of materials, with sensitivity at the level of ppm [11]. EPMA is performed by bombarding a micro-volume of a sample with a focused electron beam and collecting the X-ray photons thereby induced and emitted by various species. Because the wavelengths of these X-rays are characteristic of the emitting species, the sample composition can be easily identified by recording WDS spectra. All elements from Be to U can be analysed.

EPMA instruments are equipped with a complete kit of built-in microscopy tools that allow simultaneous X-ray (WDS or EDS), SEM and BSE imaging, plus sophisticated visible light optics which provides very flexible sample inspection with image

magnification ranging from 40 to 40.000×. EPMA usually provides much better results than standard SEM/EDS systems.

In this study, a Cameca SX100 EPMA instrument was used for analysis of AA6060-T6 surfaces.

4.3.7 Secondary ion mass spectrometry

In secondary ion mass spectrometry (SIMS) a surface is bombarded by a focused beam of primary ions (e.g. O^-, Ar^+), resulting in sputtering of the outermost atomic layers [12]. As a result secondary ion species are ejected from the surface and these secondary ions are collected as quantifiable mass spectra, as in-depth or along-surface concentration profiles, or as distribution images of the sputtered surface. The great usefulness of modern SIMS is mainly due to the unique combination of high sensitivity and good topographic resolution, both laterally (sub-micron) and in depth (down to a few atomic layers).

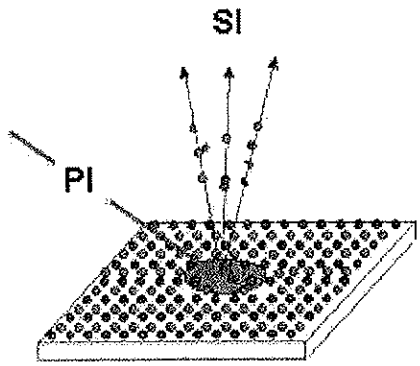

Figure 9. Schematic representation of the static SIMS principle. Large molecular ions are produced at some distance from the impact of the primary ion [11].

One may distinguish between two classes of SIMS: dynamic and static mode. Dynamic SIMS is primarily utilised for the determination of concentrations and/or topographic distributions of elements. During such analysis sputtering is continuously eroding the

specimen. Static SIMS (including the time-of-flight technique), on the other hand, is mainly directed at chemical-molecular characterisation of the outermost layers of the solid, and aspires to minimal possible erosion of the analysed surface. This mode is particularly useful in the study of organic and polymer materials.

ToF-SIMS provides very specific chemical information [13]. ToF-SIMS spectrometers provide high mass resolution, unlimited mass range and molecular imaging capabilities. This technique is also complementary to XPS for producing chemical information about surfaces. One possibility of the ToF-SIMS technique is the study of chemical interactions between aluminium surfaces and adhesives. However, the technique is very sensitive to surface contamination. Precautions should be taken in order to prepare specimens with clean surfaces.

ToF-SIMS analysis was performed with a Cameca ToF-SIMS IV instrument. A Ga gun operated at 11 keV was used as the primary ion source. The analysed area was 200×200 μm, and an Ar gun was used for sputtering.

4.3.8 Contact angle measurements

The surface energy, γ_{sv} (also designated γ below), of silanised aluminium surfaces was determined by measuring the contact angle using the sessile drop method. The measurements were performed with a NRC Contact Angle Goniometer model 100-00 from Ramè-Hart, Inc., at ambient temperature and humidity. Each measurement was averaged for ten drops of 5 μl that were placed on the surface using a micropipette.

When a drop is placed on a solid surface it may remain as a spherical drop, or spread to cover (or wet) the solid surface [14]. The angle with which the liquid subtends the solid is known as the contact angle. When wetting occurs, the contact angle is less than 90°. If the contact angle is greater than 90°, then the liquid does not wet the solid and poor adhesion between the solid surface and the liquid occurs.

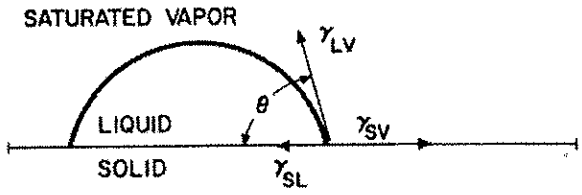

Figure 10. Contact angle equilibrium on a smooth surface [15].

The contact angle, θ, is related to the solid and liquid surface energies, γ_{sv} and γ_{lv}, and the solid/liquid interfacial energy, γ_{sl}, through the principle of virtual work expressed by the rearranged Young's equation:

$$\cos\theta = \frac{\gamma_{sv} - \gamma_{sl}}{\gamma_{lv}}$$

To achieve wetting, γ_{sv} should be large, while γ_{sl} and γ_{lv} should be small [14]. Hence, liquids of a lower surface tension will always spread over a solid surface of higher surface tension in order to reduce the total free energy of the system. This is due to the fact that the molecular adhesion between the solid and liquid is greater than the cohesion between the molecules of the liquid.

The total surface energy comprises a number of contributions from different types of force components and the total could be represented by the simple sum of these components [16]. This is often expressed as:

$$\gamma = \gamma^d + \gamma^p$$

where d represents the dispersion forces and p represents all the non-dispersion forces arising from various polar interactions. In this work the contact angle of the surfaces was determined using two test liquids: water and methylene iodide. The following

equations were used to obtain the polar and disperse components of the surfaces [15], water (subscript 1) and methylene iodide (subscript 2):

$$\gamma_1(1+\cos\theta_1) = 2\sqrt{\gamma_1^d \cdot \gamma^d} + 2\sqrt{\gamma_1^p \cdot \gamma^p}$$

$$\gamma_2(1+\cos\theta_2) = 2\sqrt{\gamma_2^d \cdot \gamma^d} + 2\sqrt{\gamma_2^p \cdot \gamma^p}$$

References

[1] O. Lunder, B. Olsen and K. Nisancioglu, *Int. J. Adhesion Adhesives* **22**, 143-150 (2002)

[2] ASTM D3762, American Society for Testing and Materials, Philadelphia, PA.

[3] J.O. Leppinen, in: Surface Characterization, D. Brune, R. Hellborg, H.J. Whitlow and O. Hunderi (Eds.), Wiley-VCH, Weinheim, 1997. p. 369-389.

[4] W. Kemp, Organic Spectroscopy, MacMillan Education, London, 1987.

[5] K. Kristiansen, in: Surface Characterization, D. Brune, R. Hellborg, H.J. Whitlow and O. Hunderi (Eds.), Wiley-VCH, Weinheim, 1997. p. 111-128.

[6] E. Johnson, in: Surface Characterization, D. Brune, R. Hellborg, H.J. Whitlow and O. Hunderi (Eds.), WILEY-VCH, Weinheim, 1997, p. 445-464.

[7] L. Mattson, in: Surface Characterization, D. Brune, R. Hellborg, H.J. Whitlow and O. Hunderi (Eds.), Wiley-VCH, Weinheim, 1997. p. 82-100.

[8] http://www.sintef.no/units/matek/2410/wyko/wykohome.htm

[9] I. Olefjord, in: Surface Characterization, D. Brune, R. Hellborg, H.J. Whitlow and O. Hunderi (Eds.), Wiley-VCH, Weinheim, 1997. p. 292-319.

[10] D. Briggs and M.P. Seah, Practical Surface Analysis; Volume 1 – Auger and X-ray Photoelectron Spectroscopy, John Wiley & Sons, New York, 1990.

[11] http://www.cameca.fr/

[12] A.R. Lodding and U.S. Södervall, in: Surface Characterization, D. Brune, R. Hellborg, H.J. Whitlow and O. Hunderi (Eds.), Wiley-VCH, Weinheim, 1997, p. 206-229.

[13] P. Bertrand and L.T. Weng, in: Surface Characterization, D. Brune, R. Hellborg, H.J. Whitlow and O. Hunderi (Eds.), Wiley-VCH, Weinheim, 1997, p. 334-353.

[14] J. Lawrence, L. Li and J.T. Spencer, Surf. Coat. Tech. **115**, 273-281 (1999)

[15] S. Wu, Polymer Interface and Adhesion, Marcel Dekker, New York, 1982.

[16] K.W. Allen, *Int. J. Adhesion Adhesives* **13**, 67-72, (1993)

Chapter 5
Summary of papers

5.1 Paper I, II and III

Organofunctional silanes are often used as coupling agents to enhance the durability of adhesively bonded aluminium joints in hydrothermal environments. The silanes will increase the density of strong bonds between the oxide and the adhesive, as well as improve the hydrolytic stability of the aluminium oxide through the formation of a crosslinked siloxane film on the surface. One of the most commonly used silanes is γ-glycidoxypropyltrimethoxysilane (GPS).

In paper I (see Chapter 6), the wedge test was used to determine the durability of adhesively bonded joints made of pretreated aluminium alloy AA6060-T6 and XD4600 one-component epoxy adhesive which was cured at 180°C. Treatment of the aluminium surfaces with a 1% aqueous solution of GPS significantly improved the durability, independent of the initial surface pretreatment. The best performance was seen by the grit-blasting + GPS pretreatment, which performed much better than the chromic-sulphuric acid based FPL-etch. In fact, under the conditions used this pretreatment performed even better than phosphoric acid anodising, which is often considered as the pretreatment giving the best obtainable durability (see Appendix). The ranking between the pretreatments was the same before and after treatment with GPS, and the silane treatment also reduced the initial crack lengths of the wedge test specimens.

The wedge test results, combined with XPS and white-light interferometry, also showed that both surface topography and hydrocarbon surface contamination have effect on durability. Increased surface roughness improves the durability, while increased surface contamination reduces the durability.

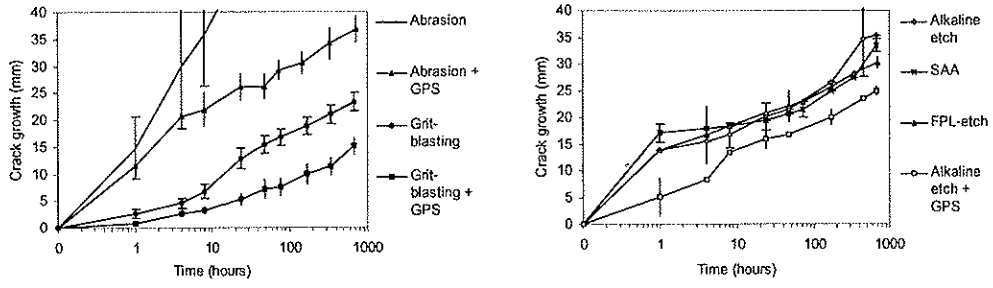

Figure 1. Durability of wedge test specimens made of pretreated AA6060-T6 at 60°C/100% r.h.

The reason for the improved durability after treatment with GPS was investigated in paper II (see Chapter 7). The chemical interaction between GPS films on aluminium and dicyandiamide (DICY), and other amines, was investigated using reflection-absorption FT-IR spectroscopy. DICY is a common curing agent used in one-component epoxy adhesives, and is also used in XD4600.

The results strongly indicated that a chemical reaction between DICY and the silane films took place. An intensity reduction of the epoxy band at 910 cm^{-1} was observed, indicating consumption of epoxy groups in the GPS film, and a new band appeared at 2190 cm^{-1} after treatment of GPS films with DICY. This latter band at 2190 cm^{-1} is indicative of the nitrile C≡N group in DICY and was assigned to the formation of a covalent bond between the curing agent and the epoxy ring of the GPS molecule. Thus, the curing agent in the epoxy resin had reacted chemically with the silane film. The curing agent will also react chemically with the epoxy resin in the formation of a polymer network, whereas the silane film is bonded to the aluminium oxide through strong AlOSi bonds. The presence of a covalent bridge between the aluminium surface and the adhesive can therefore be expected.

The formation of covalent bonds between the adhesive and the silane film are important with respect to durability of an adhesively bonded joint, as they introduce stronger bonds between the adhesive and the aluminium surface. Degradation of the bonded joint due to the effects of humid environment will then be delayed, resulting in improved

durability. The results in Paper II therefore partly explain the improved durability of GPS treated aluminium surfaces after bonding with a one-component epoxy adhesive.

The amines also catalysed the condensation of SiOH groups, and a higher degree of SiOSi crosslink density was observed.

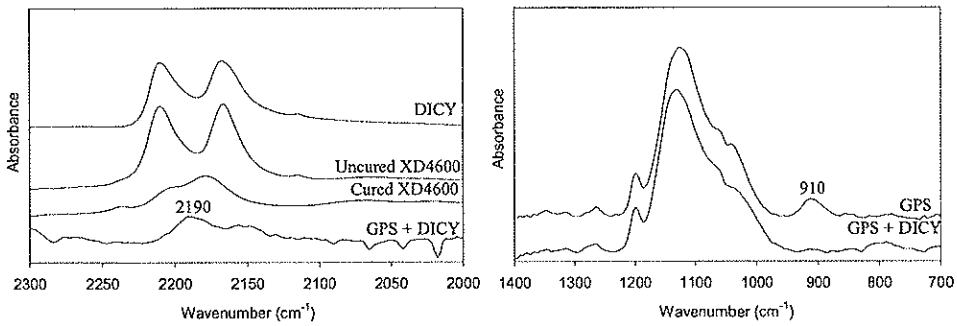

Figure 2. Reflection-absorption FT-IR spectra of GPS films on AA6060-T6, DICY curing agent on AA6060-T6, and XD4600 epoxy adhesive.

As discussed in paper II, the general understanding is that silanisation improves durability through the formation of covalent bonds between the aluminium surface and the adhesive. However, also other phenomena in the silane/adhesive interface have been reported to have effect on adhesion. Two of these are the existence of an interpenetrating network in the silane film/polymer interphase, and the compatibility of the silane film with a given adhesive.

Using silanes with and without functional groups that are chemically reactive with the epoxy adhesive, it was established that the silanes that generated the most hydrophobic surfaces performed best in wedge tests in paper III (see Chapter 8). This trend occurred independently of the ability of the silane to form covalent bonds with the adhesive. Clearly, chemical reaction was not necessary for improved durability after silanisation. A hydrophobic surface can to some extent prevent water from entering the aluminium-adhesive interface. Less water present at the surface can improve durability because the

presence of water at the crack tip is a prerequisite for the crack growth observed in wedge tests.

In paper III, it was also observed a significant difference in durability between alkaline etched surfaces that were either desmutted in concentrated nitric acid or non-desmutted. The non-desmutted surface performed better. Desmutting removes a 'smut' layer rich in magnesium oxides which are thermodynamically passive at high pH. Since epoxy adhesives are alkaline of nature, the presence of magnesium oxides on the surface is expected to improve the stability of the surface. This will also have effect on the stability of the alkaline etched and non-desmutted aluminium surfaces discussed in the next section.

5.2 Paper IV

Two models for the failure of adhesively bonded aluminium joints under the influence of moisture has been proposed earlier: one with and another without corrosion. One of the degradation mechanisms suggests that amines in the epoxy adhesive result in an alkaline environment in the polymer/oxide interphase. Consequently, the aluminium oxide is destabilised and dissolved. In the other degradation mechanism, corrosion results in an acidic environment.

In order to investigate the effect of pH on GPS treated surfaces, specimens were exposed to aqueous solutions of different pH at 40°C in paper IV (see Chapter 9). The degradation of the silane films were investigated using reflection-absorption FT-IR spectroscopy. The durability of adhesively bonded aluminium joints was investigated by exposing wedge test specimens to similar solutions. Particularly, the effect of an alkaline environment was of interest since the amine-cured XD4600 epoxy adhesive was used for bonding.

The GPS films behaved differently in acidic, neutral and alkaline environments. At pH 4, the silane was desorbed from the surface. The same trend was observed at a much

slower rate at pH 7, while the silane film was stable at pH 8. The stability of the silane film depended on the stability of the silane film itself and/or the stability of the underlying aluminium surface. The siloxane network may be rehydrolysed in acidic environments, but it is stable in alkaline environments. Also, the aluminium surface was much more stable in alkaline environment. In acidic solution, etching of the surface took place. The durability of wedge test joints was significantly reduced at very low pH (pH 2), and a trend of increasing durability with increasing pH was observed.

Two models for the degradation of the GPS treated aluminium surface in acidic environment were proposed: one involving simultaneously hydrolysis of the siloxane network and corrosion of the underlying aluminium surface, and one involving only corrosion of the aluminium surface.

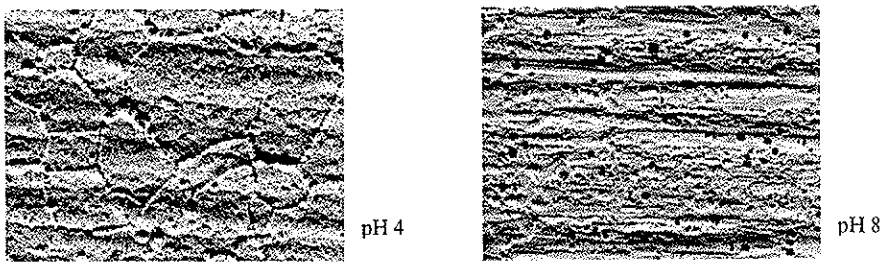

Figure 3. Scanning electron micrographs of bare AA6060-T6 surfaces exposed to buffer solutions at 40°C.

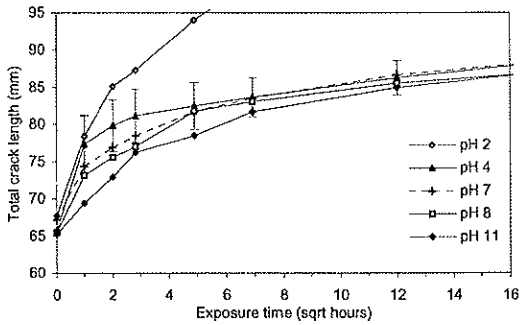

Figure 4. Durability of wedge test specimens made of GPS treated AA6060-T6. The specimens were immersed into solutions of different pH at 40°C.

5.3 Paper V and VI

In paper I, it was shown that silanisation of aluminium with GPS results in excellent durability. However, from paper IV and from the literature it was established that silanisation with GPS does not give good corrosion protection. The remaining work was therefore focused on anodising pretreatments, which have a greater potential as the sole pretreatment system for, e.g., automotive parts.

In paper V (see Chapter 10), the durability of anodised aluminium alloy AA6060-T6 bonded with XD4600 was investigated at 40°C/96% RH. The results showed that AC anodising in hot phosphoric and sulphuric acid solutions performed very well, almost as good as the well-established FPL + DC-PAA pretreatment. These three anodising processes performed significantly better than the DC-SAA process. The FPL + DC-PAA and DC-SAA pretreatments are used by the aerospace and automotive industry, respectively. However, they are quite expensive processes, whereas the AC anodising pretreatments produce thinner oxide films, are quicker and less expensive processes. They also avoid the use of toxic hexavalent chromium.

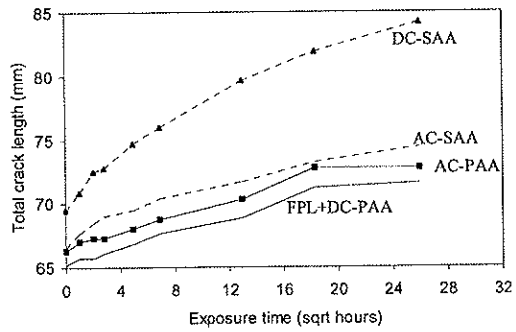

Figure 5. Durability of wedge test joints made of anodised aluminium alloy AA6060-T6 bonded with XD4600 epoxy adhesive. Exposure conditions were 40°C/96% r.h.

Sealing of the DC-SAA and AC-SAA substrates in boiling water significantly reduced the durability.

Reflection-absorption FT-IR spectroscopy showed that the DC-SAA and AC-SAA oxides contained significant amounts of sulphate. Sulphates can absorb relatively large amounts of water, and this can have a significant effect on the long-term properties of bonded joints. FT-IR spectroscopy also showed that water was released from and driven out of the oxides during curing of the adhesive at 180°C. The observations suggested that a transformation from the hydroxide, $Al(OH)_x$, to the oxide, Al_2O_3, state took place.

The effect of water in the anodic oxide film was more thoroughly investigated in paper VI (see Chapter 11). Anodised AA6006-T6 substrates were conditioned in environments of different relative humidities prior to adhesive bonding with XD4600. The thick oxide film (8 μm) produced by the DC-SAA process, was compared with the thinner oxide film (0.2 μm) of the AC-SAA process. The aluminium sulphate in these oxides to a large extent controls the amount of water present.

Pre-bond humidity was shown to have effect on the crack growth resistance of wedge test joints at 40°C/96% r.h. The difference was significant for DC-SAA substrates bonded in dry and wet environments. Adhesive bonding at 85% r.h. gave a large decrease in crack growth resistance compared with joints bonded at 45% r.h. The differences were much smaller between AC-SAA substrates, but adhesive bonding in very wet (85% r.h.) and very dry (11% r.h.) environments resulted in reduced crack growth resistance compared with 33 and 52% r.h. In joints bonded at 85% r.h., significant blister formation in the adhesive bondline was observed, and it was claimed that extensive blister formation may have a significant effect on the behaviour of the joints bonded joints. The blister formation is connected to the release of water from the conditioned adhesive and oxide films during curing of the adhesive.

The dehydration of the oxide during heating to 180°C at curing seems to have effect on the structure of the adhesive close to the oxide surface. Cross-sections of specimens bonded in wet and dry environments were investigated using TEM. Close to the oxide surfaces bonded at 85% r.h., a relatively structure free zone with very little thixotropic agent was observed. The range of this zone was about 200 nm. No such zone was observed in specimens bonded at 11% r.h. The thixotropic agent consists of silica which

is hydrophobic of nature. This silica may then be evicted from the oxide surface when water is desorbed from the oxide during curing of the adhesive.

(A) AC-SAA 85% r.h. (B) AC-SAA 11% r.h.

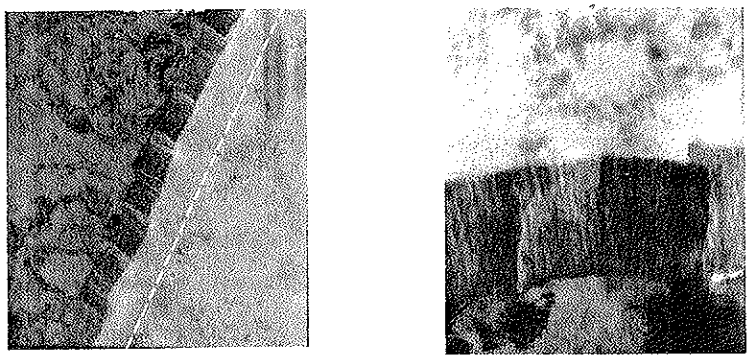

Figure 6. TEM cross-sections of AC-SAA oxides on aluminium alloy AA6060-T6 bonded with XD4600 epoxy adhesive at: (A) 85 and (B) 11% r.h.

No indications of adhesive penetration into the oxide pores could be seen in any of the specimens investigated.

Chapter 6

Silanisation of adhesively bonded aluminium alloy AA6060 with γ-glycidoxypropyltrimethoxysilane. I. Durability investigation

Bernt B. Johnsen, Kjell Olafsen, Aage Stori, Kristin Vinje

J. Adhesion Sci. Technol. **16**, 1931-1948 (2002)

Abstract

The wedge test was used to determine the durability of adhesively bonded joints of pretreated aluminium alloy AA6060 in a hydrothermal environment. Testing of joints bonded with the one-component epoxy adhesive XD4600 showed that the durability was higher for surfaces that were grit-blasted with alumina than for alkaline etched, FPL-etched, and sulphuric acid anodised surfaces. All these surfaces performed much better than those abraded with ScotchBrite®. It was discovered that increased surface roughness improved the durability, while increased surface contamination reduced the durability of the bonded joints. On a very rough surface such as the grit-blasted, the effects of surface contamination were more than outweighed by the effects of surface roughness. Treatment of some of the pretreated surfaces with a 1% aqueous solution of γ-glycidoxypropyltrimethoxysilane significantly improved the durability, but the ranking between the pretreatments was the same as before the silane treatment. The silane treatment also reduced the initial crack lengths of the wedge test specimens. The best performance was seen by the grit-blasting plus silane treatment, which performed much better than the well-established FPL-etch.

Keywords: Adhesively bonded joints; Aluminium adherend; Epoxy adhesive; Surface pretreatment; γ-Glycidoxypropyltrimethoxysilane; Wedge test; Durability.

6.1 Introduction

Adhesives have been used for many years in aerospace applications, where high durability bonded aluminium structures are obtained by using adhesives based on phenolic or epoxy resins [1]. Adhesives are currently also used in many areas in the manufacture of automobiles, but so far the use of adhesives in structural applications has been very limited. A major reason for the limited use of adhesives in structural automotive applications is the concern about the fatigue and durability behaviour of these components. The adhesive joints must perform satisfactorily under service conditions that include dynamically applied loads and exposure to hostile environments such as water and road salt [2]. Unfortunately, water is one of the most hostile environments for adhesive joints. It is, therefore, necessary to use expensive surface pretreatment processes to obtain the required long-term service life of the joints [3].

The strength and durability of adhesively bonded aluminium joints partly depend on the adhesive and partly on the metal and its surface pretreatment [4]. Hence, the pretreatment of aluminium in order to improve adhesion has been the subject of much research. A diverse range of mechanical, chemical and electrochemical pretreatments have been developed [5], and all these pretreatments may be combined with a range of chemical 'add-ons', such as primers, coupling agents or hydration inhibitors to stabilise the surface during storage or to further enhance bond durability [6].

Organofunctional silanes are widely used as coupling agents to enhance the durability of adhesive joints during exposure to moisture at elevated temperature [7]. According to Rider *et al.* [8] a silane coupling agent will perform two functions in order to improve the environmental durability of a bonded joint. Firstly, it will increase the density of strong bonds between the oxide and the adhesive. Secondly, it will improve the hydrolytic stability of the aluminium oxide. Formation of a weak hydrated layer on the aluminium surface is significantly hindered by the formation of a cross-linked multilayer film [3,9-10].

One of the most commonly used silanes is γ-glycidoxypropyltrimethoxysilane (GPS). The treatment of aluminium surfaces with aqueous solutions of GPS before adhesive bonding has been shown to improve bond durability after initial surface pretreatments such as, e.g., abrasion, grit-blasting and the FPL etch [9-13]. Several different surface characterisation techniques have been used to investigate the deposition of and the films formed by GPS on aluminium surfaces, including reflection absorption infrared (RAIR) spectroscopy, X-ray photoelectron spectroscopy (XPS) and time-of-flight secondary ion mass spectrometry (ToF-SIMS) [14-26].

In this paper the durability of an adhesively bonded system (aluminium alloy and adhesive) which is of particular interest to the automotive industry is reported. The aluminium alloy AA6060 is used by the automotive industry due to its good mechanical properties and corrosion resistance. The adhesive used for bonding of the AA6060 substrates was XD4600, which is a one-component epoxy paste cured at high temperature. The effect of several different surface pretreatments on durability was determined using a modified version of the Boeing wedge test. Common pretreatments like abrasion, grit-blasting and the FPL etch, in addition to alkaline etching and sulphuric acid anodisation (SAA) were tested. The SAA pretreatment is of great interest to the automotive industry, whereas phosphoric acid and chromic acid anodisation are of greater interest to the aerospace industry. Alkaline etching is normally used as an initial step in a pretreatment procedure, such as in SAA, in order to remove the upper surface layer of the alloy. The aluminium surfaces were characterised prior to bonding using X-ray photoelectron spectroscopy for the determination of surface composition and with white-light interferometry (WLI) for the determination of surface topography. Some of the pretreated surfaces were further treated with GPS and the durability was determined.

This, and a following paper [27], report and discuss the effect of using GPS on the stability of bond strength between an epoxy adhesive and a pretreated aluminium substrate.

6.2 Experimental

6.2.1 Materials

A one-component structural epoxy adhesive, XD4600 from Gurit-Essex, Nuneaton Warwickshire, UK, was used for adhesive bonding of all aluminium specimens. The substrate material used in this study was aluminium alloy AA6060-T6. The chemical composition of this alloy (in wt%) is; Mg 0.50, Si 0.40, Fe 0.18, Mn 0.02, others < 0.02 and balance Al. The material used as reinforcement for the wedge test specimens was extruded aluminium alloy AA7021-T1. Both aluminium materials were supplied by Hydro Aluminium, Tønder, Denmark. Both the adhesive and the aluminium alloy used as substrate material were chosen because they are of particular interest to the automotive industry. γ-Glycidoxypropyltrimethoxysilane (GPS) was obtained from Witco Europe SA (trade name: Silquest A-187). Almeco 18, used for mild alkaline degrease, was obtained from Henkel, and 0.21-0.30 mm alumina grit was supplied by Clemco Norge AS, Oslo, Norway.

6.2.2 Surface pretreatment procedures

The extruded AA6060 substrates were pretreated in several different ways before adhesive bonding. The pretreatment procedures are given in Table 1. Silanisation of the pretreated aluminium substrates was performed in a 1 wt% solution of GPS in distilled water. The pH of the solution was adjusted to 5.0 using acetic acid, and the solution was then continuously stirred for 60 min at ambient temperature, using a magnetic stirrer, for hydrolysis of the silane methoxy groups. The silane was then deposited on the aluminium substrates by immersing them in the solution for 10 min, after which they were dried at 93°C for 60 min.

6.2.3 Bond preparation and environmental testing

Wedge-style reinforced double cantilever beam (RDCB) specimens were prepared for environmental testing. The RDCB geometry was chosen in order to prevent plastic deformation of the substrates after insertion of the wedge. The RDCB geometry is also used in cyclic fatigue tests. Two 110 mm wide AA6060 substrates with thickness 2 mm

Table 1
Pretreatment procedures applied to the extruded AA6060 aluminium substrate before bonding with structural epoxy adhesive

Pretreatment	Aluminium substrate pretreatment procedure
A. Abrasion	1. Solvent degrease with a paper tissue soaked in acetone 2. Abrasion with ScotchBrite® scouring pad 3. Solvent degrease with a paper tissue soaked in acetone
B. Grit-blasting	1. Solvent degrease with a paper tissue soaked in acetone 2. Grit-blast with 0.21-0.30 mm sharp edged alumina grit 3. Blow off residual grit with N_2 gas 4. Rinse with acetone
C. Alkaline etch	1. Solvent degrease with a paper tissue soaked in acetone 2. Mild alkaline degrease in 50 g/l Almeco 18 at 70°C for 5 min 3. Alkaline etch in 5 wt% NaOH at 60°C for 100 s 4. Immerse in 1 wt% HNO_3 at room temperature for 5 min 5. Immerse in water at room temperature for 10 min 6. Dry at 120°C for 15 min
D. FPL-etch	1. Solvent degrease with a paper tissue soaked in acetone 2. Mild alkaline degrease in 50 g/l Almeco 18 at 70°C for 5 min 3. FPL-etch according to ASTM D 2651-90 4. Immerse in water at room temperature for 15 min 5. Dry at 120°C for 15 min
E. Anodising in sulphuric acid	1. Alkaline etch in NaOH 2. Desmut in H_2SO_4 3. Anodising in H_2SO_4 4. Sealing in boiling water
F. Silanisation	As A, B or C above followed by treatment with GPS (see text)

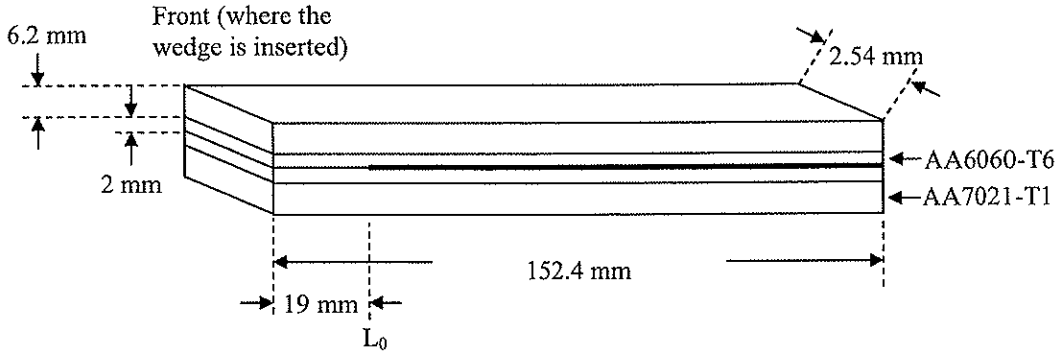

Figure 1. Schematic drawing of a reinforced double cantilever beam (RDCB) specimen seen from the side before insertion of the stainless steel wedge. Bondline thickness is 0.1 mm. Measurement of initial crack length starts at point L_0.

were bonded with XD4600, and a reinforcement made of AA7021 with thickness 6.2 mm was bonded with XD4600 at the back of each substrate. Steel spacers of thickness 0.1 mm were used to control the thickness of the bondline between the AA6060 substrates. The substrate/reinforcement bondlines were not controlled, resulting in bondline thicknesses around 0.05 mm. The bonded 'sandwich' assembly was cured in an oven at 180°C for 30 min. After curing, this 'sandwich' assembly was cut into three RDCB specimens with correct specimen geometry according to ASTM D 3762-79. The only exception from the standard was that specimen thickness was 16.5 mm. Fig. 1 gives a schematic drawing of an RDCB specimen.

Stainless steel wedges were inserted into the bondline with a tensile testing machine at a constant rate of 10 mm/min, in order to introduce a highly stressed crack tip region. After insertion of the wedges, the RDCB specimens were stored overnight at room temperature before measurement of initial crack length. Environmental testing was performed in a humid atmosphere (close to 100% relative humidity) at 60°C. During testing the specimens were resting on a Teflon grid in a beaker placed in an oven at 60°C. The vapour phase was created by liquid water at the bottom of the beaker, and the specimens were not in direct contact with this liquid water phase. Crack growth, as a result of environmental exposure, was measured at fixed intervals. A minimum of five specimens were used for each test, and crack growth was measured on both sides of each specimen. It took approximately six minutes for the atmosphere in the test beaker to re-establish itself after each measurement.

The durability of adhesively bonded joints determined by the wedge test is normally given in terms of crack growth beyond the initial crack length as a function of time in test environment. There is, however, some disadvantage in using this type of presentation only, since it does not take into account the variations in initial crack length (bond strength). As the initial crack length increases, the 'driving' force for further crack growth decreases. For example, a pretreatment giving short crack growth may misleadingly be interpreted to exhibit good durability properties if the initial crack length was long. According to Digby and Packham [4], the calculation of strain energy release rate (G_I) provides a more complete picture, because it includes information

about the strength of the initial bond. The following equation was used for the calculation of the strain energy release rate:

$$G_1 = \frac{3Ed^2h^3}{16(a+0.6h)^4},$$

where G_I = mode I strain energy release rate; E = Young's modulus; d = displacement of the load point (thickness of the wedge); h = specimen thickness; a = crack length; and 0.6 = geometric correction factor.

This equation is used for a purely comparative analysis only, and the calculated values of strain energy release rate should not be regarded as the 'real' values of strain energy release rate.

6.2.4 Surface characterisation

The surface topography of the differently pretreated AA6060 substrates was investigated with white-light interferometry (WLI). The instrument used was WYKO NT-2000 from Veeco Instruments, which was operated at the VSI instrument mode. The vertical resolution of the VSI mode is 3 nm. A magnification of 106.5× was used for all measurements. X-ray photoelectron spectroscopy (XPS) analysis was performed with a VG Microlab 3 instrument with Mg K_α as radiation source. The take-off angle was set at 45°. The analysed surfaces were pretreated according to the schedule given in Table 1, but the as-received and sulphuric acid anodised surfaces were also rinsed with acetone before analysis.

6.3 Results and discussion

6.3.1 Environmental testing of RDCB wedge test specimens

Environmental testing of abraded, grit-blasted, FPL-etched, alkaline etched or sulphuric acid anodised RDCB wedge test specimens showed that grit-blasting resulted in higher durability than all other pretreatments tested. Figs 2 and 3 also show that abrasion with

ScotchBrite® resulted in very poor durability. In fact, several of the specimens fell apart after 48 h of environmental exposure. Not only did abrasion give high crack growth, but also the initial crack length was high, giving a low initial value of strain energy release rate (G_I). The standard deviation of the abraded specimens was high, up to 20 times higher than for specimens giving good durability.

Images of the pretreated surfaces obtained by WLI (see Fig. 4) show that abrasion removed the longitudinal lines of the extruded material, indicating that some μm of the surface was removed. After abrasion it was possible to see in which direction the abrasion was performed, because the surface was covered with elongated furrows in the direction of the abrasion (also reported elsewhere [10]). The XPS results, shown in Table 2, revealed that 33.1 atomic% carbon was present on the surface after degreasing by acetone. This contamination can have effect on the durability by preventing the adhesive from interacting with the sites at the surface, thus resulting in poor adhesion.

Table 2
Surface composition (in atomic%) of as-received and pretreated AA6060 surfaces determined by X-ray photoelectron spectroscopy analysis prior to bonding

Element	AA6060 (as-received)	Abrasion	Grit-blasting	FPL-etch	Alkaline etch	SAA
Al(0)	2.5	10.4	3.8	7.2	4.3	-
Al(III)	1.7	19.3	21.6	25.3	27.4	14.4
C	58.0	33.1	31.8	16.4	14.9	41.0
O	36.7	37.2	42.8	51.0	53.4	42.4
Mg	1.1	-	-	-	-	-
N	-	-	-	-	-	2.1
Al(III)/O	0.05	0.52	0.50	0.50	0.51	0.34
Al(III)/Al(0)	0.68	1.86	5.68	3.51	6.37	-

SAA – sulphuric acid anodising.

The durabilities of the FPL-etched, alkaline etched and sulphuric acid anodised specimens were all of the same order, with fairly good durability. Although there were some differences in the initial crack lengths, the values of G_I almost approached the same levels within a few hours of environmental testing. It is very difficult to give any internal ranking to the performance of these three pretreatments, but the alkaline etch

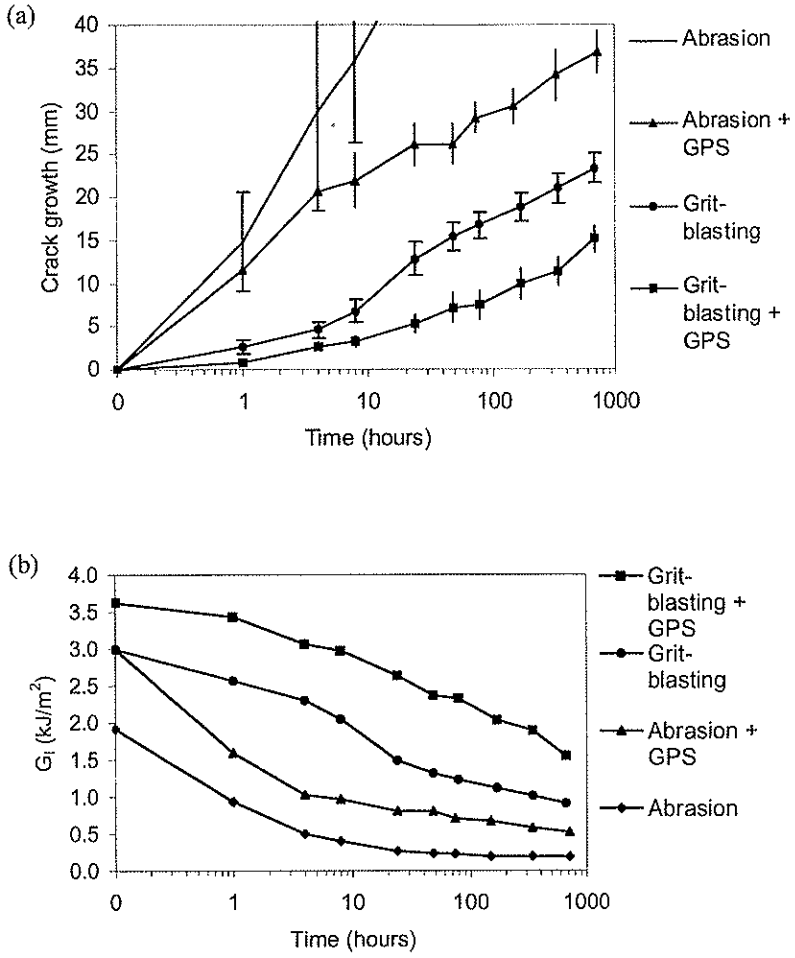

Figure 2. Durability of abraded, abraded and silanised, grit-blasted, and grit-blasted and silanised RDCB wedge test specimens in 60°C/100% r.h.: (a) crack growth and (b) strain energy release rate (G_i).

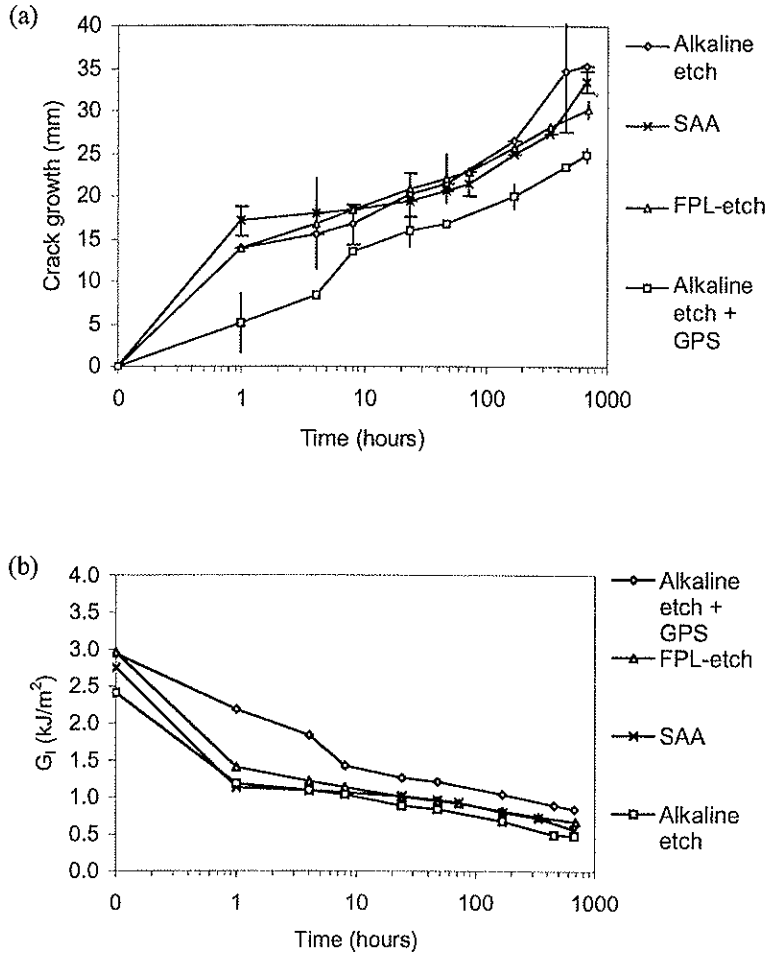

Figure 3. Durability of alkaline etched, alkaline etched and silanised, FPL-etched, and sulphuric acid anodised (SAA) RDCB wedge test specimens in 60°C/100% r.h.: (a) crack growth and (b) strain energy release rate (G_I).

pretreatment seemed to perform more poorly than the FPL etch and sulphuric acid anodising pretreatments. The alkaline etched specimens also gave a much higher standard deviation, indicating low reproducibility. The standard deviation of the sulphuric acid anodised specimens was low, indicating that anodisation gave a very reproducible surface. The standard deviation of the FPL-etched specimens was initially large, but decreased to a value similar to that of the anodised specimens.

Both etching processes resulted in a surface where the grain boundaries of the alloy were clearly visible, but etching did not remove the characteristic longitudinal lines of the extruded material (see Fig. 4d-e). The grain boundaries were more distinctive on the alkaline etched surface, and the surface seemed to be more etched than the FPL-etched surface. On the alkaline etched surface it could also be observed that etching around intermetallic surface particles had occurred, leading to the formation of small pits. Weight measurements before and after alkaline etching indicated that this process removed an upper surface layer of about 5 μm thickness. The amounts of carbon residues on the two etched surfaces were much lower than on the abraded surface. The amount of carbon on the FPL-etched and alkaline etched surfaces were 16.4, and 14.9 atomic% respectively, while the carbon content on the abraded surface was 33.1 atomic%. This is probably a contributing factor to the higher durability of the etched surfaces.

Grit-blasting with alumina gave good durability and low standard deviation, although a carbon content of 31.8 atomic% was almost equal to that of the abraded surface. As can be seen from Figs 2 and 3, the difference in durability between grit-blasting and the other pretreatments was significant during the first 48 h of the test. The value of G_I was initially high, and was maintained at a rather high level during the initial period of the test. This indicates that it took longer time for water to degrade the grit-blasted specimens. After a while the value of G_I decreased, but it never approached the values obtained with other pretreatments.

Grit-blasting produced a much rougher surface than the other pretreatments. Descriptions of the surface topography parameters measured by WLI are given in Table

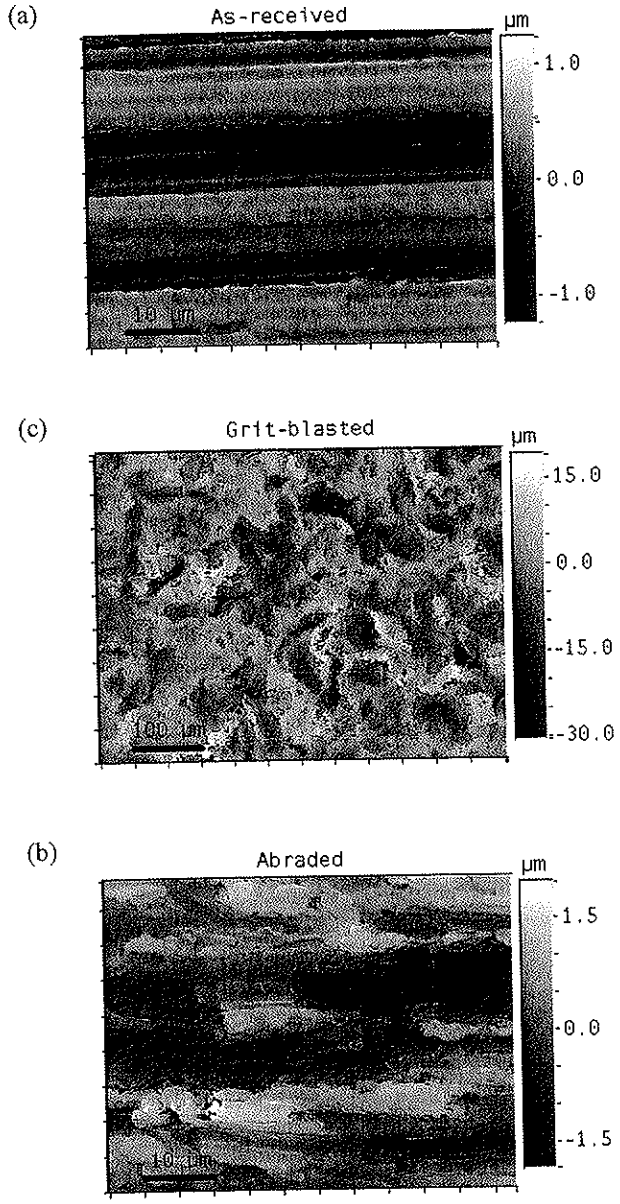

Figure 4. White-light interferometry pictures of AA6060 surfaces: (a) as-received, (b) abraded, (c) grit-blasted, (d) alkaline etched, (e) FPL-etched and (f) sulphuric acid anodised.

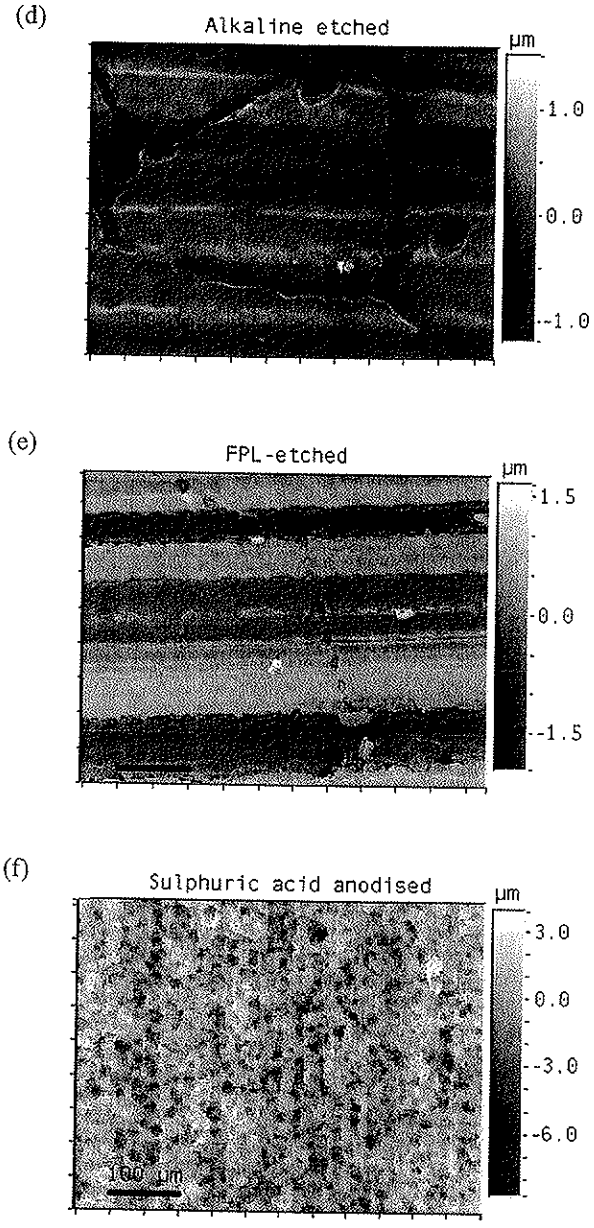

Figure 4. (cont.)

3. As can be seen from Table 4, the surface topography parameters indicated that the grit-blasted surface had much more 'extreme' topography than, e.g., the abraded surface. The increased surface area makes more sites available for interaction between the surface and the adhesive. An increased number of interfacial bonds means that an increased number of bonds must be broken by water for the crack to propagate in the interface.

Table 3
Description of surface topography parameters measured by white-light interferometry

Surface topography parameter	Definition
R_a	*Roughness average*, is the mean height as calculated over the entire measured array
R_t	*Maximum height of the profile*, is the vertical distance between the highest and lowest points of the surface
Surface area index	The ratio of the surface area to the area of an ideal plane

Table 4
Surface topography parameters of pretreated surfaces determined by white-light interferometry analysis prior to bonding

Pretreatment	AA6060 (as-received)	Abrasion	Grit-blasting	FPL-etch	Alkaline etch	SAA
R_a (μm)	0.22	0.93	4.44	0.57	0.60	0.98
R_t (μm)	2.24	8.11	35.95	5.44	5.36	10.33
Surface area index	1.03	1.16	3.06	1.09	1.14	1.95

SAA – sulphuric acid anodising.

It has been shown by Venables [28] that the microroughness of the surface has an effect on the durability of adhesively bonded aluminium. The pore structures formed by the phosphoric acid and chromic acid anodising processes increase the durability compared with, e.g., the FPL etch. Although microroughness obviously is important with respect to durability, the macroroughness can also have a significant effect. Rider *et al.* [29] showed this in experiments with a flat surface and a surface with 'extreme' topography

of equal surface composition. The increase in surface area was only 1.5 fold, but the fracture toughness improved by two orders of magnitude. The authors proposed that a rough surface would lead to higher stress intensity at the peaks than in the hollows. The density of micro-cavities (where diffusion of water can take place) may then be significant only in the region of the peaks of a roughened surface.

A high degree of contamination on the surface can result in the formation of a high density of micro-cavities between the surface and the adhesive. The carbon content on the grit-blasted surface was equivalent to the carbon content on the abraded surface, but dramatic differences in durability were observed. It seems that contamination is of major importance on the relatively flat abraded surface, but of minor importance on the rough grit-blasted surface. This supports the statement by Rider *et al.* [29] that the presence of micro-cavities in the hollows of a rough surface is of lesser importance than the presence of such micro-cavities at the peaks.

Fig. 5 shows scanning electron micrographs of the crack growth area of grit-blasted and alkaline etched wedge test joints. These surfaces gave good and medium durabilities, respectively. The dark areas in the figure represent adhesive that is present on the aluminium side of the fracture. On the alkaline etched surface the failure was almost purely interfacial, with only a few areas of cohesive failure (one of these areas is shown in Fig. 5b). However, adhesive was more or less evenly distributed on the grit-blasted surface. Thus, it seems that a substantial part of the failure on the grit-blasted surface in our study was cohesive within the adhesive. This behaviour could not be observed for any of the other surfaces. If high stress intensities at the peaks of the surface in some areas forces the crack to grow into the adhesive, this will increase the durability. Crack growth in the adhesive is dependent on the rate of hydrolysis of the polymer, a process that normally takes longer time than desorption of the polymer from the surface. Another factor that may have effect on the durability of a rough surface is mechanical interlocking of the adhesive. This will also increase the durability of the bonded surface.

(a)

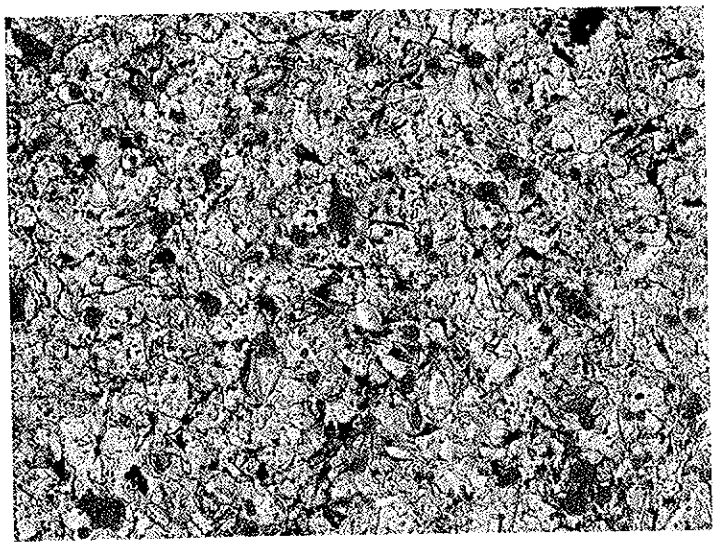

(b)

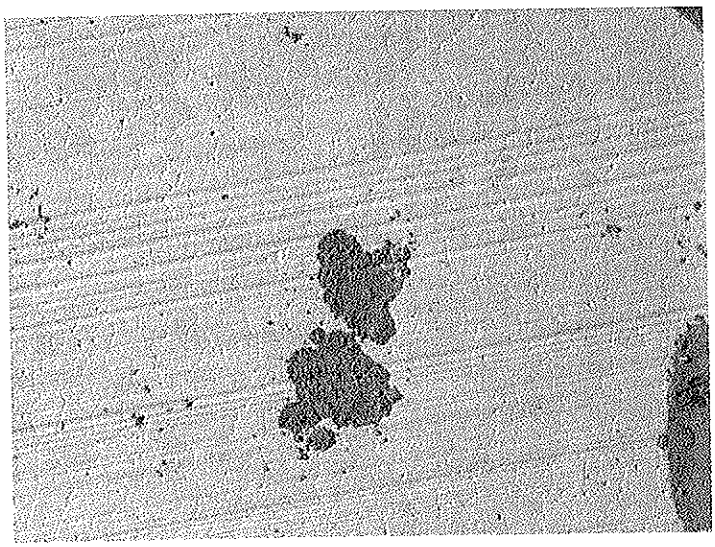

Figure 5. Scanning electron micrographs of the crack growth areas of RDCB wedge test joints: (a) grit-blasted and (b) alkaline etched. Magnification is 100×.

The anodising process also created a surface with larger surface area, but the anodised surface was much 'smoother' than the grit-blasted surface and the effects of higher stress intensity or mechanical interlocking will not occur on this surface.

6.3.2 *Effect of treatment with GPS*

Substrates which had been abraded, grit-blasted and alkaline etched were treated with GPS. It was observed that treatment with GPS significantly increased the durability. Figs 2 and 3 show that the crack growth reduced, and that the values of strain energy release rate increased, after the silane treatment. This indicates that it took longer time for water to hydrolyse or weaken the interfacial bonds in the specimens treated with GPS. The G_I values of the treated surfaces never reached the same low levels as that of the untreated surfaces. This was especially apparent for the grit-blasted and GPS treated specimens, which gave high G_I values over a longer period of time, as the value of G_I decreased at a slower rate. The combined effect of grit-blasting and silanisation slowed down the degradation process, and treatment with GPS typically reduced the standard deviation by a factor of three.

The durability of the abraded surface was significantly improved after treatment with GPS. Several of the abraded specimens which were not treated with GPS fell apart within a few days of environmental exposure, while none of the specimens treated with GPS fell apart during the test. Besides increasing the number of strong bonds in the interface, one mechanism by which silanisation can improve the durability is by filling the cracks and crevices in the abraded surface, effectively hindering diffusion of water along these paths. Kono *et al.* [26] observed that open areas in an alkaline etched aluminium surface appeared to be rather filled after treatment with GPS. This is in accordance with our own observations of silane film thickness. It was visually observed that even a 1% solution of GPS gave thicker films on some spots on the surface.

The positive effect of treatment with GPS on durability can also be seen when comparing the G_I curves of the alkaline etched specimens with and without treatment with GPS. The value of G_I for the untreated specimens was reduced to half of the initial value after only one hour, while the G_I value of the treated specimens was reduced to half of the initial value after 8 h. This occurred even if the initial value of G_I was higher for the treated specimens. Hence, the durability was significantly higher for the GPS treated specimens.

The initial pretreatment before treatment with GPS has effect on durability. An internal ranking shows that the durability of the grit-blasted surface was higher than the durability of the alkaline etched surface, which again was higher than the durability of the abraded surface. The same order of performance could be seen after treatment with GPS. The alkaline etched surface also performed better than the abraded surface after treatment with GPS. It is possible that the carbon contamination on the abraded surface prevents the silane from interacting with the sites on the surface, resulting in a higher density of micro-cavities. The result is decreased adhesion and durability.

6.3.3 General considerations

Surface analysis by XPS revealed that the pretreatment processes significantly altered the surface composition of the as-received surface (see Table 2). Carbon residues heavily contaminated the as-received surface after degreasing with acetone and drying. It is suspected that the presence of a high amount of carbon residues on the surface will prevent the adhesive from interacting with sites on the surface, resulting in reduced adhesion. Every pretreatment reduced the amount of carbon. Another particular difference between the as-received and pretreated surfaces was the change in Al(III)/O and Al(III)/Al(0) ratios. The Al(III)/O ratio of the as-received surface was low. This low ratio cannot be explained by the presence of aluminium hydroxides. Other sources of oxygen, such as e.g. magnesium hydroxides, acetone residues and other contaminants, may also be present on the surface. Also the Al(III)/Al(0) ratio was low on the as-received surface. This could imply that some elemental aluminium was present in the oxide layer of the as-received surface. The presence of elemental aluminium in the oxide layer indicates that removal of the upper surface layer is important in order to improve the corrosion properties of the surface. After extrusion there may be a heavily deformed surface region that contains fragmented intermetallic particles and inclusions of oxide particles [30]. This makes the surface more susceptible to corrosion and the upper surface layer should, therefore, be removed before adhesive bonding.

The surfaces of the forcibly opened wedge test specimens could be divided into three distinct zones by visual inspection after the exposure test. Insertion of the wedge resulted in cohesive failure within the adhesive, exposure to environment produced

interfacial failure at the interface between the adhesive and the aluminium surface, while opening of the specimens after testing once again gave cohesive failure. As mentioned earlier, the failure mode of the grit-blasted specimens during environmental exposure looked mainly interfacial, but there were small particles of aluminium on the adhesive side of the fracture and adhesive on the aluminium side of the fracture. Thus, some cohesive failure was observed.

As can be seen from Table 5, there were differences in the initial crack lengths of the RDCB wedge test joint specimens. This effect occurred despite the fact that all the initial cracks gave cohesive failure within the adhesive. The only exception was in the case of the grit-blasted surface. In some areas the initial cracks in these joints propagated very close to the aluminium/adhesive interface. Introduction of the wedge into the bondline will produce high stresses in the joint. On a rough surface such as the grit-blasted, regions of high stress intensity may be formed close to the surface [29], thereby forcing the crack to grow closer to the interface. This higher stress intensity at the interface may be reflected in the relatively long initial crack length of the grit-blasted joints compared with, e.g., the FPL etched joints.

Table 5
Initial crack lengths of RDCB wedge test joints

Pretreatment	Initial crack length (mm)	
	Before treatment with GPS	After treatment with GPS
Abrasion	70.2 (2.7)	62.2 (1.8)
Grit-blasting	65.3 (5.5)	59.1 (2.6)
FPL-etch	62.5 (1.6)	-
Alkaline etch	66.0 (3.8)	62.6 (1.1)
SAA	63.7 (1.7)	-

SAA – sulphuric acid anodising.

The initial crack length was shorter for the surfaces that had been treated with GPS than the corresponding untreated surfaces. Despite the initially shorter crack lengths, the durability of the joints treated with GPS was better than the durability of the untreated joints. The same trend could be seen when comparing the different pretreatments: joints

with shorter initial crack length gave better durability. The only exception was the relatively long initial crack in case of the grit-blasted surface, which possibly can be related to higher stress intensities at the rough surface. This suggests that there is a correlation between the bond strength in dry environment and the performance in humid environment. Since the initial cracks were cohesive within the adhesive, we are not able to explain this correlation which needs further investigations.

6.4 Conclusion

Grit-blasting with alumina gave better durability than alkaline etching, FPL-etching, and sulphuric acid anodising, which again gave better durability than abrasion with ScotchBrite®. It seems that both surface topography and surface contamination play important roles with respect to durability. Increased surface roughness improves the durability, while increased surface contamination reduces the durability. On a very rough surface such as the grit-blasted, the effects of surface contamination are more than outweighed by the effects of surface roughness.

Treatment with a 1% aqueous solution of GPS significantly improved the durability of pretreated surfaces, and the ranking between the pretreatments was the same as before treatment with GPS. The silane treatment also reduced the initial crack lengths in the wedge test specimens. The best performance was seen by the grit-blasting plus silane treatment, which performed much better than the well-established FPL-etch in wedge tests. Since this pretreatment is a relatively simple process that gives a very durable surface, it may have the potential as a repair system for damaged automotive parts.

Acknowledgements

Thanks are due to Hydro Automotive Structures and The Research Council of Norway for financial support.

References

[1] M. Brémont and W. Brockmann, *J. Adhesion* **58**, 69-99 (1996)

[2] R.A. Dickie, L.P. Haack, J.K. Jethwa, A.J. Kinloch and J.F. Watts, *J. Adhesion* **66**, 1-37 (1998)

[3] A.J. Kinloch, *Proc. Institution Mech. Eng.* **211**, 307-335 (1997)

[4] R.P. Digby and D.E. Packham, *Int. J. Adhesion Adhesives* **15**, 61-71 (1995)

[5] G.W. Critchlow and D.M. Brewis, *Int. J. Adhesion Adhesives* **16**, 255-275 (1996)

[6] K.B. Armstrong, *Int. J. Adhesion Adhesives* **17**, 89-105 (1997)

[7] M.R. Horner, F.J. Boerio and H.M. Clearfield, in: Silanes and Other Coupling Agents, K.L. Mittal (Ed.), VSP, Utrecht, 1992. p. 241-262.

[8] A.N. Rider, D.R. Arnott, A.R. Wilson and O. Vargas, *Mater. Sci. Forum* **189/190**, 235-240 (1995)

[9] A.N. Rider and D.R. Arnott, *Surf. Interface Anal.* **24**, 583-590 (1995)

[10] D.R. Arnott, A. R. Wilson, A.N Rider, L.T. Lambriandis and N.G. Farr, *Appl. Surface Sci.* **70/71**, 109-113 (1993)

[11] R.P. Digby and S.J. Shaw, *Int. J. Adhesion Adhesives* **18**, 261-264 (1998)

[12] W. Thiedman, F.C. Tolan, P.J. Pearce and C.E.M. Morris, *J. Adhesion* **22**, 197-210 (1987)

[13] A.N. Rider and D.R. Arnott, *Int. J. Adhesion Adhesives* **20**, 209-220 (2000)

[14] P.R. Underhill, G. Goring and D.L. DuQuesnay, *Appl. Surface Sci.* **134**, 247-253 (1998)

[15] P.R. Underhill, G. Goring and D.L. DuQuesnay, *Int. J. Adhesion Adhesives* **18**, 307-311 (1998)

[16] P.R. Underhill, G. Goring and D.L. DuQuesnay, *Int. J. Adhesion Adhesives* **18**, 313-317 (1998)

[17] P.R. Underhill, G. Goring and D.L. DuQuesnay, *Int. J. Adhesion Adhesives* **20**, 195-199 (2000)

[18] M.-L. Abel, J. F. Watts and R.P. Digby, *Int. J. Adhesion Adhesives* **18**, 179-192 (1998)

[19] M.-L. Abel, R.P. Digby, I.W. Fletcher and J.F. Watts, *Surface Interface Anal.* **29**, 115-125 (2000)

[20] M.-L. Abel, A. Rattana and J.F. Watts, *J. Adhesion* **73**, 313-340 (2000)

[21] A. Rattana, M.-L. Abel and J.F. Watts, in: Proc. 24th Annual Meeting of the Adhesion Society, Williamsburg, 2001. p. 202-204.

[22] J. Hermes, A. Rattana, M.-L. Abel and J.F. Watts, in: Proc. 24th Annual Meeting of the Adhesion Society, Williamsburg, 2001. p. 374-376.

[23] Y.L. Leung, M.Y. Zhou, P.C. Wong and K.A.R. Mitchell, *Appl. Surface Sci.* **59**, 23-29 (1992)

[24] G.A. Woods, S. Haq, N.V. Richardson, S. Shaw, R. Digby and R. Raval, *Surface Sci.* **433-435**, 199-204 (1999)

[25] C.M. Bertelsen and F.J. Boerio, *Prog. Org. Coatings* **41**, 239-246 (2001)

[26] M. Kono, X. Sun, R. Li, K.C. Wong, K.A.R. Mitchell and T. Foster, *Surface Rev. Lett.* **8**, 43-50 (2001)

[27] B.B. Johnsen, K. Olafsen, A. Stori and K. Vinje, *J. Adhesion Sci. Technol.* **17**, 1283-1298 (2003)

[28] J.D. Venables, *J. Materials Sci.* **19**, 2431-2453 (1984)

[29] A.N. Rider, C.L. Olsson-Jacques and D.R. Arnott, *Surface Interface Anal.* **27**, 1055-1063 (1999)

[30] A. Afseth, J.H. Nordlien, G.M. Scamans and K. Nisancioglu, *Corrosion Sci.* **43**, 2093-2109 (2001)

Chapter 7

Reflection-absorption FT-IR studies of the specific interaction of amines and an epoxy adhesive with GPS treated aluminium surfaces

Bernt B. Johnsen, Kjell Olafsen, Aage Stori

Int. J. Adhesion Adhesives **23**, 155-163 (2003)

Abstract

Aluminium surfaces were silanised with γ-glycidoxypropyltrimethoxysilane and the silane films were then further treated with different amines. Investigation before and after treatment, using reflection-absorption FT-IR spectroscopy, strongly indicated that a chemical reaction between the amines and the silane films took place, as observed in the intensity reduction of the epoxy band at 910 cm^{-1}. Increased SiOSi crosslink density was also observed. Treatment with dicyandiamide also showed the appearance of a band which was assigned to the formation of a covalent bond between the curing agent and the epoxy ring of the silane. The results partly explain the improved durability of GPS treated aluminium surfaces after bonding with one-component epoxy adhesives.

Keywords: Epoxides; Infrared spectra; Adhesion by chemical bonding; γ-Glycidoxy-propyltrimethoxysilane.

7.1 Introduction

Adhesives have been used for many years in industrial applications, where high durability bonded aluminium structures can be obtained by using adhesives based on, e.g., epoxy resins [1]. Unfortunately, it is necessary to use expensive surface pretreatment processes to obtain the required long-term service life of the bonded joints [2]. Chromium-based processes, such as the chromic-sulphuric acid FPL etch, are extensively used in the aerospace industry. However, hexavalent chromium is reported to be toxic to most living species [3]. Environmental factors together with stricter legislation has therefore led researchers to look for alternative, more environmentally friendly, pretreatment processes.

Organofunctional silanes are widely used as coupling agents to enhance the durability of adhesive joints [4]. The silanes generally have a hydrolysable group (e.g. -OCH_3) and an organofunctional group (e.g. an epoxy group) usually selected to be chemically reactive with a given adhesive. After the hydrolysis reaction, the silane can enable the formation of strong Al-O-Si bonds between the hydroxyl groups on the metal surface and the hydrolysed groups of the silane. Hence, a silane coupling agent will perform two functions in order to improve the environmental durability of a bonded joint [5]. Firstly, it will increase the density of strong bonds between the oxide and the adhesive. Secondly, it will improve the hydrolytic stability of the aluminium oxide. Formation of a weak hydrated layer on the aluminium surface is significantly hindered by the formation of a cross-linked multilayer film [2,6-7].

One of the most commonly used silanes is γ-glycidoxypropyltrimethoxysilane (GPS). The treatment of aluminium surfaces with aqueous solutions of GPS before adhesive bonding has been shown to improve bond durability [6-10], and the deposition of GPS and the films formed by GPS on aluminium surfaces have been investigated with a variety of techniques, including FT-IR spectroscopy, X-ray photoelectron spectroscopy and time-of-flight secondary ion mass spectrometry [11-22]. Abel *et al.* [15] used the

latter technique to show that the strong Al-O-Si bond is formed between hydrolysed GPS and aluminium surfaces.

Adhesive joints made of aluminium alloy AA6060 and XD4600 epoxy adhesive have in previous work been shown to give improved durability after silanisation with GPS of the substrates to be bonded [23]. The general understanding is that silanisation improves durability through the formation of strong, covalent bonds between the aluminium surface and the adhesive. By far the most common curing agents used with epoxy based adhesives are amines [24]. Therefore, in this work GPS films on aluminium surfaces were further treated with different amines and an epoxy adhesive in order to investigate the chemical interactions between the two phases and in order to get a better understanding of the effects amines have on GPS films. Analysis of the GPS films was performed with FT-IR spectroscopy in the reflection mode. Any detected chemical interactions between the amines and the GPS films can possibly, at least partially, explain why silanisation with GPS gives the observed improved durability.

Dicyandiamide (DICY) shown in Fig. 1, is one of the most widely used latent hardeners for epoxy resins, and it is the most common agent for high-temperature curing of one-component adhesive formulations [24-25]. The curing agent will not dissolve in the epoxy resins at low temperatures, and the adhesives are therefore cured at high temperatures where DICY dissolves and reacts chemically with the resins. The curing mechanism of epoxy resins by dicyandiamide has been studied in detail by Zahir [25] and Saunders *et al.* [26]. The chemical interactions between DICY and GPS films are of particular interest, therefore DICY was therefore deposited onto GPS silanised surfaces, and the specimens were heat-treated in order to simulate the curing conditions of a one-component structural epoxy adhesive. One important question mark is whether covalent bonding between DICY and the GPS film takes place or not, resulting in the formation of strong bonds between the aluminium surface and the adhesive.

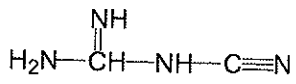

Figure 1. The chemical structure of DICY.

7.2 Experimental

7.2.1 Materials

The substrate material used in this study was extruded aluminium alloy AA6060-T6, which was supplied by Hydro Aluminium, Tønder, Denmark. γ-Glycidoxypropyl-trimethoxysilane (GPS) was obtained from Witco Europe SA (trade name: Silquest A-187), dicyandiamide (DICY) and dimethylformamide (DMF) from Fluka, ethanolamine from Janssen Chimica, dimethylbenzylamine from Aldrich and the two-component epoxy adhesive Araldite 2020 from Ciba. The curing agent of Araldite 2020 contains isophoronediamine. The one-component structural epoxy adhesive XD4600, was delivered by Dow Automotive, Freienbach, Switzerland. XD4600 contains DICY curing agent.

7.2.2 Specimen preparation and surface treatment

Aluminium specimens of size 50 × 25 mm^2 were prepared by a successive sequence of abrasion with a ScotchBrite® scouring pad (3M), solvent degreasing with a paper tissue soaked in acetone, and alkaline etching, before further treatment. The etching process was performed in 10 wt% NaOH at 60°C for 50 s. The specimens were then rinsed in 1 wt% HNO_3 at room temperature for 5 min, and in distilled water at room temperature for 10 min. They were then dried at 60°C.

Silanisation was performed in a 1 wt% solution of GPS in distilled water. The pH of the solution was adjusted to 5.0 using acetic acid, and the solution was then continuously stirred for 60 min at ambient temperature, using a magnetic stirrer, for hydrolysis of the silane methoxy groups. The silane was then deposited on the aluminium substrates by immersing them in the solution for 10 min, after which they were dried at 93°C for 60 min. In order to follow the condensation process of the SiOH silanols, one specimen was placed into the FT-IR spectrometer directly after the deposition step. The ambient conditions in the test chamber were 25°C and 35% relative humidity.

GPS silanised aluminium surfaces were treated with different amines or adhesives in order to investigate the chemical interactions of the amines/adhesives with the GPS films. The latent curing agent DICY was deposited onto the GPS silanised specimens by immersing the specimens into a 1 wt% solution in dimethylformamide (DMF) at ambient temperature for a period of 20 min. The specimens were then dried at 40°C for 1 h in order to drive off the solvent, after which the specimens were heat-treated at 180°C for 30 min (typical curing conditions for one-component epoxy adhesives). After they had cooled to room-temperature, the specimens were extracted with DMF to remove unreacted DICY from the surface. They were then once again dried at 40°C for 1 h before analysis by FT-IR spectroscopy. XD4600 epoxy adhesive was also deposited onto the GPS silanised specimens from a 1 wt% solution in DMF. However, in order to remove adhesive fillers the solution was filtered with a Millipore Millex-FH filter.

GPS films were also treated with ethanolamine, dimethylbenzylamine and the curing part of Araldite 2020 epoxy adhesive. The ethanolamine treatment was conducted by immersing the specimens into pure ethanolamine at 60°C for 60 min, while treatment with dimethylbenzylamine was performed in a 1% solution in methanol at 60°C for 60 min. Dimethylbenzylamine is a common tertiary amine catalyst used in epoxy adhesive systems. The GPS films were coated with the curing part of Araldite 2020 and heat-treated at 60°C for 3 h (recommended curing cycle for Araldite 2020). The curing part contains isophoronediamine and trimethylhexamethylenediamine. After these different treatments the specimens were extracted with methanol and dried at 40°C for 1 h before analysis by FT-IR spectroscopy. GPS films were also treated with pure DMF and pure methanol, according to the procedures described above, for reference purposes.

A GPS gel was prepared from a 30 wt% solution of GPS at pH 5.0. The hydrolysed solution was dried at 93°C, and the dried gel was ground up, baked into a KBr-pellet and analysed with FT-IR spectroscopy. The dried gel was also reacted with ethanolamine at 60°C.

7.2.3 Reflection-absorption infrared spectroscopy

The treated aluminium specimens were investigated with reflection-absorption infrared spectroscopy (RAIR). The analysis was performed with a Perkin Elmer 1725X FT-IR Spectrometer where the specimens were mounted on an external reflectance accessory. The spectra were recorded as an average of 100 scans with a resolution 4 cm^{-1} in the range 400-4000 cm^{-1}. However, when following the SiOH condensation process only 10 scans were recorded for each analysis. The angle of the infrared beam to the normal of the specimen surface was 80°. A bare aluminium specimen (not treated with GPS) was used to obtain a background spectrum for the RAIR analysis. Transmission infrared spectra were obtained by deposition of the chemical compound on KBr-pellets.

7.3 Results

The transmission infrared spectrum of GPS is shown in Fig. 2. Two of the most interesting bands in the spectrum can be identified as $SiOCH_3$ methoxy groups at 822 cm^{-1} and epoxy rings at 910 cm^{-1}. The silane undergoes chemical changes during the hydrolysis and drying processes. During hydrolysis of the silane the $SiOCH_3$ groups will transform into SiOH silanols. These silanols will condense during the drying step, resulting in the formation of a cross-linked SiOSi network. In the dried GPS films (as shown in Fig. 2) the bands in the range 1000-1130 cm^{-1} are mainly attributed to SiOSi vibrations, while the broad band at 3370 cm^{-1} is attributed to SiOH silanols.

The condensation process of the SiOH silanol groups was monitored by placing a silanised specimen in the FT-IR spectrometer directly after the deposition step. As can be seen from Fig. 3, no band was present at 822 cm^{-1}, indicating full hydrolysis of the methoxy groups. Two strong bands could be seen at 919 and 1105 cm^{-1}. These bands are attributed to SiOH and SiOSi groups, respectively. The intensity of the band at 919 cm^{-1} decreased with time, and it was also shifted towards a lower wavenumber, while the intensity of the band at 1105 cm^{-1} increased and was shifted towards a higher wavenumber. The latter indicates a higher density of SiOSi linkages, and thus a higher degree of crosslink density in the film. The condensation process, which started immediately after deposition, was monitored for 4 h, at which time it had declined

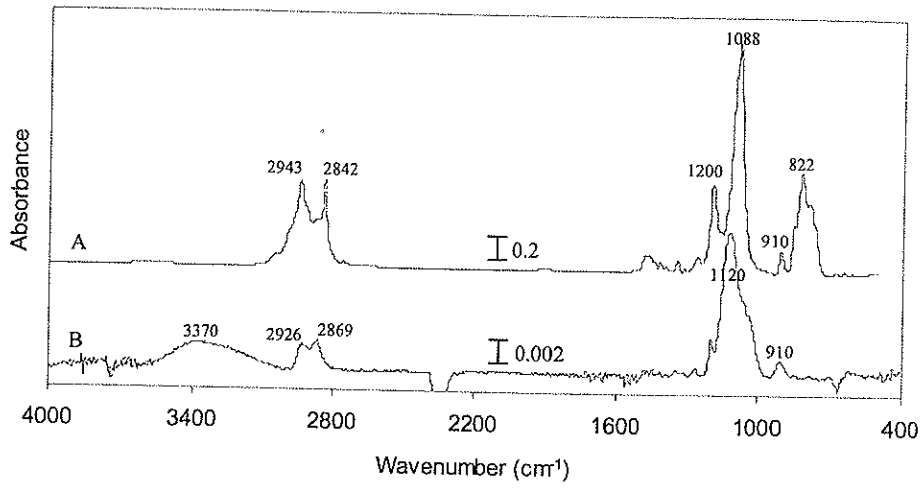

Figure 2. (A) Transmission infrared spectrum of GPS on KBr-pellet and (B) a typical reflection-absorption infrared spectrum of a dried GPS film on AA6060-T6 aluminium deposited from a 1% solution of GPS in water.

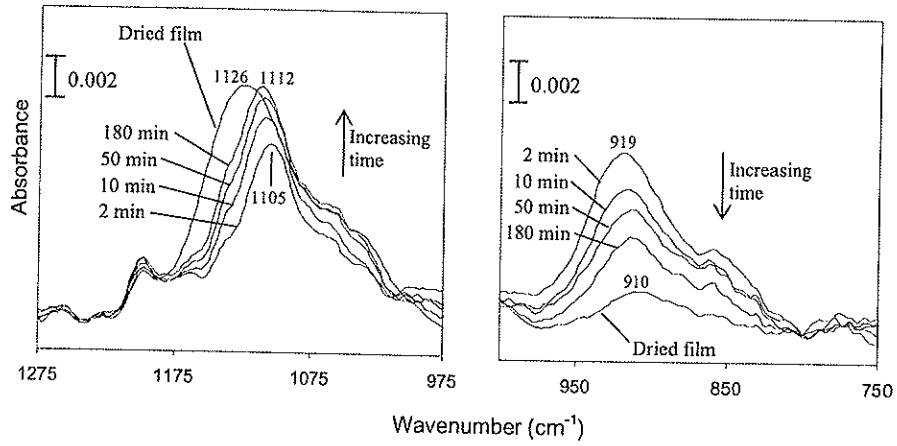

Figure 3. Reflection-absorption infrared spectra of the condensation process of hydrolysed GPS on AA6060-T6 aluminium deposited from a 1% solution of GPS in water. The ambient conditions were 25°C and 35% relative humidity. The spectra have been shifted vertically for clarity.

considerably. However, a post-drying at 93°C for 60 min had a significant effect, resulting in further condensation. After post-drying the two bands were shifted to 910 and 1126 cm^{-1}, and the intensity of the former band was significantly lower than before drying. Similar spectra of GPS films were obtained by drying at 93°C directly after the deposition step (Figs 4-7). However, the SiOH band at 3370 cm^{-1} was sometimes not detectable, indicating that almost all SiOH groups were consumed during the drying process.

All GPS films that were treated with different amines showed a significant reduction of the band at 910 cm^{-1} compared with the untreated GPS films (Figs 4-7). Another change that was common for all amine treatments was the shift of the band at 1120 cm^{-1} towards a higher wavenumber. However, treatment with DICY also resulted in one specific change. After the treatment a minor band was observed at 2190 cm^{-1} (Fig. 9). Reference specimens that were treated with pure DMF or pure methanol did not show any significant changes in the RAIR spectra. Hence, neither treatment with solvent nor heat-treatment at 180°C had effect on the structure of the GPS films.

Fig. 10 shows the transmission infrared spectra of filtered epoxy adhesive before and after curing at 180°C for 30 min. Most of the bands that are indicative of the epoxy resin did not undergo any changes. The intense bands at 1510 and 1608 cm^{-1} are due to the aromatic ring, while the strong bands at 1184 and 1246 cm^{-1} are from ether and substituted aromatic groups, respectively [27]. However, the epoxy band at 914 cm^{-1} totally disappeared, and the emergence of a broad hydroxyl band at 3385 cm^{-1} indicates opening of the epoxy rings. This is consistent with the disappearance of N-H stretching modes around 3350 cm^{-1}, the nitrile (C≡N) band at 2210 cm^{-1} and the band of the salt form of DICY ($^{-}N=C=N^{+}$) at 2167 cm^{-1} [28]. Hence, the amine curing agent has reacted chemically with the epoxy resin.

A significant reduction in the band at 910 cm^{-1} was also observed after treatment of a GPS surface with filtered epoxy adhesive (Fig. 11). Increased crosslink density was also observed by the shift of the band at 1120 cm^{-1}. The appearance of the two bands indicative of aromatic ether groups at 1510 cm^{-1} and substituted aromatic rings at 1251

cm^{-1} on the treated surface, showed that adhesive was present on the surface after this treatment. The deposited adhesive film was strongly bonded to the GPS coated surface, and was not washed away by extraction in DMF.

Table 1
Some of the infrared frequencies discussed in this study.

Vibrational assignment	GPS			DICY	Uncured epoxy adhesive
	bulk	hydrolysed	dried film		
$SiOCH_3$	822				
SiOH		919, 3370	3370		
SiOSi			1120-1126		
epoxy ring			910		914
C≡N				2210	2210
$^{-}N=C=N^{+}$				2167	2167
$R_2N\text{-}C\equiv N$				2190[a]	2179[b]

[a]Present in the spectrum of GPS films after treatment with DICY.
[b]Only present in cured epoxy adhesive.

7.4 Discussion

Taking into consideration Figs 2 and 3 it is clear that both the SiOH group and the epoxy ring have absorbing frequencies in the same region. A major problem with these overlapping absorption bands can be masking of the signal from the epoxy rings, complicating the interpretation of the obtained results. Underhill *et al.* [14] observed a small peak at 908 cm^{-1}, which was due to the epoxy group in the GPS molecule. This band overlapped with the SiOH peak at 916 cm^{-1}. The presence of two absorbing groups in this region can make it difficult to assign the reduction of a band in the region to the reduction of either SiOH or epoxy groups.

In Fig. 3 the condensation reaction of hydrolysed SiOH groups can be observed. During condensation at room temperature the intensity of the SiOH band at 919 cm^{-1} decreases and is shifted to 914 cm^{-1}. A post-cure at 93°C reduces the intensity further and shifts

the band to 910 cm^{-1}. It has been reported that the drying of the GPS film and the condensation of SiOH groups is essentially over within 12 min [11], indicating that the drying process is very rapid at room temperature. This is a much faster drying process than we observed in our study. Fig. 3 shows that the drying process reached a halt after 180 min at an ambient temperature of 23°C and 35% relative humidity, and after 240 min no further development was observed. However, the post-drying at 93°C had a significant effect, showing that the drying process was not completed at room temperature.

7.4.1 Effect of amine treatments

All dried GPS films that were treated with amines showed significant changes after treatment (Figs 4-7). It has been proposed that amines can catalyse the condensation reactions of hydrolysed silanes [29], and it is clear that the treatment of GPS films on aluminium with different amines results in further condensation of the silane film. For all treatments the SiOSi band at 1120 cm^{-1} in the dried films is shifted towards 1126 cm^{-1}, indicating a higher crosslink density. The observed wavenumbers could to some extent vary, but there was always a shift towards higher wavenumbers after the amine treatments. However, although the SiOSi band is shifted towards a higher wavenumber, the intensity of this band is only insignificantly altered. One exception was after treatment with the curing part of Araldite 2020 where increased intensity and a shift to 1123 cm^{-1} was observed (Fig. 7). The curing agent contains a band at 1117 cm^{-1}, so this may well be due to the presence of chemically bound curing agent on the surface. Increased intensity of C-H streching bands in the area 2850-2950 cm^{-1} was also observed.

An interesting observation is the intensity reduction of the band at 910 cm^{-1}. Primary amines (e.g. ethanolamine and the curing part of Araldite 2020) are expected to react covalently with epoxy rings, while tertiary amines (e.g. dimethylbenzylamine) are expected to catalyse opening and polymerisation of epoxy rings [30]. Although both the SiOH groups and the epoxy rings have absorbing frequencies in the region around 910 cm^{-1}, here we attribute the observed intensity reduction to the reduction in the number of epoxy rings. We base this assumption on different observations. A shift of the band at

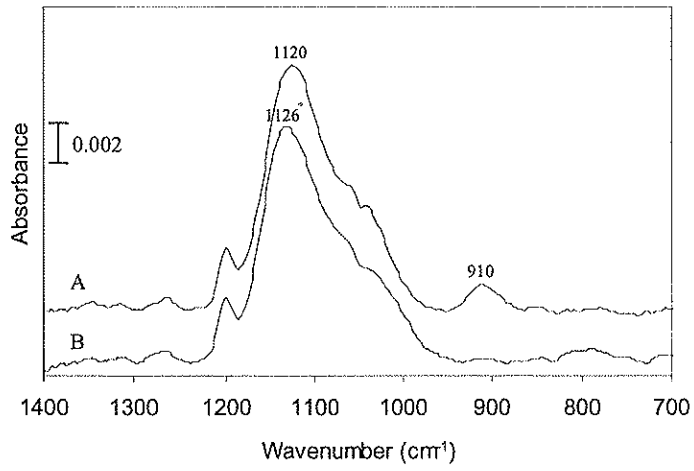

Figure 4. Reflection-absorption infrared spectra of GPS films on AA6060-T6 aluminium deposited from a 1% solution of GPS in water: (A) Untreated and (B) after further treatment with dicyandiamide curing agent deposited from a 1% solution in DMF.

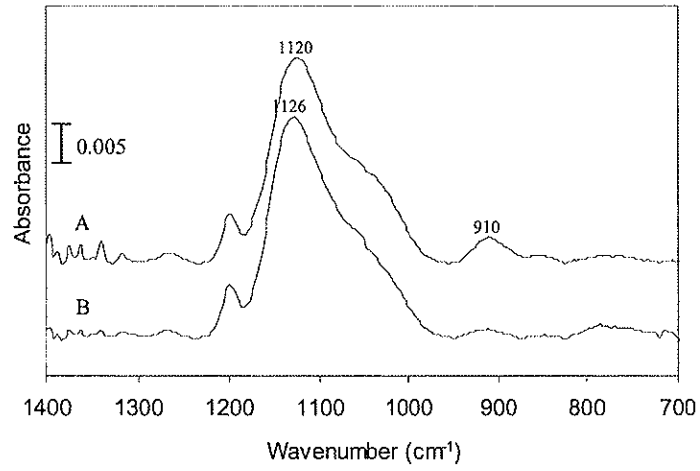

Figure 5. Reflection-absorption infrared spectra of GPS films on AA6060-T6 aluminium deposited from a 1% solution of GPS in water: (A) Untreated and (B) after further treatment with ethanolamine.

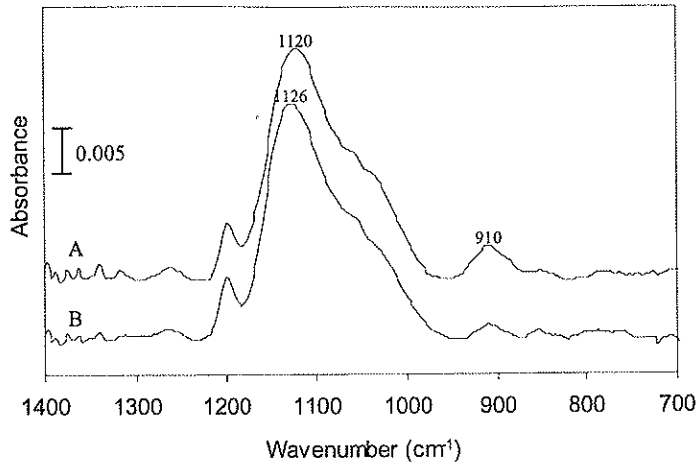

Figure 6. Reflection-absorption infrared spectra of GPS films on AA6060-T6 aluminium deposited from a 1% solution of GPS in water: (A) Untreated and (B) after further treatment with 1% dimethylbenzylamine in methanol.

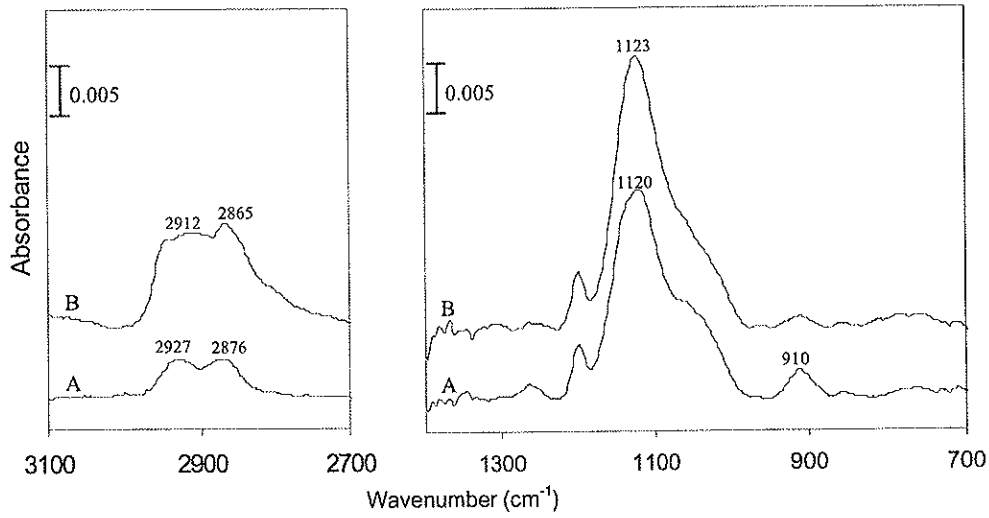

Figure 7. Reflection-absorption infrared spectra of GPS films on AA6060-T6 aluminium deposited from a 1% solution of GPS in water: (A) Untreated and (B) after further treatment with the amine curing agent of Araldite 2020.

1120 cm^{-1} was observed, but the treatments did not (usually) have any effect on the SiOH band at 3370 cm^{-1}. So it seems that only few SiOH groups were consumed during the amine treatment processes. The main part of the intensity reduction of the band at 910 cm^{-1} must then be due to the consumption of epoxy rings. Thus, there does not seem to be any connection between the intensity reduction of 3370 and 910 cm^{-1} during amine treatments. The intensity reduction was also observed in GPS films where no band at 3370 cm^{-1} was detected, i.e., in films where the condensation process of SiOH groups was almost complete and still a band at 910 cm^{-1} was present. Another observation is that during condensation there is a shift of the SiOH band at 919 cm^{-1} towards the band of the epoxy ring at 910 cm^{-1}. This suggests that the band at 910 cm^{-1} in the dried GPS films mainly is the result of absorption from epoxy rings. Also, when a mixture of pure GPS and the curing part of Araldite 2020 was cured at 60°C, the band at 910 cm^{-1} disappeared.

For comparison reasons, also a dried GPS gel was analysed with FT-IR spectroscopy. The spectrum contains a strong O-H stretching band at 3436 cm^{-1} and the epoxy ring/SiOH band at 906 cm^{-1} (Fig. 8). Also, two strong bands appear at 1106 and 1035 cm^{-1}, of which the latter peak is unresolved in the spectra of the GPS films. These bands are attributed to SiOSi vibrations, since longer or more branched siloxane chains results in a broader and more complex SiOSi absorption, with two or more absorbing bands. Some interesting observations were made when reacting the GPS gel with ethanolamine. The intensity of the O-H band at 3436 cm^{-1} was significantly increased, while the intensity of the epoxy/SiOH band at 906 cm^{-1} was significantly decreased (Fig. 8). This shows that a reaction between the epoxy rings and the amine groups in ethanolamine has taken place. The increased intensity of the 3436 cm^{-1} band is due to hydroxyls produced during opening of the epoxy rings and from hydroxyls in the chemically bonded ethanolamine molecules. The remaining part of the 906 cm^{-1} band may be unreacted SiOH groups. These observations support the assumption that the epoxy rings in the GPS films have reacted with amines during the amine treatments. The N-H band at 1629 cm^{-1} also indicates the reaction of the epoxy rings. However, increased crosslink density in the GPS gel was not observed after treatment with ethanolamine.

7.4.2 Treatment with DICY and epoxy adhesive

The reaction between the GPS silanised surface and DICY or an epoxy adhesive can be compared with the reactions taking place during curing of the adhesive. Fig. 10 shows the transmission infrared spectra of filtered epoxy adhesive before and after cure. Most of the bands which are indicative of the epoxy resin do not undergo any changes, i.e. the bands at 1246 and 1510 cm^{-1}. However, the epoxy band at 914 cm^{-1} totally disappears, and the emergence of a broad hydroxyl band at 3385 cm^{-1} indicates opening of the epoxy ring. This is consistent with the disappearance of N-H stretching modes around 3350 cm^{-1}, the nitrile (C≡N) band at 2210 cm^{-1} and the band of the salt form of DICY ($^-N{=}C{=}N^+$) at 2167 cm^{-1} [28]. Thus, the amine curing agent has reacted chemically with the epoxy rings in the resin.

The curing mechanism of epoxy resins by dicyandiamide has been studied in detail by Zahir [25] and Saunders *et al.* [26]. According to Zahir, the reaction of phenyl glycidyl ether with dicyandiamide leads mainly to products with two different structural units, namely a dialkyl cyanamide:

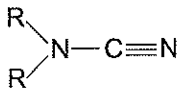

and an organic base, derivatives of 2-amine-2-oxazoline (or its tautomer 2-imino-oxazolidine):

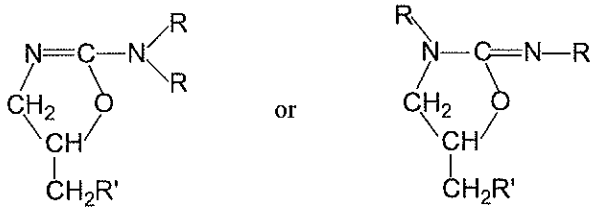

where

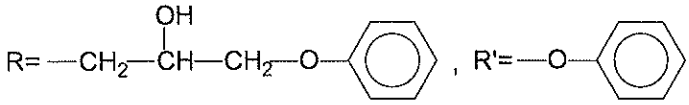

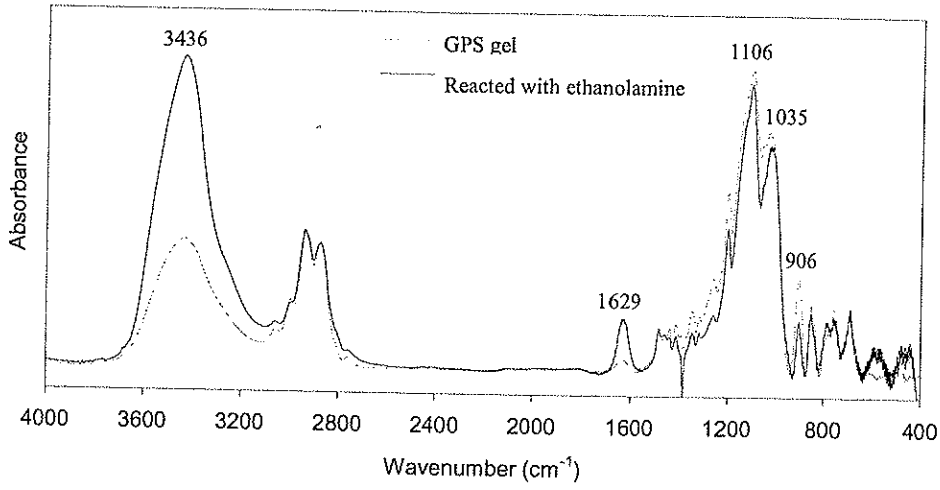

Figure 8. Transmission FT-IR spectra of GPS gel prepared from a 30% solution of GPS in water; before and after reaction with ethanolamine.

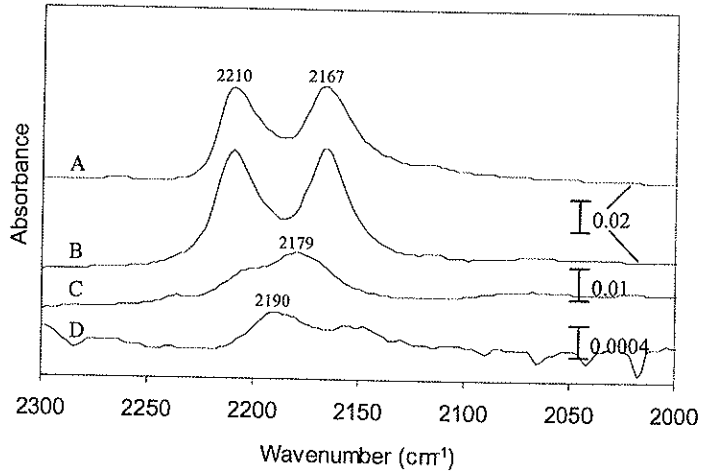

Figure 9. Infrared spectra in the 2000-2300 cm^{-1} region of: (A) dicyandiamide curing agent on AA6060-T6 aluminium, (B) uncured XD4600 epoxy adhesive on KBr-pellet, (C) cured XD4600 epoxy adhesive on KBr-pellet and (D) dicyandiamide treated GPS on AA6060-T6 aluminium.

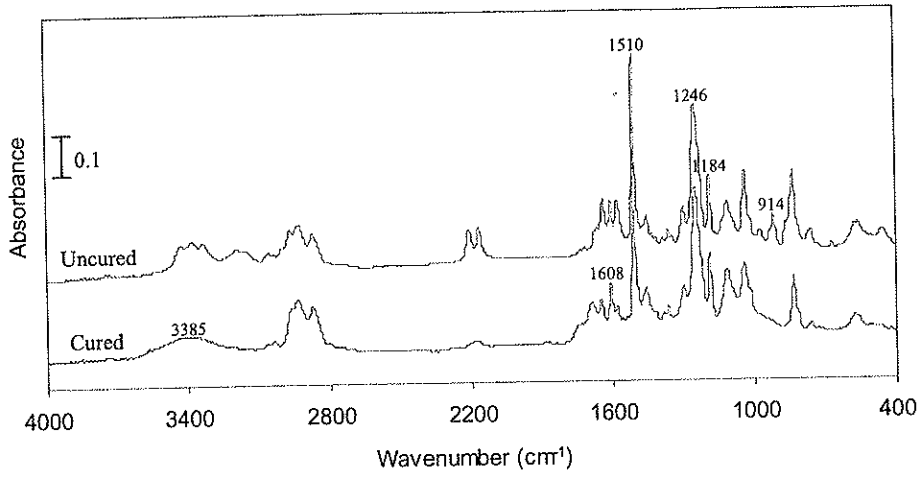

Figure 10. Transmission infrared spectra of uncured (above) and cured (below) filtered XD4600 epoxy adhesive on KBr-pellets deposited from a 1% solution of XD4600 in DMF.

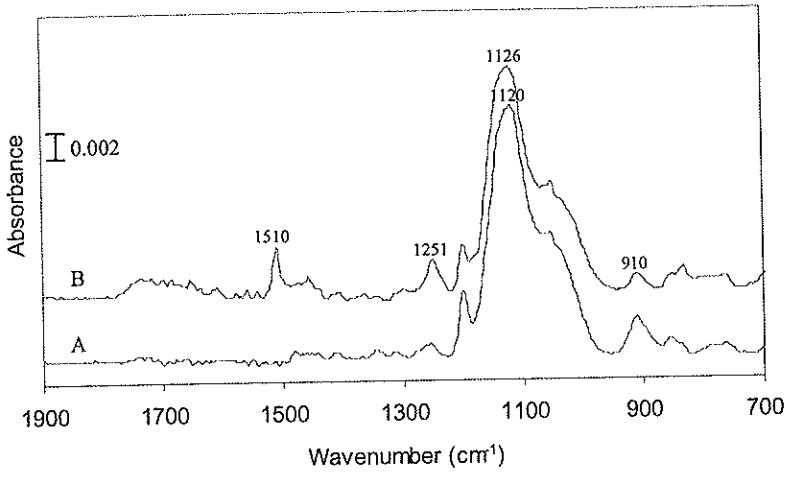

Figure 11. Reflection-absorption infrared spectra of GPS films on AA6060-T6 aluminium deposited from a 1% solution of GPS in water: (A) Untreated and (B) after further treatment with filtered XD4600 epoxy adhesive deposited from a 1% solution in DMF.

In addition, urea carbonyl and urethane ester groups may be formed in the resin via the intramolecular and/or intermolecular rearrangement reactions of the above products. We expect that the glycidyl groups of GPS can interact with DICY in the same manner as the glycidyl groups of epoxy resins. Hence, the molecular structures as shown above can be expected in a chemical reaction between GPS and DICY.

Fig. 9 depicts the infrared spectra in the 2000-2300 cm^{-1} region of DICY deposited onto aluminium, of uncured and cured epoxy adhesive, and of a GPS surface treated with DICY. The DICY treated GPS surface was extracted with DMF solvent after heat-treatment at 180°C in order to remove loosely adsorbed DICY before analysis with FT-IR. Both the C≡N band at 2210 cm^{-1} and the $^{-}N=C=N^{+}$ band at 2167 cm^{-1} are present in the spectra of DICY and epoxy adhesive. After curing of the adhesive, a new band is formed in the region between the two original bands, namely at 2179 cm^{-1}. A band in the same region also appears on the GPS surface after treatment with DICY. This band at 2190 cm^{-1} is not present on the surface before treatment with DICY or the GPS surface that was treated only with DMF. The band is weak, but it is not present in the spectra of other amine treatments. Other authors have attributed bands in this area to the nitrile group in DICY [25,28,31]. Taking into consideration the work of Zahir [25], here we tentatively assign the band at 2190 cm^{-1} to be the dialkyl cyanamide structure shown above, or possibly an alkyl cyanamide structure, R-NH-C≡N. The shift from 2179 to 2190 cm^{-1} can be explained by the different substituents of the cyanamide in the reaction with either epoxy adhesive or GPS, resulting in altered vibration frequency.

Deposition and curing of an epoxy adhesive film on a GPS coated aluminium surface has the same effect as deposition of DICY followed by heat-treatment at 180°C (Fig. 11). Both an intensity reduction of the epoxy band at 910 cm^{-1}, as well as increased crosslink density was observed. This shows that the curing agent of the epoxy adhesive is responsible for the changes occurring. The presence of an adhesive film on the surface is shown by the ether band at 1251 cm^{-1} and the strong aromatic band at 1510 cm^{-1}. However, the bands at 2179 or 2190 cm^{-1} could not be observed on the surface.

The adhesive film is very thin in order to enhance the interface reactions and the signal is possibly too weak for detection of these bands.

As discussed above, treatment with DICY suggested that a covalent bond was formed between DICY and the GPS film. The curing agent will also react chemically with the epoxy resin in the formation of a polymer network, and the presence of a covalent bridge between the aluminium surface and the adhesive can therefore be expected. The existence of a covalent bond between a GPS film on aluminium and an epoxy adhesive has been shown by Rattana *et al.* [32], using ToF-SIMS. They showed that the amine curing agent interacted covalently with the epoxy ring of the GPS molecule and the DGEBA resin, forming a network of covalent bonds from the aluminium surface through to the bulk of the adhesive. Thus, it is possible for an amine-cured epoxy adhesive system to interact covalently with a GPS film on aluminium. These covalent bonds are of importance with respect to the durability of an adhesively bonded joint, as they introduce stronger bonds between the adhesive and the surface. Degradation of the bonded joint due to the effects of humid environment will then be delayed, resulting in improved durability. This was shown in a previous publication where AA6060-T6 surfaces silanised with GPS was shown to give better durability after bonding with epoxy adhesive than the unsilanised surfaces [23].

The band at 910 cm^{-1} did not totally disappear during treatment with amines or epoxy adhesive. The silane film exists in the form of a crosslinked siloxane network on the surface, as illustrated by Bell *et al.* [33], and it is possible that only the epoxy rings in the outer surface layer of the GPS films are accessible for reaction with the curing agent. The thickness of the siloxane network acts as a barrier that prevents diffusion of curing agent towards the surface. Hence, after treatment of the GPS films with amines or adhesive, only the epoxy rings in the outer siloxane layer will react. The epoxy rings closer to the surface are not accessible for chemical reaction. Thus, they will not react and can still be detected after the treatment.

7.5 Conclusion

Alkaline etched surfaces of aluminium alloy AA6060-T6 were coated with GPS and then further treated with different amines. Investigation of the GPS films before and after treatment using RAIR showed that significant changes occurred during the treatments. All amine treatments strongly indicated that a chemical reaction between the amines and the GPS films took place, as observed in the intensity reduction of the epoxy band at 910 cm^{-1}. The amines also catalysed the condensation of SiOH groups, and a higher degree of SiOSi crosslink density was observed in the films.

Treatment with DICY, a common curing agent used in one-component epoxy adhesives, also showed the appearance of a band at 2190 cm^{-1} in addition to increased crosslink density and an intensity reduction at 910 cm^{-1}. The band at 2190 cm^{-1} is indicative of the nitrile C≡N group in DICY and is assigned to the formation of a covalent bond between the curing agent and the epoxy ring of the GPS molecule.

Treatment of the GPS films with epoxy adhesive resulted in the same changes as treatment with amines. The existence of covalent bonds between a GPS film on aluminium and an epoxy adhesive is of importance with respect to the durability of a bonded joint. Stronger bands are introduced, resulting in improved durability in humid environment. The results from this study explains the improved performance of GPS treated aluminium surfaces reported earlier [23].

Acknowledgements

Thanks are due to Hydro Automotive Structures and The Research Council of Norway for financial support.

References

[1] M. Brémont and W. Brockmann, *J. Adhesion* **58**, 69-99 (1996)

[2] A.J. Kinloch, *Proc. Institution Mech. Eng.* **211**, 307-335 (1997)

[3] N.L. Rogers, in: Adhesive Bonding of Aluminum Alloys, E.W. Thrall and R.W. Shannon (Eds.), Marcel Dekker, New York, 1985. p. 41-50.

[4] M.R. Horner, F.J. Boerio and H.M. Clearfield, in: Silanes and Other Coupling Agents, K.L. Mittal (Ed.),VSP, Utrecht, 1992. p. 241-262.

[5] A.N. Rider, D.R. Arnott, A.R. Wilson and O. Vargas, *Mater. Sci. Forum* **189/190**, 235-240 (1995)

[6] A.N. Rider and D.R. Arnott, *Surf. Interface Anal.* **24**, 583-590 (1995)

[7] D.R. Arnott, A.R. Wilson, A.N. Rider, L.T. Lambriandis and N.G. Farr, *Appl. Surface Sci.* **70/71**, 109-113 (1993)

[8] R.P. Digby and S.J. Shaw, *Int. J. Adhesion Adhesives* **18**, 261-264 (1998)

[9] W. Thiedman, F.C. Tolan, P.J. Pearce and C.E.M. Morris, *J. Adhesion* **22**, 197-210 (1987)

[10] A.N. Rider and D.R Arnott, *Int. J. Adhesion Adhesives* **20**, 209-220 (2000)

[11] P.R Underhill, G. Goring and D.L. DuQuesnay, *Appl. Surface Sci.* **134**, 247-253 (1998)

[12] P.R Underhill, G. Goring and D.L. DuQuesnay, *Int. J. Adhesion Adhesives* **18**, 307-311 (1998)

[13] P.R Underhill, G. Goring and D.L. DuQuesnay, *Int. J. Adhesion Adhesives* **18**, 313-317 (1998)

[14] P.R Underhill, G. Goring and D.L. DuQuesnay, *Int. J. Adhesion Adhesives* **20**, 195-199 (2000)

[15] M.-L. Abel, J.F. Watts and R.P. Digby, *Int. J. Adhesion Adhesives* **18**, 179-192 (1998)

[16] M.-L. Abel, R.P. Digby, I.W. Fletcher and J.F. Watts, *Surface Interface Anal.* **29**, 115-125 (2000)

[17] M.-L. Abel, A. Rattana and J.F. Watts, *J. Adhesion* **73**, 313-340 (2000)

[18] A. Rattana, M.-L. Abel and J.F. Watts, in: Proc. 24th Annual Meeting of the Adhesion Society, Williamsburg, 2001. p. 202-204.

[19] Y.L. Leung, M.Y. Zhou, P.C. Wong and K.A.R. Mitchell, *Appl. Surface Sci.* **59**, 23-29 (1992)

[20] G.A. Woods, S. Haq, N.V. Richardson, S. Shaw, R. Digby and R. Raval, *Surface Sci.* **433-435**, 199-204 (1999)

[21] C.M. Bertelsen and F.J. Boerio, *Prog. Org. Coatings* **41**, 239-246 (2001)

[22] M. Kono, X. Sun, R. Li, K.C. Wong, K.A.R. Mitchell and T. Foster, *Surface Rev. Lett.* **8**, 43-50 (2001)

[23] B.B. Johnsen, K. Olafsen, A. Stori and K. Vinje, *J. Adhesion Sci. Technol.* **16**, 1931-1948 (2002)

[24] A.V. Pocius, Adhesion and Adhesives Technology, Carl Hanser Verlag, Munich, 1997.

[25] S.A. Zahir, *Adv. Org. Coat. Sci. Tech.* **4**, 83-102 (1982)

[26] T.F. Saunders, M.F. Levy and J.F. Serino, *J. Polym. Sci.* **5**, 1609-1617 (1967)

[27] S.-H. Hong and J.-S. Tsai, *Macromol. Mater. Eng.* **276/277**, 59-65 (2000)

[28] F. Fondeur and J.L. Koenig, *Appl. Spectrosc.* **47**, 1-6 (1993)

[29] F.D. Osterholtz and E.R. Pohl, *J. Adhesion Sci. Technol.* **6**, 127-149 (1992)

[30] J.A. Brydson, Plastics Materials, Butterworth & Co, London, 1975.

[31] R.O. Carter, R.A. Dickie, J.W. Holubka and N.E. Lindsay, *Ind. Eng. Chem. Res.* **28**, 48-51 (1989)

[32] A. Rattana, J.D. Hermes, M.-L. Abel and J.F. Watts, *Int. J. Adhesion Adhesives* **22**, 205-218 (2002)

[33] J.P. Bell, R.G. Schmidt, A. Malofsky and D. Mancini, in: Silanes and Other Coupling Agents, K.L. Mittal (Ed.),VSP, Utrecht, 1992, p. 241.

Chapter 8

The role of covalent bonding in silane pretreatment of adhesively bonded aluminium

Bernt B. Johnsen, Kjell Olafsen, Aage Stori

J. Adhesion, submitted

Abstract

The importance of covalent bonding between aluminium surfaces treated with 1 wt% aqueous silane solutions and an epoxy adhesive has been investigated. Both reactive and unreactive organosilanes were used. The silane treated surfaces were characterised by contact angle measurements and reflection-absorption infrared spectroscopy, and the durability of bonded joints was determined using the wedge test at 40°C/96% RH. The general understanding is that silanisation improves durability through the formation of strong, covalent bonds between the metal surface and the adhesive. However, the results indicate that also the hydrophobicity of the surface is important with respect to durability in humid environments. Chemical reaction is not necessary for improved durability. Hydrophobic surfaces can prevent water from entering the aluminium-adhesive interface. Since water is a prerequisite for the crack growth observed in wedge tests, the durability is improved with increasing surface hydrophobicity.

Keywords: Adhesive bonding; Aluminium; Silanes; Wedge test; Adhesion mechanisms.

8.1 Introduction

Adhesives have been used for many years in industrial applications, where high durability bonded aluminium structures can be obtained by using adhesives based on epoxy resins [1]. Unfortunately, it is necessary to use expensive surface pretreatment processes to obtain the required long-term service life of the bonded joints [2]. Chromate-containing processes, such as chromic acid and phosphoric acid anodising (the substrates are normally etched in a chromic acid solution prior to anodising) are extensively used in the aerospace industry. However, hexavalent chromium is reported to be toxic to most living species [3]. Environmental factors together with stricter legislation has therefore led researchers to look for alternative, more environmentally friendly, pretreatment processes.

Organofunctional silanes are widely used as coupling agents to enhance the durability of adhesive joints [4]. The silanes generally have a hydrolysable group (e.g. $-OCH_3$) and an organofunctional group (e.g. an epoxy group) usually selected to be chemically reactive with a given adhesive. After hydrolysis, the silane can enable the formation of strong AlOSi bonds between the hydroxyl groups on the metal surface and the hydrolysed groups of the silane. Hence, a silane coupling agent is said to perform two functions in order to improve the environmental durability of a bonded joint [5]. Firstly, it will increase the density of strong bonds between the oxide and the adhesive. Secondly, it will improve the hydrolytic stability of the aluminium oxide. Formation of a weak hydrated layer on the aluminium surface is significantly hindered by the formation of a cross-linked siloxane film [2,6-7].

One of the most commonly used silanes is γ-glycidoxypropyltrimethoxysilane (GPS). The treatment of aluminium surfaces with aqueous solutions of GPS before adhesive bonding has been shown to improve bond durability [6-10]. Abel *et al.* [11] used time-of-flight secondary ion mass spectrometry (ToF-SIMS) to show that the strong AlOSi bond is formed between hydrolysed GPS and aluminium surfaces, while the existence of a covalent bond between a GPS film on aluminium and an epoxy adhesive was also

shown by ToF-SIMS by Rattana *et al.* [12]. The amine curing agent interacted covalently with the epoxy rings of the GPS molecule and the DGEBA resin, forming a network of covalent bonds from the aluminium surface through to the bulk of the adhesive. These covalent bonds are claimed to be of importance with respect to the durability of an adhesively bonded joint, as they introduce stronger bonds between the adhesive and the surface. Degradation of the bonded joint due to the effects of humidity may then be delayed, resulting in improved durability.

Thus, the general understanding is that silanisation improves durability through the formation of strong, covalent bonds between the aluminium surface and the adhesive. However, it has also been reported that other phenomena in the silane/adhesive interface have effect on the adhesion. The existence of an interpenetrating network in the silane film/polymer interphase can have effect on bond properties. This effect can occur if contact is made between a polymer and uncrosslinked siloxanols which still have some degree of solubility [13-14]. In addition, the compatibility of unreactive siloxanes with polymer matrices depends upon wettability or solubility parameters for these materials [15].

In a previous publication, it was shown that silanisation of aluminium alloy AA6060-T6 with GPS significantly improves bond durability independent of the initial surface pretreatment [16]. This was partly assigned to the covalent interaction between the GPS molecule and the dicyandiamide curing agent in the epoxy adhesive used for bonding [17]. The aim of the present study is to investigate the importance of covalent bonding between the silane and the adhesive. The bond properties of silanes with different organofunctional groups are investigated: one silane with a functional group that is chemically reactive with the epoxy adhesive (GPS), and three silanes with organosubstituted groups which are believed to be unreactive with the epoxy adhesive (acetoxypropyltrimethoxysilane, methoxypropyltrimethoxysilane and propyltrimethoxy-silane). However, these silanes have varying degrees of secondary interactions with epoxy adhesives, and the surface energy after of aluminium substrates are different after deposition of the silanes.

8.2 Experimental

8.2.1 Materials

The substrate material used in this study was extruded aluminium alloy AA6060-T6. The composition of this alloy by weight is 0.46% Mg, 0.40% Si, 0.18% Fe, 0.021% Mn, 0.002% Cu, 0.015% Zn, 0.01% Ti, Al balance [18]. Extruded aluminium alloy AA7021-T1 was used as reinforcement material for the wedge test specimens. Both aluminium materials were supplied by Hydro Aluminium, Tønder, Denmark.

The one-component structural epoxy adhesive Betamate XD4600 was delivered by Dow Automotive, Freienbach, Switzerland. The following four silanes were delivered by ABCR, Karlsruhe, Germany: γ-glycidoxypropyltrimethoxysilane (GPS), acetoxypropyltrimethoxysilane (AcPS), methoxypropyltrimethoxysilane (MePS), and propyltrimethoxysilane (PS). The chemical structure of the silanes are shown in Table 1. Almeco 18, used for mild alkaline degrease, was obtained from Henkel.

Table 1
The chemical structure of the silanes used in this study

Silane	Chemical structure	Abbreviation
γ-Glycidoxypropyltrimethoxysilane	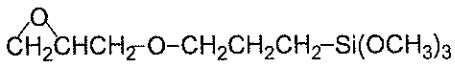	GPS
Acetoxypropyltrimethoxysilane	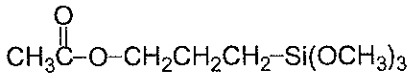	AcPS
Methoxypropyltrimethoxysilane	CH_3–O–$CH_2CH_2CH_2$–Si(OCH_3)$_3$	MePS
Propyltrimethoxysilane	$CH_3CH_2CH_2$–Si(OCH_3)$_3$	PS

8.2.2 Surface pretreatment procedures

The AA6060-T6 substrates were submitted to the pretreatment sequences described in Table 2 before silane treatment. Silanisation of the alkaline etched aluminium substrates was performed in 1 wt% silane solutions of deionized water and methanol. The water/methanol ratio was 80/20 by weight, and the pH of the water was adjusted to 5.0 using acetic acid. The silane solution was continuously stirred for 60 min at ambient for hydrolysis of the silane methoxy groups. Silanisation was performed by immersing the aluminium substrates into the solution for 10 min, after which they were rinsed in deionized water and dried at 93°C for 60 min. Substrates used for wedge tests were cooled to room temperature and immediately bonded. The applied silane treatment process has been shown to work well for GPS [6-10,16]. However, it is uncertain if this is the optimum process for the other silanes that were employed in this study.

Table 2
Pretreatment procedures applied to the AA6060-T6 substrates

Pretreatment	Aluminium substrate pretreatment procedure
Alkaline etch + desmut	Solvent degrease with a paper tissue soaked in acetone Mild alkaline degrease in 50 g/l Almeco 18 at 70°C for 5 min Alkaline etch in 10 wt% NaOH at 60°C for 50 s Rinse in spring water, then distilled water Desmut in 65 wt% HNO_3 at ambient for 90 s Rinse in spring water, then distilled water Dry at 60°C
Alkaline etch	Solvent degrease with a paper tissue soaked in acetone Mild alkaline degrease in 50 g/l Almeco 18 at 70°C for 5 min Alkaline etch in 10 wt% NaOH at 60°C for 50 s Rinse in spring water, then distilled water Dry at 60°C
Grit-blasting	Solvent degrease with a paper tissue soaked in acetone Grit-blast with 0.21-0.30 mm sharp edged alumina grit Blow off residual grit with N_2 gas Rinse with acetone
Phosphoric acid anodising (PAA)	As Alkaline etch + desmut followed by Anodise in 10 wt% H_3PO_4 at 25°C for 20 min at a constant voltage of 10 V Rinse in spring water, then distilled water Dry at 60°C

In order to obtain a relatively flat surface for the analysis, the specimens used for measurement of contact angles and analysis with reflection-absorption infrared spectroscopy were prepared by abrading them with a ScotchBrite® scouring pad (3M), and degreasing, prior to the alkaline etching + desmutting procedure.

8.2.3 Contact angle measurements

The surface energy, γ, of the silanised aluminium surfaces was determined by measuring the contact angle using the sessile drop method. The measurements were performed with a NRC Contact Angle Goniometer model 100-00 from Ramè-Hart, Inc., at ambient temperature and humidity. Ten drops of 5 µl were averaged for each measurement. The contact angle, θ, was determined for two test liquids: water and methylene iodide. The surface energy can then be divided into its polar, γ^p, and dispersive, γ^d, components:

$$\gamma = \gamma^p + \gamma^d$$

The following equations were used to obtain the polar and dispersive components of the surfaces [19], water (subscript 1) and methylene iodide (subscript 2):

$$\gamma_1(1+\cos\theta_1) = 2\sqrt{\gamma_1^d \cdot \gamma^d} + 2\sqrt{\gamma_1^p \cdot \gamma^p}$$

$$\gamma_2(1+\cos\theta_2) = 2\sqrt{\gamma_2^d \cdot \gamma^d} + 2\sqrt{\gamma_2^p \cdot \gamma^p}$$

The values used for the surface energy, γ, the dispersive component, γ^d, and the polar component, γ^p, were as reported in the literature [20]. These values were 72.2, 22.0, and 50.2 mN/m for water and 50.8, 48.5, and 2.3 mN/m for methylene iodide, respectively.

8.2.4 *Bond preparation and environmental testing*

Wedge-style reinforced double cantilever beam (RDCB) specimens were prepared for environmental testing. Two AA6060-T6 substrates and two AA7021-T1 reinforcements were bonded with XD4600 into a 'sandwich' assembly. Steel spacers were used to control the thickness of the bondline between the AA6060-T6 substrates. After curing in an oven at 180°C for 30 min, the 'sandwich' assembly was cut into RDCB specimens with the geometry shown in Fig. 1. The bonding procedure has been described in greater detail elsewhere [16]. Stainless steel wedges were inserted into the bondline, and environmental testing was performed at 40°C and 96% relative humidity. Phosphoric acid anodising (PAA) was used as benchmark reference.

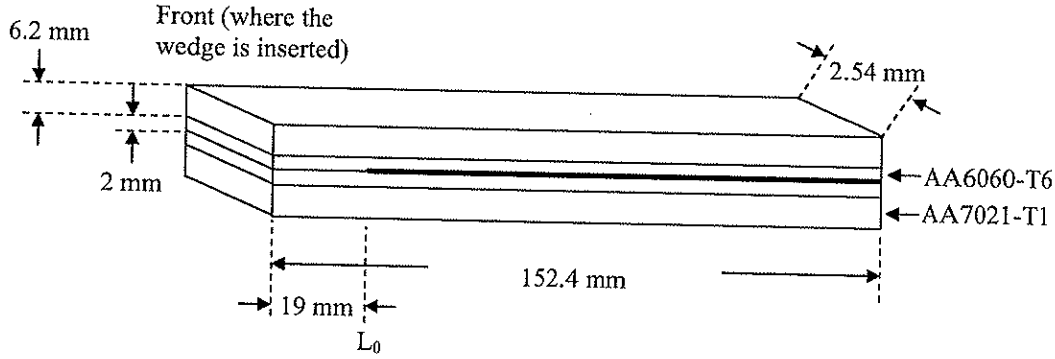

Figure 1. Schematic drawing of a RDCB specimen before insertion of the stainless steel wedge. Geometry according to ASTM D 3762-79, except for specimen thickness. Bondline thickness is 0.1 mm. Measurement of crack length starts at point L_0.

8.2.5 *Reflection-absorption infrared spectroscopy*

Reflection-absorption infrared (RAIR) spectroscopy was used to investigate the silane treated aluminium substrates. The analysis was performed with a Perkin Elmer 1725X FT-IR Spectrometer, and the use of an external reflectance accessory enabled the infrared beam to be focused on the samples at 80° relative to the surface normal. The spectra were recorded as an average of 100 scans with a resolution 4 cm^{-1} in the range 400-4000 cm^{-1}. Transmission infrared spectra were obtained by deposition of the silane on KBr-pellets.

8.3 Results

8.3.1 Environmental durability

The total crack lengths during environmental exposure for the etched and silane treated substrates are shown in Fig. 2. The initial failure before environmental exposure in these specimens was cohesive within the adhesive. During environmental exposure the failure was interfacial between the adhesive and the surface. There was a significant difference in durability between the surfaces that were desmutted and not desmutted, with the not desmutted surface performing better of the two. Similar trends have also been observed by Lunder *et al.* [18] in lap shear tests. They claimed that the observations could be related to a difference in magnesium surface concentration. Alkaline etching of AA6060-T6 causes a 'smut' layer rich in magnesium oxide/hydroxide, but practically all magnesium is removed by desmutting in concentrated nitric acid. The epoxy adhesive used in the present work contains dicyandiamide as curing agent, and it has been reported that such systems are alkaline of nature [21]. Residues set free during curing of the adhesive, reacts with water, forming a strongly alkaline environment. The presence of magnesium oxide on the aluminium surface is expected to improve the stability in alkaline environment due to the fact that magnesium oxides are thermodynamically passive at high pH.

The durability of the substrates that were alkaline etched only (not desmutted) was significantly improved by silanisation with both GPS and AcPS (see Fig. 2). The durability was excellent for both silanes. In fact, both silane treatments resulted in durabilities that were comparable to phosphoric acid anodising (PAA). Of the existing pretreatments for adhesive bonding of aluminium, PAA is widely considered to give the most durable joints [22-23].

Silanisation of the alkaline etched and desmutted substrates resulted in lower durability. This is directly opposite of what was expected, at least for GPS, since GPS in several studies has been shown to improve the durability of adhesively bonded aluminium [6-10,16]. This is also the case for other surfaces in this study. A possible explanation for

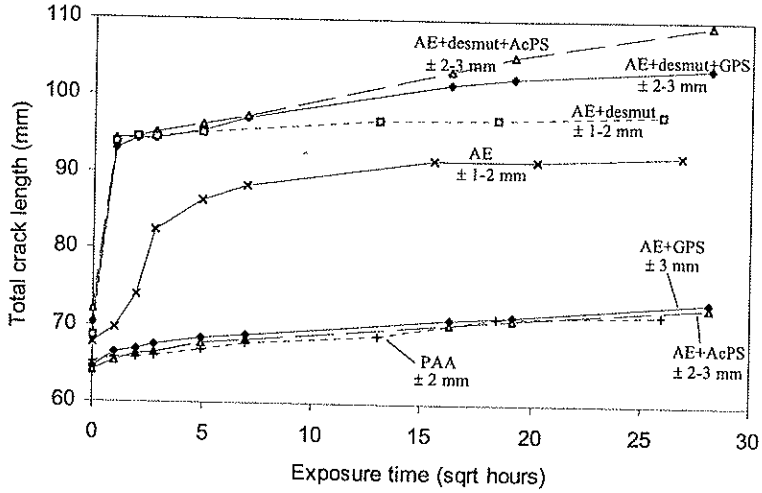

Figure 2. Total crack length as a function of exposure time for RDCB wedge test specimens. Substrate material was aluminium alloy AA6060-T6 that was alkaline etched and alkaline etched + desmutted prior to silane treatment and bonding with XD4600 epoxy adhesive. Test environment was 40°C and 96% relative humidity (AE denotes alkaline etching).

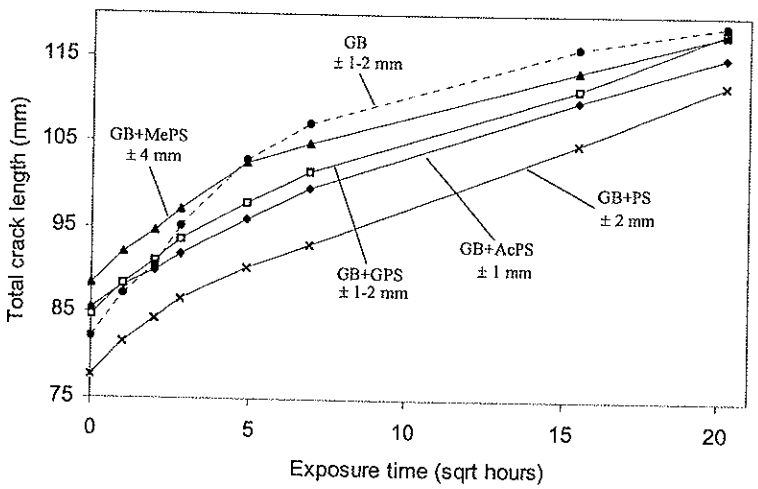

Figure 3. Total crack length as a function of exposure time for RDCB wedge test specimens. Substrate material was aluminium alloy AA6060-T6 that was grit-blasted with alumina prior to silane treatment and bonding with XD4600 epoxy adhesive. Test environment was 40°C and 96% relative humidity (GB denotes grit-blasting).

the decrease in durability can be the presence of acidic residues on the surface after desmutting in nitric acid. It is known that the SiOSi bonds in a siloxane film can rehydrolyse in acidic environments [24]. Any residues of acid left on the aluminium surface after rinsing in water can then have a degrading effect on the silane films, as the films rehydrolyse into smaller oligomeric species, resulting in a loss of cohesive strength. GPS gave better durability than AcPS.

Since the durabilities of both GPS and AcPS on the alkaline etched surface were equal and comparable to PAA, and since both silanes gave poor durability on the alkaline etched and desmutted surface, it was decided to test the silanes on another surface. It was determined to use grit-blasted surfaces. The treatment of this surface with GPS has in a previous study been shown to give very good durability, which was better than that of the grit-blasted surface [16].

The durability of the grit-blasted and silane treated wedge test joints are shown in Fig. 3. All silane treated surfaces performed better than the only grit-blasted surface, that is, all silane treatments had a positive effect on durability. However, the joints treated with PS clearly gave the best performance. The PS surface gave both shorter initial crack length and lower crack growth than the grit-blasted surface. According to the theory of covalent bonding, GPS should have performed better than the unreactive silanes that were tested. The GPS surface gave a higher initial crack length than the grit-blasted surface, but the durability was better. The durability of the AcPS surface was slightly lower than that of the GPS surface.

8.3.2 Contact angle measurements

The results of the contact angle measurements are shown in Table 3. The surface energy of the alkaline etched and desmutted aluminium surface was higher than the surface energies, γ, of the silane treated surfaces. The dispersive components, γ^d, of the silane treated surfaces were higher or equal to the corresponding value of the etched surface. However, large differences in the polar component, γ^p, of the surface energy were

detected. The polar components of the silane treated surfaces were lower, in some cases significantly lower, than the polar component of the etched surface.

Table 3
Measured contact angles and calculated surface energies of the silanised aluminium surfaces

Treatment	Contact angle (degrees)		Surface energy (mN/m)		
	H_2O	CH_2I_2	γ^p	γ^d	γ
Alkaline etch + desmutting	28.0	32.7	36.2	29.2	65.4
	- not rinsed before drying -				
GPS	58.0	25.2	13.9	37.6	51.6
AcPS	48.8	38.7	23.5	29.5	53.1
MePS	69.4	49.5	11.5	27.8	39.4
PS	100.5	61.8	0.5	27.2	27.7
	- rinsed before drying -				
GPS	76.0	39.0	5.7	35.5	41.2
AcPS	63.8	46.5	14.6	28.4	42.9
MePS	68.3	48.4	10.8	31.1	41.9
PS	86.2	44.5	2.3	35.0	37.3
Grit-blasting	73.0	38.3	7.1	35.2	42.2
	- rinsed before drying -				
GPS	105.8	35.5	0.6	46.1	46.7
AcPS	81.5	37.3	3.1	38.0	41.1
MePS	-	-	-	-	-
PS	119.0	52.5	2.2	38.3	40.5

There were significant differences in the surface energies of the silane treated surfaces that were not rinsed before drying. The largest difference was found in the polar component of the surface energy, which varied from 0.5 to 23.5 mN/m. The effect of the substituted organic group on the polarity of the surface followed the decreasing order:

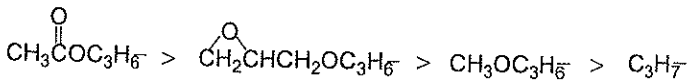

The large difference in the polar component can be explained by the polarity of the substituted organic groups. The propyl-group is a highly unpolar hydrocarbon, while the acetoxypropyl-, glycidoxypropyl- and methoxypropyl-groups contain oxygen atoms that contribute to increased polarity.

The substituted organic group also had effect on the dispersive component of the surface energy. The following decreasing order was observed:

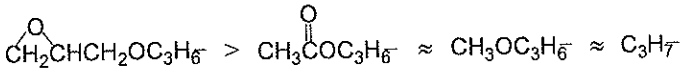

Lee [15] determined the surface energy of different silane films on glass substrates. The effect of the functional group on wettability of silanes was examined for both unreactive and reactive compounds. It was observed somewhat different surface energies of different silane films on glass substrates, as compared to what we observed on aluminium substrates. Exactly the same values can not be expected since the substrates are different. Nevertheless, the major trends are comparable, although there were some significant differences. Lee [15] found that the polar component was much higher than the dispersive component on the GPS treated surface, opposite of what we observed (low value of the polar and high value of the dispersive component). It is surprisingly that he found such a large difference in the polar component between GPS and AcPS, 40.1 and 16.8 mN/m, respectively. The polar component of the AcPS surface was comparable to that of the PS surface, which was 13.6 mN/m. We also observed a very low value of the dispersive component of the PS surface, compared with the observations of Lee [15].

The surface energies of the silane treated surfaces that were rinsed before drying were all of approximately the same order (see Table 3). The surface energies of the GPS and AcPS surfaces were significantly decreased after rinsing, while the surface energy of the PS surface was significantly increased. The differences in the polar components of the rinsed surfaces were smaller than on the unrinsed surface. The polar component varied from 2.3 to 14.6 mN/m, but PS still gave the lowest value, while AcPS gave the highest

value. Also, the GPS and PS surfaces gave the highest values of the dispersive component, 35.5 and 35.0 mN/m, respectively.

Great care should be taken when interpreting the data from the contact angle measurements of the grit-blasted surfaces, also shown in Table 3. The very rough surface may result in contact angle hysteresis. In this case the intrinsic contact angle is different from the visually observed contact angle [19]. However, it seems clear that the silane treatments changed the chemical properties of the grit-blasted surface. The total surface energies are all of the same order, but the data indicates that the silane treated surfaces were more hydrophobic than the grit-blasted surface.

The surface energies of the grit-blasted and alkaline etched surfaces cannot be directly compared due to different levels of surface roughness, but it seems that the surface energy of the grit-blasted surface is lower than that of the alkaline etched surface. The grit-blasted surface also performed inferior in wedge tests. The difference in surface energy can be connected to surface contamination. It was observed that the surfaces were heavily contaminated during the grit-blasting process. The alumina grit used for grit-blasting was recycled inside the chamber in which the grit-blasting was performed, creating a very contaminated atmosphere in the chamber. The acetone degreasing may have been less effective for removal of this contamination from the surfaces.

8.3.3 Infrared spectroscopy

The transmission infrared spectra of the silanes are shown in Fig. 4. In all spectra a strong band at 1088 cm^{-1} and a weaker band at 822 cm^{-1} are attributed to the unhydrolysed $SiOCH_3$ group. These bands can be monitored in order to determine the degree of hydrolysis. The bands at 1195 cm^{-1} are attributed to Si-C, while the C-H stretching modes can be seen at 2942 (for PS at 2958) and 2841 cm^{-1}. The spectra of the different silanes contain some peaks which are characteristic of each silane. In the spectrum of GPS the band of the epoxy ring can be seen at 910 cm^{-1}, while the C=O and C-O stretching modes can be seen in the spectrum of AcPS at 1741 and 1240 cm^{-1}, respectively. The vibrational assignments are based on ref. [25].

(A) GPS

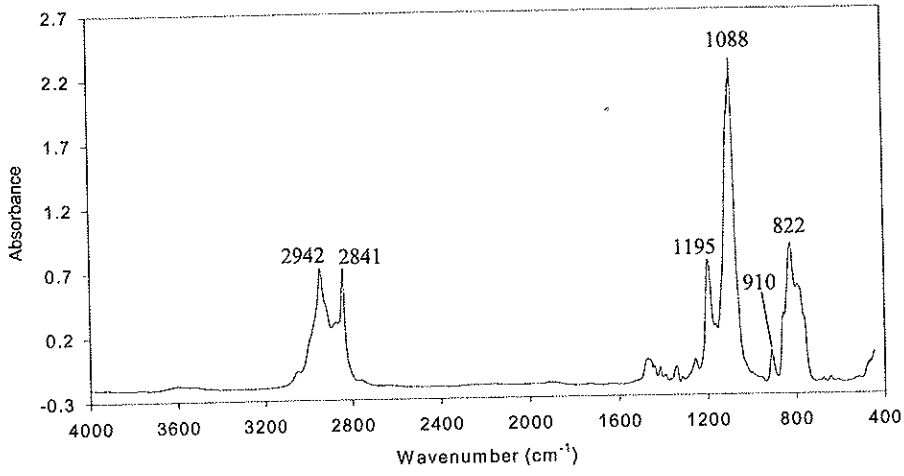

(B) AcPS

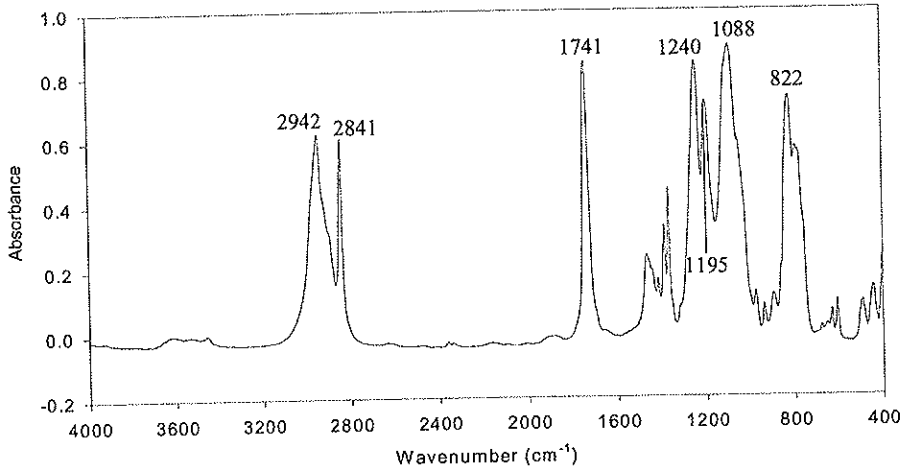

Figure 4. Transmission infrared spectra of silanes: (A) GPS, (B) AcPS, (C) MePS, and (D) PS.

(C) MePS

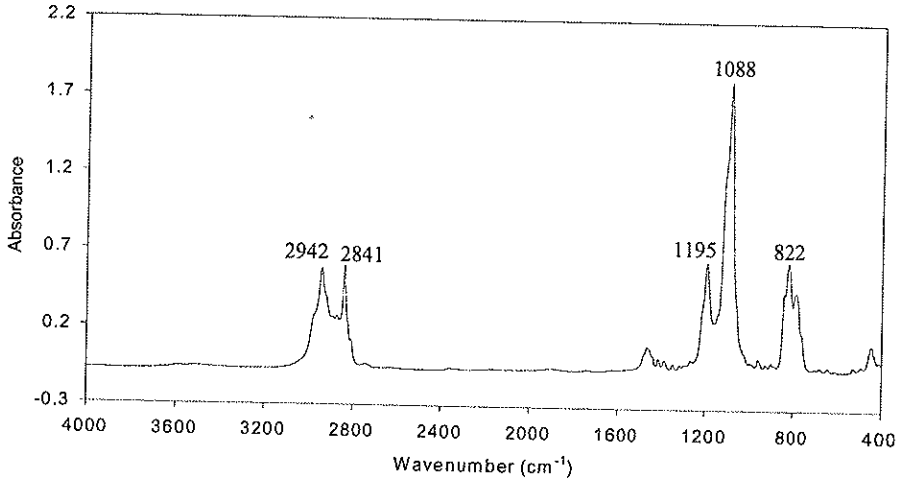

(D) PS

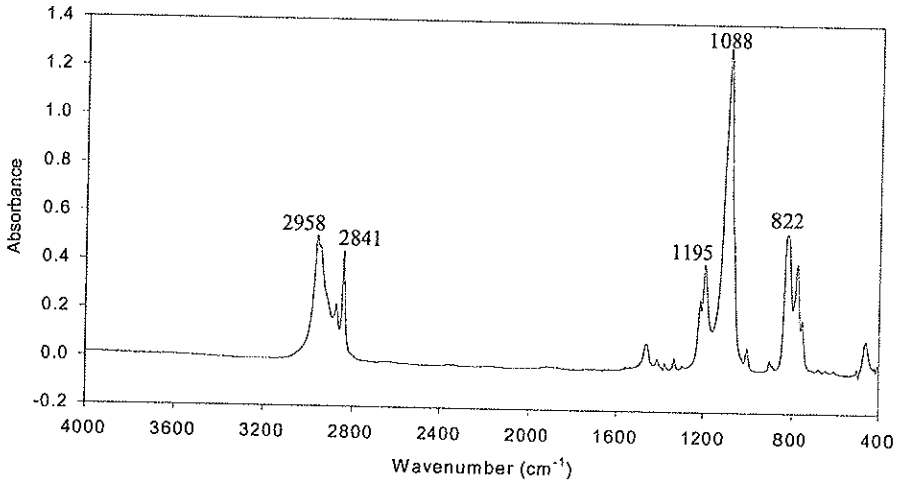

Figure 4. (cont.)

(A) GPS

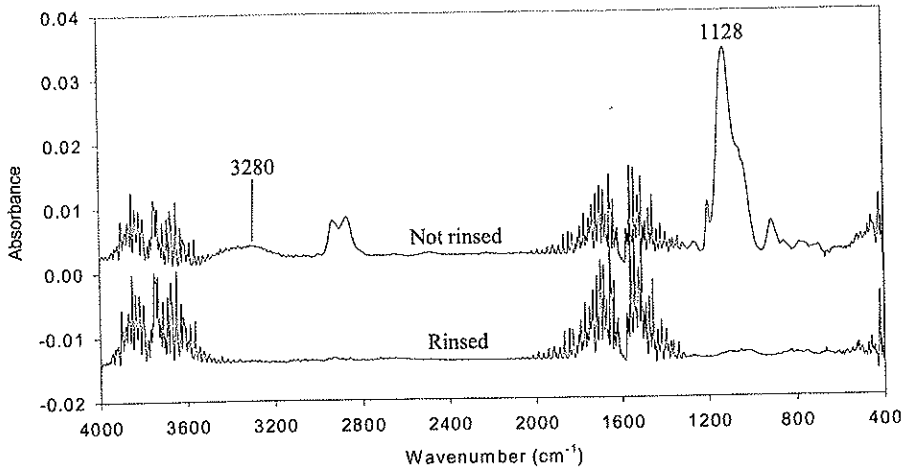

(B) AcPS

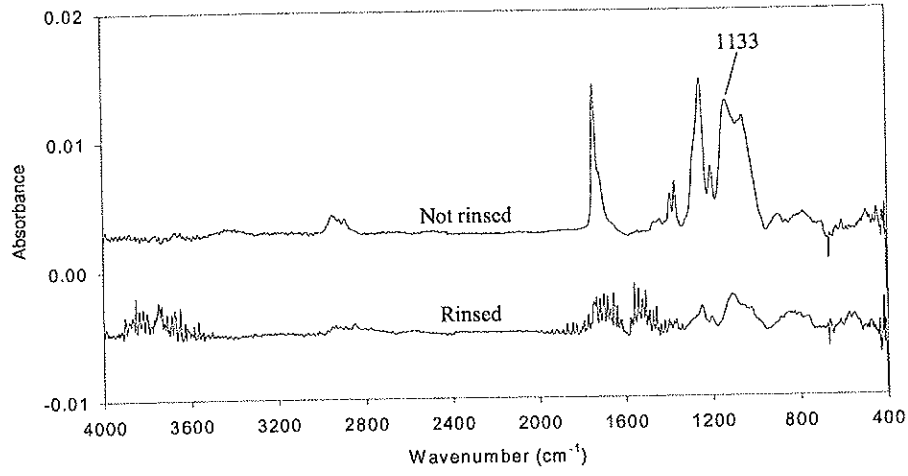

Figure 5. RAIR spectra of alkaline etched and desmutted AA6060-T6 surfaces treated with silanes: (A) GPS, (B) AcPS, (C) MePS, and (D) PS. Spectra were obtained from surfaces that were rinsed and not rinsed prior to drying.

(C) MePS

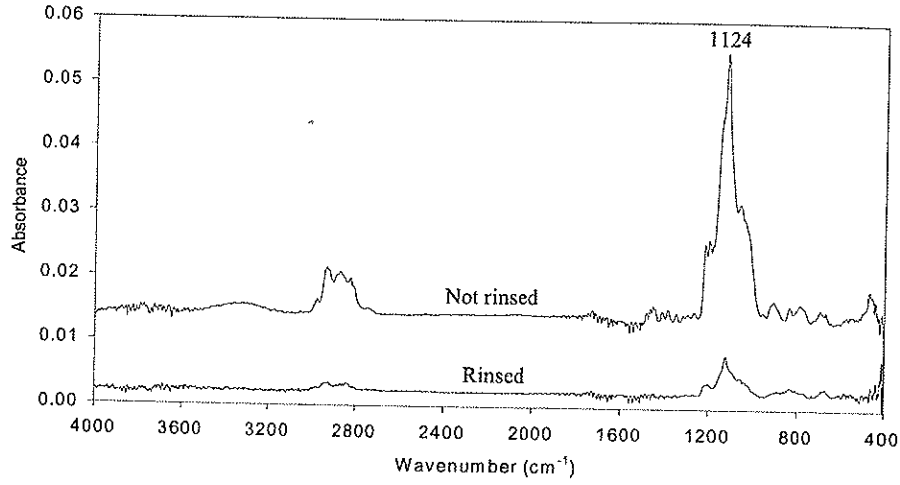

(D) PS

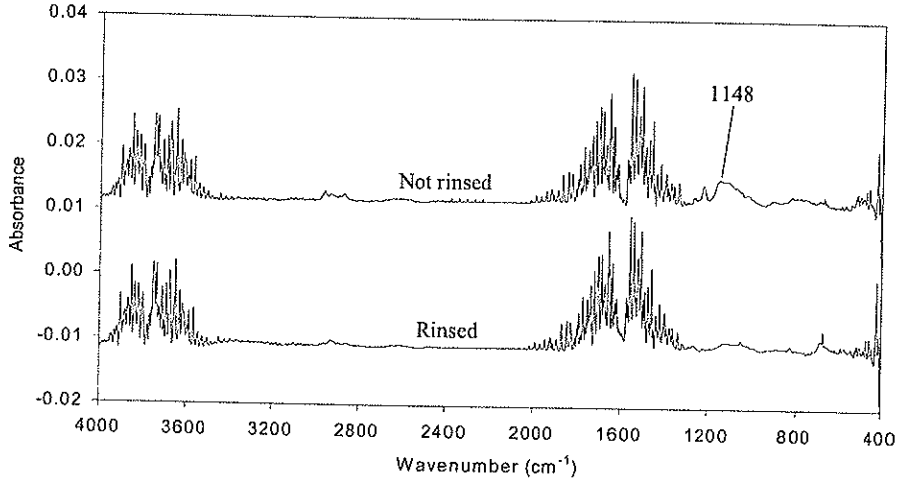

Figure 5. (cont.)

Fig. 5 shows RAIR spectra of the silane films on alkaline etched and desmutted aluminium surfaces. During the drying process, the hydrolysed silanes condense in the formation of a crosslinked siloxane network on the aluminium surface. The existence of the siloxane network can be seen by the presence of the strong SiOSi band at 1128 cm^{-1} (GPS), 1133 cm^{-1} (AcPS), 1124 cm^{-1} (MePS) and 1148 cm^{-1} (PS) in the spectra of films that were not rinsed before drying. The hydrolysed SiOH groups have condensed in the formation of SiOSi bonds. The O-H stretching band at 3280 cm^{-1} in the spectrum of GPS indicates that the silane film is not fully condensed. PS seemed to produce a thinner siloxane film than the other silanes. The intensity of the SiOSi band at 1148 cm^{-1} was low. Some spectra exhibited noise above 3400 cm^{-1} and between 2000 and 1300 cm^{-1}, which is due to water.

If a siloxane network is present, as in this case, the 1088 cm^{-1} band of the $SiOCH_3$ group can be masked by the strong SiOSi absorption. Then the signal can not be used to determine the degree of hydrolysis. However, the band at 822 cm^{-1} is not present in the spectra of the silane films. This indicates that the silanes were fully hydrolysed after one hour in the water/methanol solution.

Rinsing had a significant effect on silane film thickness, as can be seen from Fig. 5. After rinsing, little silane could be detected with RAIR. The rinsing process removes any loosely absorbed silane and leaves only a thin siloxane network/silane film. No GPS, and only traces of PS, could be detected after rinsing. However, AcPS and MePS seemed to leave a thin, detectable siloxane film after rinsing.

Wedge test joints with silane films that were not rinsed before drying performed catastrophically. The failure seemed to occur cohesively in the thick silane films or in the silane-adhesive interfaces. Hence, high silane film thickness had a very negative effect on durability. The exact thicknesses of the silane films were not measured.

8.4 Discussion

Silane treated surfaces performed better than untreated surfaces in wedge tests (except for alkaline etched and desmutted surfaces). AcPS performed just as well as GPS on the alkaline etched surface, and PS performed best on the grit-blasted surface. It is likely that the epoxy group in GPS will react with amine curing agents in the epoxy adhesive, forming a covalent 'bridge' between the surface and the adhesive. However, AcPS or MePS are less likely to react with the adhesive, while PS contains no organofunctional group with the potential to react with the adhesive. Still, PS performed best on the grit-blasted surface, while AcPS and GPS performed equal on the alkaline etched surface. This indicates that chemical reaction is not necessary for improved durability. This was also a conclusion drawn by Walker [14]. Physical effects as chain tangling and interpenetrating networks, and the effects of weak secondary interactions, may play an important role. Plueddemann [13] concluded that the performance of the silane coupling agent might depend as much on physical properties, resulting from the method of application, as on the chemistry of the organofunctional silane used.

A possible explanation for the observed behaviour may be connected to the hydrophobicity of the bonded surface. The contact angle measurements showed that the hydrophobicity of both the alkaline etched and grit-blasted surfaces was changed after the silane treatments. The surfaces were more hydrophobic after silane treatment. Based on contact angle measurements, PS is expected to generate the most hydrophobic surface. A hydrophobic surface can to some extent prevent water from entering the interface. More water enters surfaces which are less hydrophobic. The presence of water at the crack tip is a prerequisite for the crack growth observed in wedge tests. Wedge test joints have been exposed to dry environments of up to 60°C without showing any, or very few, signs of crack growth. Thus, the presence of water at the crack tip is essential for rapid bond degradation.

As mentioned earlier, GPS has been shown to improve durability. This is normally explained by covalent bonding to the adhesive and increased hydrolytic stability of the

surface. The contact angle measurements showed that GPS resulted in a rather hydrophobic/unpolar surface. It is possible that the hydrophobicity of the surface contributes to the observed effect on durability in addition to the positive effect of covalent bonding. This effect has been neglected in previous studies.

Another important requirement for good adhesion is the compatibility between the surface and the adhesive. The maximum strength of an adhesively bonded joint is to be expected when the surface energies of the adhesive and the surface are equal [26], or, in other words, when the interfacial free energy is at its minimum value. Thus, the interfacial free energy depends on both the surface energies of the surface and the adhesive. It has been reported that decreased interfacial free energy leads to increased adhesive strength [27-28]. Different adhesives have different surface energies, which results in different interfacial free energies. The XD4600 epoxy adhesive used in this study seems to be more compatible with unpolar surfaces. Kim and Ajersch [29] measured the surface energy of films of XD4300 epoxy adhesive, which was a predecessor to XD4600. They found that the polar component of the surface energy was 2.5 mN/m, while the dispersive component was 27.5 mN/m. They also claimed that good dry adhesion and high water resistance are obtained when the dispersive component is high and the polar component is low.

The initial failures in the grit-blasted specimens were a mixture of cohesive and interfacial failure. The cohesive part of the failure was very close to the aluminium surface, and there was more interfacial failure in specimens with a longer initial crack. Cohesive failure in the initial crack was not observed in a previous study of similar joints [16]. These joints also gave much shorter initial cracks. We believe that the long initial cracks in the present study are a result of surface contamination, creating a weak boundary layer between the surface and the adhesive. On the grit-blasted surface in this study, PS gave the shortest initial crack. PS contains an unpolar organofunctional group and may more effectively than other, more polar silanes, wet or interact with the contaminated grit-blasted surface.

More corrosion of the aluminium surface could be observed in the failure area of the grit-blasted specimens that were not treated with silanes before bonding. Very little corrosion could be observed on the silane treated surfaces. This suggests that the different silane films had a protecting effect. It has been shown by XPS that a film of GPS on aluminium has a protecting effect against hydration of the surface [6-7].

8.5 Conclusion

The importance of covalent bonding between silane treated aluminium surfaces and an epoxy adhesive was investigated. Silanes with and without organofunctional groups with the potential to form covalent bonds with the adhesive were used. The results showed that the hydrophobicity of the bonded surface was an important factor with respect to durability. The silanes that generated the most hydrophobic surfaces performed best in wedge tests. This trend occurred independently of the ability of the organofunctional group to react with the adhesive. Thus, chemical reaction is not necessary for improved durability after silanisation. The hydrophobicity of the surface can to some extent prevent water from entering the aluminium-adhesive interface. More water enters surfaces that are less hydrophobic. Less water present at the surface can improve durability because the presence of water at the crack tip is a prerequisite for the crack growth observed in wedge tests.

There was a significant difference in durability between alkaline etched surfaces that were desmutted and not desmutted in concentrated nitric acid. The not desmutted surface performed better. The observations can be related to a difference in magnesium surface concentration. Desmutting removes a 'smut' layer rich in magnesium oxide [18]. The epoxy adhesive is alkaline of nature, and the presence of magnesium oxide on the aluminium surface is expected to improve the stability in alkaline environment due to the fact that magnesium oxides are thermodynamically passive at high pH.

Acknowledgements

Thanks are due to Hydro Automotive Structures and The Research Council of Norway for financial support.

References

[1] M. Brémont and W. Brockmann, *J. Adhesion* **58**, 69-99 (1996)

[2] A.J. Kinloch, *Proc. Institution Mech. Eng.* **211**. 307-335 (1997)

[3] N.L. Rogers, in: Adhesive Bonding of Aluminum Alloys, E.W. Thrall and R.W. Shannon (Eds.), Marcel Dekker, New York, 1985. p. 41-50.

[4] M.R. Horner, F.J. Boerio and H.M. Clearfield, in: Silanes and Other Coupling Agents, K.L. Mittal (Ed.), VSP, Utrecht, 1992. p. 241-262.

[5] A.N. Rider, D.R. Arnott, A.R. Wilson and O. Vargas, *Mater. Sci. Forum* **189/190**, 235-240 (1995)

[6] A.N. Rider and D.R. Arnott, *Surf. Interface Anal.* **24**, 583-590 (1995)

[7] D.R. Arnott, A.R. Wilson, A.N. Rider, L.T. Lambriandis and N.G. Farr, *Appl. Surface Sci.* **70/71**, 109-113 (1993)

[8] R.P. Digby and S.J. Shaw, *Int. J. Adhesion Adhesives* **18**, 261-264 (1998)

[9] W. Thiedman, F.C. Tolan, P.J. Pearce and C.E.M. Morris, *J. Adhesion* **22**, 197-210 (1987)

[10] A.N. Rider and D.R. Arnott, *Int. J. Adhesion Adhesives* **20**, 209-220 (2000)

[11] M.-L. Abel, J.F. Watts and R.P. Digby, *Int. J. Adhesion Adhesives* **18**, 179-192 (1998)

[12] A. Rattana, J.D. Hermes, M.-L. Abel and J.F. Watts, *Int. J. Adhesion Adhesives* **22**, 205-218 (2002)

[13] E.W. Plueddeman, Silane Coupling Agents, Plenum Press, New York, 1982. p. 111-140.

[14] P. Walker, in: Silanes and Other Coupling Agents, K.L. Mittal (Ed.), VSP, Utrecht, 1992. p. 21-48.

[15] L.-H. Lee, in: Adhesion Science and Technology, Vol. 9B, L.-H. Lee (Ed.), Plenum Press, New York, 1975. p. 647-663.

[16] B.B. Johnsen, K. Olafsen, A. Stori and K. Vinje, *J. Adhesion Sci. Technol.* **16**, 1931-1948 (2002)

[17] B.B. Johnsen, K. Olafsen and A. Stori, *Int. J. Adhesion Adhesives* 23, 155-163 (2003)

[18] O. Lunder, B. Olsen and K. Nisancioglu, *Int. J. Adhesion Adhesives* **22**, 143-150 (2002)

[19] S. Wu, Polymer Interface and Adhesion, Marcel Dekker Inc., New York, 1982. p. 133-168.

[20] A.J. Kinloch, Adhesion and Adhesives, Chapman & Hall, New York, 1987.

[21] W. Brockmann, O.-D. Hennemann, H. Kollek and C. Matz, *Int. J. Adhesion Adhesives* **3**, 115-143 (1986)

[22] G.W. Critchlow and D.M. Brewis, *Int. J. Adhesion Adhesives* **16**, 255-275 (1996)

[23] G.W. Critchlow, *Trans. IMF* **76**, B6-B10 (1998)

[24] B.B. Johnsen, K. Olafsen, A. Stori and K. Vinje, *J. Adhesion Sci. Technol.* **17**, 1283-1298 (2003)

[25] C.N.R. Rao, Chemical Applications of Infrared Spectroscopy, Academic Press, New York, 1963.

[26] G.A. Dyckerhoff and P.-J. Sell, *Angew. Makromol. Chem.* **21**, 169-185 (1972)

[27] K.L. Mittal, *Polym. Eng. Sci.* **17**, 467-473 (1977)

[28] J. Wang and D. Feldman, *J. Adhesion Sci. Technol.* **7**, 565-576 (1991)

[29] G. Kim and F.J. Ajersch, *Mater. Sci.* **29**, 676-681 (1994)

Chapter 9

Silanisation of adhesively bonded aluminium alloy AA6060 with γ-glycidoxypropyltrimethoxysilane. II. Stability in degrading environments

Bernt B. Johnsen, Kjell Olafsen, Aage Stori, Kristin Vinje

J. Adhesion Sci. Technol. **17**, 1283-1298 (2003)

Abstract

Alkaline etched aluminium alloy AA6060 treated with of γ-glycidoxypropyl-trimethoxysilane was investigated. The stability of the silane films in degrading environments was investigated by exposing them to acidic and alkaline solutions at 40°C, followed by analysis with reflection-absorption infrared spectroscopy. Desorption of the silane from the surface occurred at pH 4, and at a much slower rate at pH 7, while the silane film was stable at pH 8. Two models for the degradation of the silanised aluminium surface in acidic environment were proposed: one involving simultaneously hydrolysis of the siloxane network and corrosion of the underlying aluminium surface, and one involving only corrosion of the aluminium surface. The durability of the silane treated surface was determined using wedge tests on joints made with XD4600 one-component epoxy adhesive. The durability was significantly reduced in highly acidic environment (pH 2), but no significant differences in durability were observed in the pH range from 4 to 11, except that the durability was slightly higher in higher alkaline environment during the initial period of testing. Better durability in an alkaline environment is connected to a better stability of both the siloxane network and the aluminium surface in this environment.

Keywords: Adhesive bonding; Aluminium; γ-Glycidoxypropyltrimethoxysilane; Reflection-absorption infrared spectroscopy; Durability.

9.1 Introduction

Adhesives have been used for many years in aerospace applications, where high durability bonded aluminium structures are obtained using adhesives based on phenolic or epoxy resins [1]. Adhesives are currently also used in many areas in the manufacture of automobiles, but so far the use of adhesives in structural applications has been limited. A major reason for the limited use of adhesives in structural automotive applications is the concern about the poor fatigue and durability behaviour of the bonded components. The adhesive joints must perform satisfactorily under service conditions that include dynamically applied loads and exposure to hostile environments such as water and road salt [2]. Unfortunately, water is one of the most hostile environments for adhesive joints. It is, therefore, necessary to use expensive surface pretreatment processes to obtain the required long-term service life of the joints [3].

The amorphous aluminium oxides produced by most surface pretreatments are not thermodynamically stable in moist environments and produce a complex range of oxide-hydroxides in presence of water: boehmite (AlOOH), bayerite ($Al(OH)_2$) and gibbsite ($Al(OH)_3$) [4]. Even in slightly acidic environments the following reactions may occur [5]:

$$Al_2O_3 + H_2O \rightarrow 2AlOOH$$

$$AlOOH + H_2O \rightarrow Al(OH)_3$$

The growth of hydration products will generate stresses that will result in local crack growth, thus the hydration products will reduce the local strength of the bond.

Brockmann *et al.* [5] proposed two models for the failure of adhesively bonded aluminium joints under the influence of moisture: one with and one without corrosion. One of the degradation mechanisms suggests that ammonia and low molecular weight amines are released when curing the epoxy adhesive systems, and these diffuse into the

polymer/oxide interphase. If water then penetrates into the bondline and comes in contact with these amines, an alkaline environment in which aluminium oxides are unstable will be formed at the adhesive/aluminium interface. Consequently, the aluminium oxide is destabilised and dissolved according to the reaction:

$$Al_2O_3 + 3H_2O + 2OH^- \rightarrow 2Al(OH)_4^-$$

Thus, the effect of alkaline environment on the durability of adhesively bonded aluminium joints is especially interesting from a practical point of view when amine-cured epoxy adhesive systems are utilised. Another degradation mechanism is the bondline corrosion where acidic hydrogen attacks the area around a weakly corroded zone, and causes failure in the oxide.

Organofunctional silanes are widely used as coupling agents to enhance the durability of adhesive joints during exposure to moisture at elevated temperatures [6]. A silane coupling agent will perform two functions in order to improve the environmental durability of a bonded joint [7]. First, it will increase the density of strong bonds between the oxide and the adhesive. Second, it will improve the hydrolytic stability of the aluminium oxide. The formation of a weak hydrated layer on the aluminium surface is significantly hindered by the formation of a cross-linked multilayer silane film and the ability to couple effectively with the adhesive [3,9-10]. One of the most common silanes for adhesive bonding is γ-glycidoxypropyltrimethoxysilane (GPS). The treatment of aluminium surfaces with GPS before bonding has been shown to improve bond durability [8-12]. In a previous paper it was shown that treatment with GPS significantly improved the adhesion and durability of adhesively bonded aluminium alloy AA6060 [13]. The positive effect of GPS was significant, regardless of the initial aluminium surface treatment.

Although much work has been done to investigate the deposition of GPS on aluminium [14-26], very little work has been done to investigate the stability of GPS films in degrading environments involving moisture and elevated temperature. One study of the

stabilising effect of silane films on aluminium surfaces was done by Arnott *et al.* [9], who used XPS to follow the growth rate of aluminium oxide in humid air at 50°C. It was shown that a film of GPS caused a marked reduction in the oxide growth during the first 10 min of exposure. The subsequent increase in oxide growth suggested that the protective GPS was leached from the surface. Once GPS is depleted from adsorption sites on the oxide surface, these sites are vulnerable to hydration, which will result in accelerated oxide conversion.

Taking into account that degradation of adhesively bonded aluminium joints may result in acidic or alkaline environment in the bondline, the study of the effects of these environments would be of interest. As mentioned above, silanisation with GPS improves adhesion and stabilises the aluminium surface in humid environment, but the effects of pH on GPS treated aluminium has, to our knowledge, not been investigated before. In this work the effect of acidic and alkaline environments on the stability of GPS on aluminium was investigated by exposing aluminium slides treated with GPS to aqueous solutions of different pH. The silane films were then investigated by reflection-absorption infrared (RAIR) spectroscopy in order to see if the structure of the silane film was altered or if the silane was leached from the aluminium surface. In order to investigate if the silane film protected the aluminium surface efficiently, bare aluminium slides were also exposed to the same environments. Another aim of this study was to investigate whether exposure to different levels of pH had an effect on the durability of adhesively bonded aluminium joints. This was done by exposing wedge test specimens to aqueous solutions of different pH.

9.2 Experimental

9.2.1 Materials

A one-component structural epoxy adhesive, XD4600 from Dow Automotive, Freienbach, Switzerland, was used for adhesive bonding of all aluminium specimens. The substrate material used in this study was extruded aluminium alloy AA6060-T6. The chemical composition of this alloy is; Mg 0.50 wt%, Si 0.40 wt%, Fe 0.18 wt%, Mn 0.02 wt%, others < 0.02 wt% and balance Al. The material used as reinforcement for the wedge test specimens was extruded aluminium alloy AA7021-T1. The aluminium materials were supplied by Hydro Aluminium, Tønder, Denmark. The particular adhesive and the aluminium alloy used as substrate material were chosen because they are of particular interest to the automotive industry. A model alloy AA6060 containing no Fe was also investigated. The composition of this model alloy is: Mg 0.50 wt%, Si 0.40 wt%, Mn 14 ppm and balance Al. Fe is not detectable. γ-Glycidoxypropyltrimethoxysilane (GPS) was obtained from Witco Europe SA (trade name: Silquest A-187).

9.2.2 Surface pretreatment procedures

The extruded AA6060 substrates were solvent degreased with a paper tissue soaked in acetone before abrasion with a ScotchBrite® scouring pad (3M). The substrates were then solvent degreased in acetone once more and dried at 60°C before alkaline etching. The etching process was performed in 10 wt% NaOH at 60°C for 50 s. The substrates were then rinsed in 1 wt% HNO_3 at room temperature for 2 min and in distilled water at room temperature for 10 min. They were then dried at 120°C for 15 min.

Silanisation was performed with a 1 wt% solution of GPS in distilled water. The pH of the solution was adjusted to 5.0 using acetic acid, and the solution was then continuously stirred for 60 min at ambient temperature, using a magnetic stirrer, for hydrolysis of the silane methoxy groups. The silane was deposited on the aluminium substrates used for wedge tests by wetting the surface by the silane solution for 10 min. The substrates were given a short rinse with distilled water before drying at 93°C for 60

min. Small specimens of size 20 × 45 mm^2 used for reflection-absorption infrared (RAIR) spectroscopy studies were silanised by immersing them in the silane solution for 10 min. The small specimens were also dried at 93°C for 60 min after silanisation.

9.2.3 Bond preparation and environmental testing

Wedge-style reinforced double cantilever beam (RDCB) specimens were prepared for environmental testing. The RDCB geometry was chosen in order to avoid plastic deformation of the substrates after insertion of the wedge. Two 110 mm wide AA6060 substrates with thickness 2 mm were bonded with XD4600, and a reinforcement made of AA7021 with thickness 6.2 mm was bonded with XD4600 at the back of each substrate. Steel spacers of thickness 0.1 mm were used to control the thickness of the bondline between the AA6060 substrates. The thickness of the substrate/reinforcement bondline was not controlled, but it was around 0.05 mm. The bonded 'sandwich' assembly was cured in an oven at 180°C for 30 min. After curing, this 'sandwich' assembly was cut into three RDCB specimens with specimen geometry according to ASTM D 3762-79. The only exception from the standard was that specimen thickness was 16.5 mm. All specimens were prepared at the same time, and five specimens were randomly picked out for each series. Fig 1 presents a schematic drawing of a RDCB

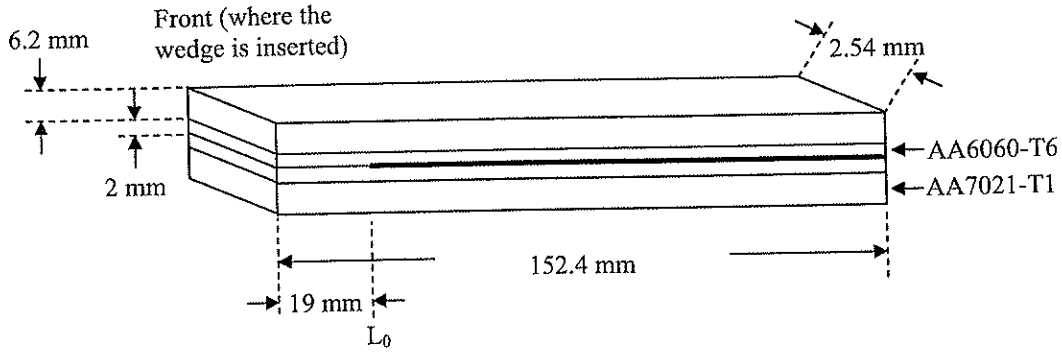

Figure 1. Schematic drawing of a reinforced double cantilever beam (RDCB) specimen before insertion of the stainless steel wedge. Geometry according to ASTM D 3762-79, except for specimen thickness. Bondline thickness is 0.1 mm. Measurement of initial crack length starts at point L_0.

specimen. Stainless steel wedges were inserted into the bondline with a tensile testing machine at a constant rate of 10 mm/min in order to introduce a highly stressed crack tip region. After insertion of the wedges, the RDCB specimens were stored overnight before measurement of initial crack length followed by environmental testing. Crack growth, as a result of environmental exposure, was measured at fixed intervals on both sides of each specimen.

The effect of acidic and alkaline environments on the durability of alkaline etched and GPS treated specimens was investigated by immersing the stressed RDCB specimens into solutions of different pH at 40°C. The pH of the solutions was in the range from 2 to 11. Na_2HPO_4/citric acid buffer solutions were used for pH 4, 7 and 8, while H_3PO_4 and NaOH were used for adjustment of the solutions giving pH 2 and 11, respectively. Stock solutions of 0.2 mol/L $Na_2HPO_4 \cdot 2H_2O$ and 0.1 mol/L citric acid were used for preparation of the buffer solutions given in Table 1.

Table 1
The composition of the buffer solutions. Stock solutions of 0.2 mol/L $Na_2HPO_4 \cdot 2H_2O$ and 0.1 mol/L citric acid were used for preparation of the buffer solutions

pH	Na_2HPO_4 (mL)	Citric acid (mL)
4.0	38.55	61.45
7.0	82.35	17.65
8.0	97.25	2.75

Table 2
Experimental matrix for alkaline etched AA6060 specimens exposed to different pH buffer solutions at 40°C and analysed with reflection-absorption infrared spectroscopy

pH	4	7	8
GPS film on AA6060	+	+	+
Bare AA6060	+	+	+
Bare model alloy of AA6060	+		+

9.2.4 *Stability of GPS films on aluminium*

Environmental effects on GPS films on aluminium were investigated by exposing the silanised specimens to solutions of different pH. The experimental matrix is shown in Table 2. The specimens were immersed in Na_2HPO_4/citric acid buffer solutions of pH 4, 7 and 8, at an elevated temperature of 40°C. The degradation of the GPS films was followed by removing the specimens from the buffer solutions at different times for analysis with RAIR. All specimens were thoroughly rinsed in distilled water and dried at 40°C before analysis. Reference specimens of bare, unsilanised aluminium substrates were also exposed and analysed for comparison purposes.

RAIR analysis was performed on a Perkin Elmer 1725X FT-IR Spectrometer where the specimens were mounted on an external reflectance accessory. The spectra were recorded as an average of 100 scans with a resolution 4 cm^{-1} in the range 400-4000 cm^{-1}. The use of an external reflectance accessory enabled the infrared beam to be focused on the sample at an angle 80° relative to the surface normal. A bare aluminium specimen (not treated with GPS) was used to obtain the background spectrum for the RAIR analysis. Elemental analysis was performed with a Cameca SX100 electron probe microanalyser. ToF-SIMS analysis was performed with a Cameca NanoSIMS 50 instrument. A Ga gun was used as the primary ion source.

9.3 Results and discussion

9.3.1 *Environmental effects on GPS films*

The infrared spectra of aluminium surfaces treated with GPS and exposed to different pH buffer solutions are shown in Fig. 2. The spectra obtained at different times have been shifted vertically for clarity. As can be seen from the spectra, the behaviour of the silane film in solutions of different pH at 40°C was different. At pH 4 (Fig. 2a) the silane gradually desorbed from the surface, as can be seen in the intensity reduction of the Si-O-Si band at 1118 cm^{-1} and the band of the epoxy ring at 910 cm^{-1}. After total exposure of 48 h the detected signal from the film was much lower, indicating a significantly lower amount of silane on the surface. This trend continued until 336 h

where no trace of the silane was detected with the infrared technique used here. During exposure, any alteration of the chemical structure of the silane film could not be detected with RAIR.

Investigations by a light microscope showed that grain-boundaries on the three surfaces exposed to pH 4 solution were much more distinct than on the initially unexposed surfaces, and simultaneously, a more 'bright' surface colour developed. Scanning electron microscopy (SEM) investigations of bare aluminium surfaces exposed to the same environments confirmed this observation. Fig. 3 shows SEM micrographs of surfaces that were exposed to solutions of pH 4 and 8. At pH 4, an etching effect of the whole surface can be observed. No extrusion lines are visible and the etching effect is enhanced at the grain boundaries. At pH 8, only slight etching takes place. The extrusion lines remain visible, but the grain boundaries cannot be seen. Thus, the acidic environment had a more degrading effect on the aluminium surface than the alkaline environment.

The effect of exposing the silane treated specimens to pH 7 (Fig. 2b) was the same as at pH 4, although at a much lower rate. A significantly less amount of silane was seen on the surface only after 336 h of total exposure. However, the silane seemed to have totally desorbed from the surface after 672 h. While the silane films deposited on specimens that were exposed to neutral and acidic environments desorbed from the surfaces, there was no such trend for the GPS treated specimen exposed to alkaline environment at pH 8 (Fig. 2c). Up to 672 h there was no sign of desorption of silane from the surface.

There are two possible models of how the observed degradation of the GPS treated aluminium surface in an acidic environment can take place. One is linked to the degradation of the silane film and the other is linked to the corrosion of the underlying aluminium surface. Corrosion of the aluminium surface can occur if water and H^+/OH^--ions diffuse through the silane film towards the surface. Hydration or etching of the aluminium oxide then takes place and the silane is leached from the surface and goes

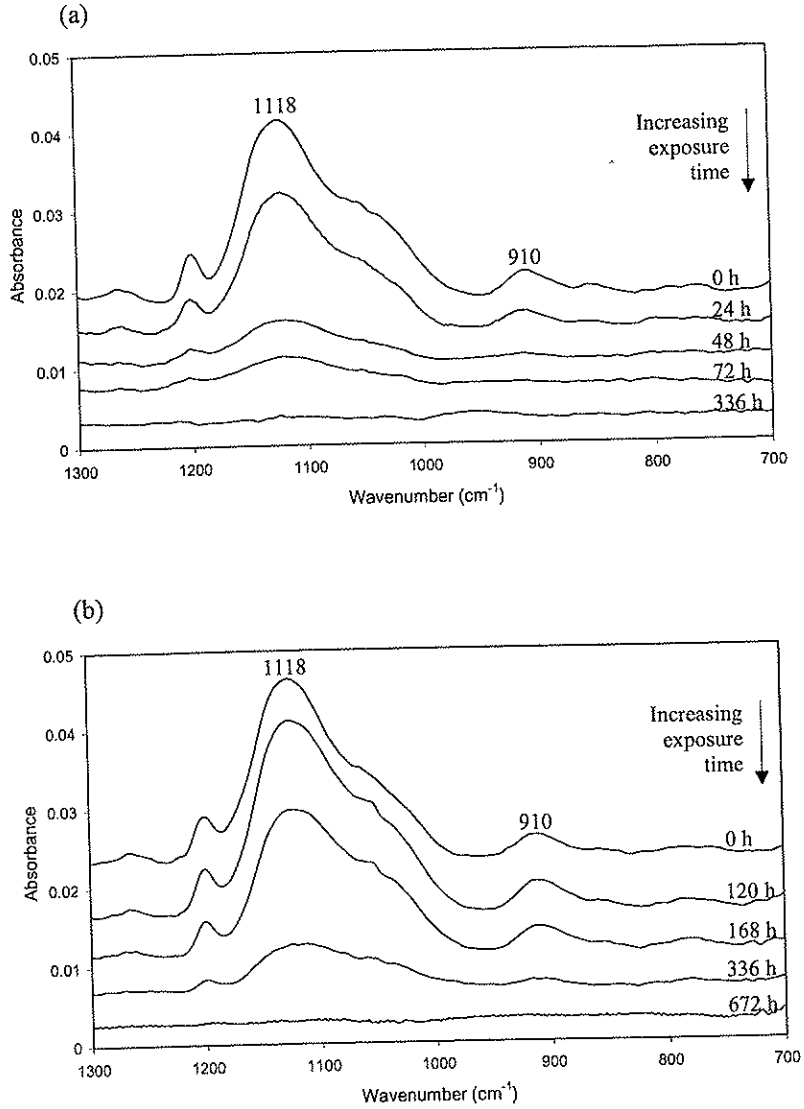

Figure 2. Reflection-absorption infrared spectra of GPS coated AA6060 surfaces immersed in buffer solutions at 40°C: (a) pH = 4, (b) pH = 7 and (c) pH = 8. The total time of environmental exposure is indicated in the figures.

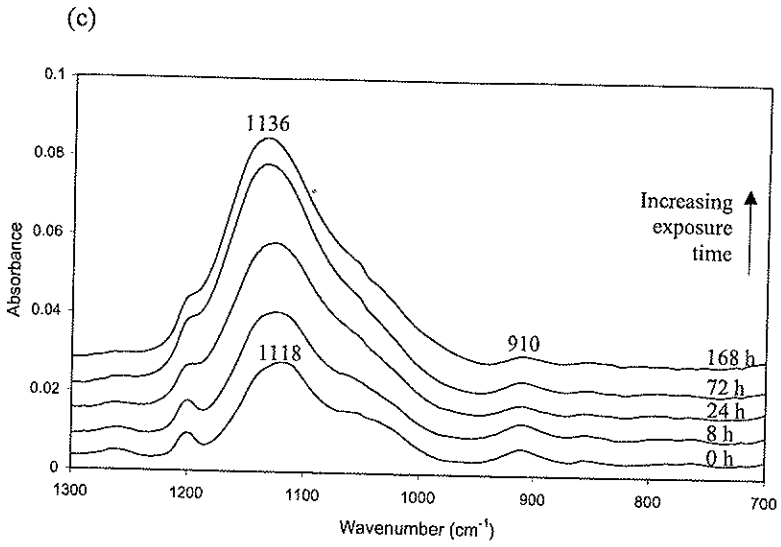

Figure 2. (cont.)

into solution. Other authors have also shown that GPS fails to prevent corrosion of the aluminium surface [27]. The second model, i.e., the degradation of the silane film, is connected to hydrolysis of the siloxane network. We conducted experiments where a 10% solution of GPS in water was adjusted to pH 11 using NaOH. After about one hour under constant stirring the solution turned milky, suggesting that condensation to long polysiloxane species had taken place. The effect of pH on silane condensation is that low pH's tend to result in small oligomeric molecules, while high pH's result in long polysiloxane chains [28]. A portion of the milky solution was acidified to pH 4 using H_3PO_4. After 2-3 h the pH 4 solution became much more transparent, and eventually turned almost completely transparent overnight. A gelatinous precipitate was also observed. At the same time, a white precipitate in the pH 11 solution was observed. These observed effects are probably connected to further condensation of the polysiloxanes in the pH 11 solution, and rehydrolysis of the Si-O-Si bonds in the pH 4 solution, forming smaller oligomeric species. Hence, at low pH the silane film on aluminium could be rehydrolysing into smaller oligomeric species. These small molecules could then be lost during the rinsing operation before analysis. Thus, in the RAIR analysis, an intensity reduction, but no alteration of the chemical structure of the

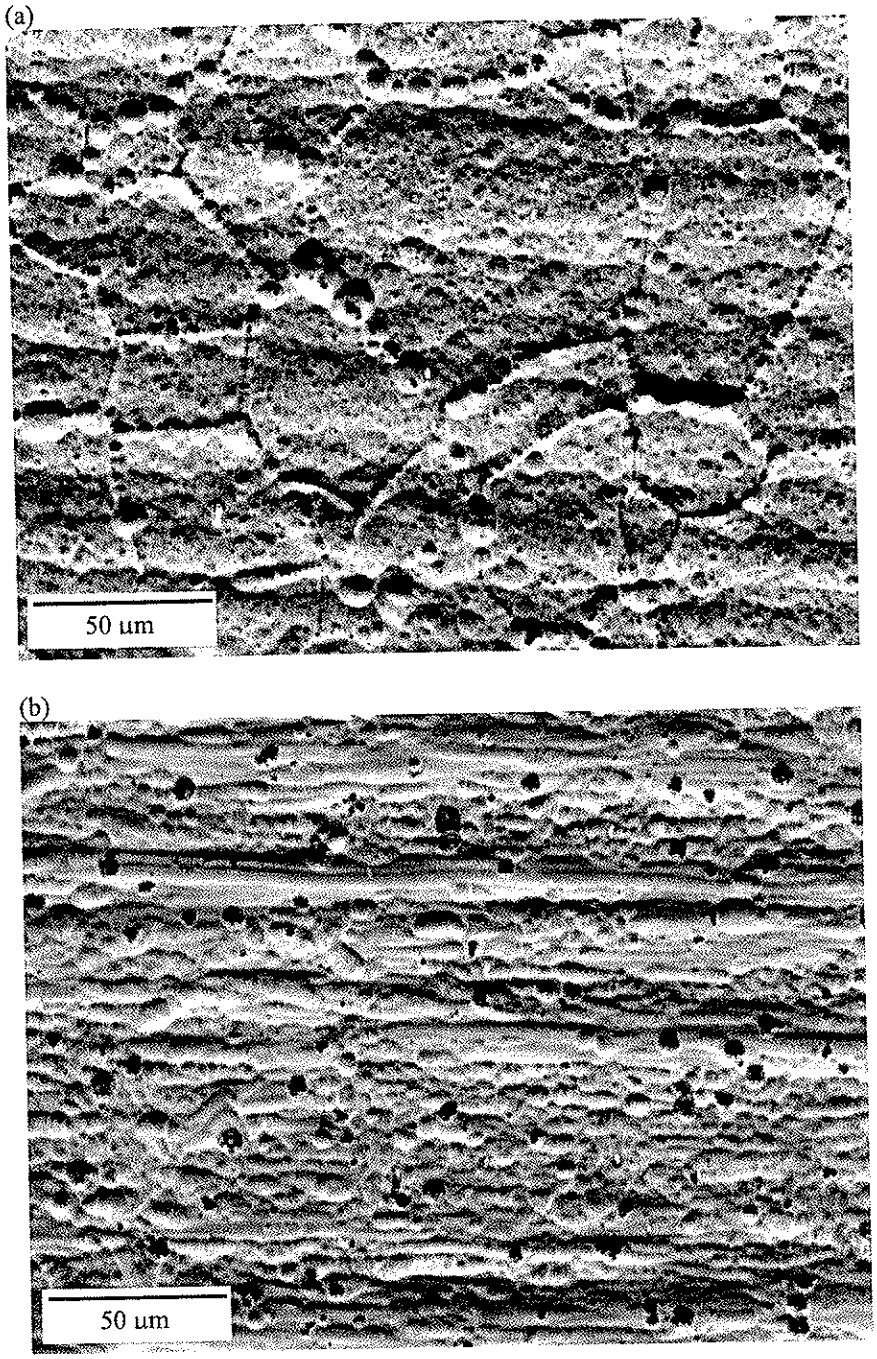

Figure 3. Scanning electron micrographs of bare AA6060 surfaces exposed to buffer solutions at 40°C for 672 h: (a) pH 4 and (b) pH 8.

silane films would be observed. Simultaneously, corrosion of the aluminium surface (as described above) could occur. In this model, the loss of silane and corrosion of the underlying aluminium surface would be two simultaneous, but unrelated processes. It is difficult to determine which one of the two models: corrosion of the aluminium surface *or* simultaneous loss of silane and corrosion of the underlying surface, best describes the observations in this study. However, the latter model is probably more likely.

As can be seen in Fig. 2c, there were significant changes in the infrared spectra at pH 8 over time. A band appeared at 1136 cm^{-1}. This band was initially partly overlapped by the Si-O-Si band at 1118 cm^{-1}, but after 24 h, the band at 1136 cm^{-1} was very strong, and the intensity of the band clearly increased with increasing time of exposure. Another broad band emerged at 3435 cm^{-1}, and the intensity of this band was also very strong after 24 h. The intensity of the bands at 1136 and 3435 cm^{-1} continued to increase until 168 h of environmental exposure, after which no significant changes were observed. Simultaneously, a brown colour that seemed to be evenly distributed on the surface developed. However, it was observed visually that the silane film had a protecting effect on localised spots with higher film thickness.

The bare aluminium specimen exposed to pH 8 behaved in a very similar fashion to the specimen treated with GPS. The same two strong bands at 1136 and 3435 cm^{-1} emerged and the brown surface colour also developed on the bare aluminium surface. It was suspected that the brown surface colour developed at pH 8 on the AA6060 surface was due to the formation of Fe oxide/hydroxide on the surface. This hypothesis was disproved by the fact that a model alloy AA6060, which did not contain any trace of Fe, also behaved very similarly.

The bare AA6060 surfaces that were exposed to buffer solutions at pH 4 and 8 were analysed using an electron microprobe analyser. The results of the elemental analysis are shown in Table 3. During the analysis a large number of dark spots were observed on the surface exposed to pH 8 (as shown in Fig. 3). Further analysis of these spots revealed that they contained much more Na, P and O than other parts of the surface. The spots must be traces of the Na_2HPO_4/citric acid buffer solution, which had been

adsorbed on the surface. SEM observations revealed that the material had precipitated in small surface pits during exposure and before drying and analysis with RAIR. Fig. 4 shows a scanning electron micrograph of some typical precipitates.

Table 3
Elemental analysis of bare AA6060 surfaces exposed to buffer solutions of pH 4 and pH 8 for 672 h (surface composition in atomic %)

Element	pH 4	pH 8	
Al	98.80	98.31	49.40[1]
Mg	0.53	0.52	0.20
Si	0.41	0.42	0.27
Fe	0.15	0.07	0.53
Cu	0.06	-	0.14
Mn	0.02	0.02	0.03
Zn	0.03	0.07	0.70
Na	-	0.14	4.00
Ca	-	0.05	1.80
P	-	0.40	11.70
O	-	-	31.23

[1]Elemental analysis of a typical surface precipitate on the pH 8 surface (see example in Fig. 4).

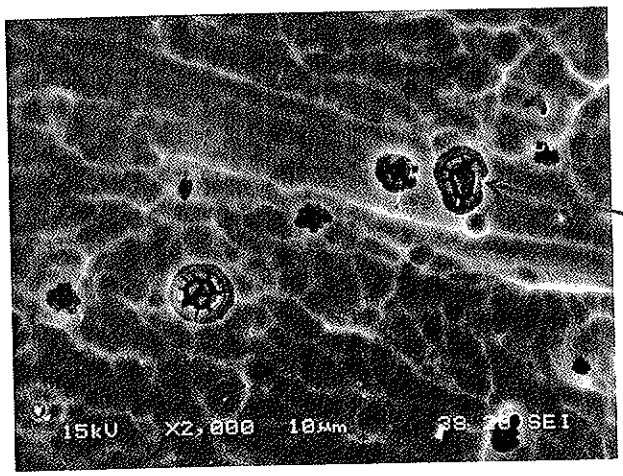

Figure 4. Scanning electron micrograph of precipitates on a bare AA6060 surface exposed to buffer solution of pH 8 at 40°C for 672 h. Magnification is 2000×.

9.3.2 Exposure of RDCB wedge test specimens to acidic and alkaline environments

The pH of the solutions, to which the different aluminium specimens were exposed, was selected with respect to the stability range of aluminium oxide. Since aluminium oxides are mostly stable in the pH range from 4 to 8 [5,29], these values were selected along with the neutral value, pH 7, and two more extreme values, pH 2 and 11. The two extreme values are well outside the stable pH range of the aluminium oxides, and an effect on durability was expected to occur at these pH values if the silane was unable to protect the aluminium surface.

High acidity had a very detrimental effect on the durability of RDCB wedge test joints made with GPS treated surfaces. All joints produced failure at the adhesive/aluminium interface. Fig. 5 gives the crack length during environmental exposure beyond the initial crack point. As can be seen, the crack growth in the joints exposed to pH 2 was much higher than for the joints exposed to higher levels of pH. As for the joints exposed in the

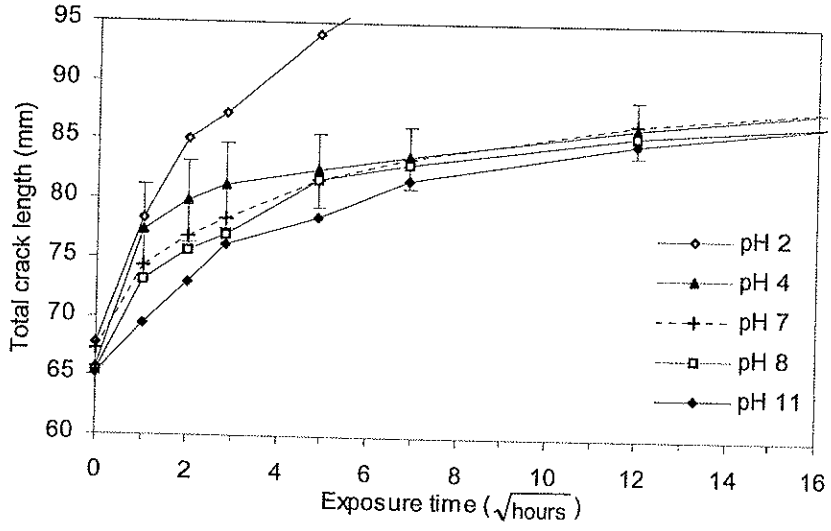

Figure 5. Total crack length as a function of exposure time for RDCB wedge test specimens. Substrate material was aluminium alloy AA6060 that was abraded, alkaline etched and treated with GPS before bonding with XD4600 epoxy adhesive. The specimens were immersed into solutions of different pH at 40°C.

pH range from 4 to 11, it was more difficult to draw any conclusions with respect to difference in durability. These joints seemed to behave very similarly, and the crack length values stabilised at approximately the same level after 48 h. However, there seemed to be some differences in durability during the first 24 h of testing, and the joints exposed to lower pH levels seemed to give higher crack growth rates in this period. It is noteworthy that the crack growth was directly related to pH in this period. Thus, pH 11 gave lower crack growth than pH 8, pH 8 gave lower crack growth than pH 7, and so on. As discussed earlier, the RAIR studies also showed better stability of the GPS treated aluminium specimens in alkaline than in acidic environment. However, in the RAIR studies significant differences in the pH range from 4 to 8 were observed, whereas only small differences were observed in the same range in the durability studies. The acidity was increased to pH 2 before any significant difference in durability was detected.

The reduced durability at pH 2 depends on both the stability of the silane film and the stability of the aluminium surface. As discussed earlier, the crosslinked siloxane film may be rehydrolysed in acidic solutions, resulting in the formation of lower molecular weight species. The hydrolysis of Si-O-Si bonds would have a negative effect on durability. Also, the aluminium surface itself was much more stable in alkaline than in acidic environment, in which an etching effect was observed (see Fig. 3a). This may have a significant influence on the durability of the joints.

It was remarkable that high alkalinity (pH 11) did not result in lower durability than the neutral value. pH 11 is well outside the stable pH range of the aluminium oxides, and it was expected that this would cause instability in the oxide layer according to the following dissolution reaction:

$$Al_2O_3 + 3H_2O + 2OH^- \rightarrow 2Al(OH)_4^-$$

It has been shown by Lunder *et al.* [30] that alkaline etching of AA6060 causes a 'smut' layer rich in Mg oxide/hydroxide. The Mg concentration at the surface is about 20 times

higher than in the bulk metal. Practically all Mg is removed by desmutting in concentrated nitric acid, but should not be affected by the short rinse in diluted nitric acid used in this study. The presence of Mg oxide in the aluminium oxide film is expected to improve the stability in alkaline environment due to the fact that Mg oxides are thermodynamically passive at high pH. On the other hand, Mg oxides dissolve readily in acidic solutions. These effects may contribute to the observed instability of the AA6060 surface in acidic environment, and vice versa in alkaline environments, which again will have effect on the durability of wedge test joints and on the stability of GPS films. The stabilising effect of Mg oxides when dicyandiamide-cured epoxy adhesives are applied, as in this study, has also been reported elsewhere [1]. Fig. 6 presents a ToF-SIMS image of the lateral distribution of Mg on the alkaline etched AA6060-T6 aluminium surface. The results of the elemental analysis in Table 3 correlated well with the given composition of the alloy, but the depth of analysis (1-2 μm) is too deep to detect any real surface effects on the metal surface. Nevertheless, the protecting effect of the silane layer should not be neglected. Treatment with GPS

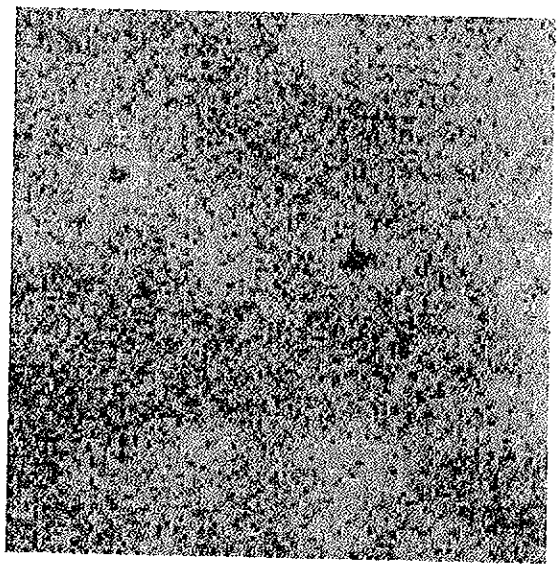

Figure 6. ToF-SIMS image showing the lateral distribution of Mg on the alkaline etched AA6060-T6 aluminium surface. Field of view is 100×100 μm.

results in improved durability [8-13], and in the study by Arnott *et al.* [9], it was shown that a film of GPS on aluminium caused a marked reduction in the oxide growth during the first 10 min of exposure to humid air. The exposure times in the present study are, however, much longer than those used by Arnott *et al.* [9], providing longer time for diffusion of water and H^+/OH^--ions through the GPS films towards the aluminium surface. Still, the silane film can very well have a significant effect on the degradation rate - slowing down the degradation process as compared to unsilanised joints.

An uncertain factor with the wedge test is the local pH near or just ahead of the crack tip. The slow diffusion of species through the adhesive or along the interface could result in strong pH gradients since the amines in the epoxy adhesive have a high buffering capacity. Maybe the pH must be as low as pH 2 before the solution pH has effect on the pH near the crack tip. In this case the pH at the crack tip would be approximately the same for the pH 4 to pH 11 solutions. There was also a problem with maintaining the pH of the solutions at the desired value; this was especially apparent for the pH 11 solution. After one week of testing, the pH dropped to around 9.5. The pH of the other solutions had also been slightly altered. New, fresh solutions were prepared every week due to these changes in pH.

9.4 Conclusion

Films of GPS on alkaline etched aluminium alloy AA6060 behaved differently in acidic, neutral and alkaline environments. In acidic environment (pH 4) the silane was desorbed from the surface. The same trend was observed in neutral environment (pH 7), although at a much slower rate, but in alkaline environment (pH 8) the silane film was stable. The GPS is present on the aluminium surface in the form of a crosslinked siloxane network. The stability of the silane film depends on the stability of the silane film itself and/or the stability of the underlying aluminium surface. It is unclear which one of the effects contributes most to the observed behaviour of the silane films. The siloxane network may be rehydrolysed in acidic environment, forming smaller oligomeric species that go into solution. However, the siloxane bonds are stable in

alkaline environments. It was also shown that the aluminium surface was much more stable in alkaline than in acidic environments. In acidic solution an etching effect of the surface occurred.

The durability of alkaline etched aluminium alloy AA6060 treated with GPS was significantly reduced in highly acidic environment (pH 2), but no significant differences in durability were observed in the pH range from 4 to 11. However, the durability was somewhat higher in more alkaline environments during the initial period of testing. Better durability in an alkaline environment is probably connected to a better stability of the siloxane network as well as of the aluminium surface.

Acknowledgements

Thanks are due to Hydro Automotive Structures and The Research Council of Norway for financial support. The authors also wish to thank Dr C. J. Simensen at SINTEF Materials Technology for help with the ToF-SIMS analysis.

References

[1] M. Brémont and W. Brockmann, *J. Adhesion* **58**, 69-99 (1996)

[2] R.A. Dickie, L.P. Haack, J.K. Jethwa, A.J. Kinloch and J.F. Watts, *J. Adhesion* **66**, 1-37 (1998)

[3] A.J. Kinloch, *Proc. Institution Mech. Eng.* **211**, 307-335 (1997)

[4] R.A. Pethrick, D. Hayward, K. Jeffrey, S. Affrossman and P. Wilford, *J. Mater. Sci.* **31**, 2623-2629 (1996)

[5] W. Brockmann, O.-D. Hennemann, H. Kollek and C. Matz, *Int. J. Adhesion Adhesives* **6**, 115-143 (1986)

[6] M.R. Horner, F.J. Boerio and H.M. Clearfield, in: Silanes and Other Coupling Agents, K.L. Mittal (Ed.), VSP, Utrecht, 1992. p. 241-262.

[7] A.N. Rider, D.R. Arnott, A.R. Wilson and O. Vargas, *Mater. Sci. Forum* **189/190**, 235-240 (1995)

[8] A.N. Rider and D.R. Arnott, *Surf. Interface Anal.* **24**, 583-590 (1995)

[9] D.R. Arnott, A.R. Wilson, A.N Rider, L.T. Lambriandis and N.G. Farr, *Appl. Surface Sci.* **70/71**, 109-113 (1993)

[10] R.P. Digby and S.J. Shaw, *Int. J. Adhesion Adhesives* **18**, 261-264 (1998)

[11] W. Thiedman, F.C. Tolan, P.J. Pearce and C.E.M. Morris, *J. Adhesion* **22**, 197-210 (1987)

[12] A.N. Rider and D.R. Arnott, *Int. J. Adhesion Adhesives* **20**, 209-220 (2000)

[13] B.B. Johnsen, K. Olafsen, A. Stori and K. Vinje, *J. Adhesion Sci. Technol.* **16**, 1931-1948 (2002)

[14] P.R. Underhill, G. Goring and D.L. DuQuesnay, *Appl. Surface Sci.* **134**, 247-253 (1998)

[15] P.R. Underhill, G. Goring and D.L. DuQuesnay, *Int. J. Adhesion Adhesives* **18**, 307-311 (1998)

[16] P.R. Underhill, G. Goring and D.L. DuQuesnay, *Int. J. Adhesion Adhesives* **18**, 313-317 (1998)

[17] P.R. Underhill, G. Goring and D.L. DuQuesnay, *Int. J. Adhesion Adhesives* **20**, 195-199 (2000)

[18] M.-L. Abel, J.F. Watts and R.P. Digby, *Int. J. Adhesion Adhesives* **18**, 179-192 (1998)

[19] M.-L. Abel, R.P. Digby, I.W. Fletcher and J. . Watts, *Surface Interface Anal.* **29**, 115-125 (2000)

[20] M.-L. Abel, A. Rattana and J.F. Watts, *J. Adhesion* **73**, 313-340 (2000)

[21] A. Rattana, M.-L. Abel and J.F. Watts, in: Proc. 24th Annual Meeting of the Adhesion Society, Williamsburg, 2001. p. 202-204.

[22] A. Rattana, J.D. Hermes, M.-L. Abel and J.F. Watts, *Int. J. Adhesion Adhesives* **22**, 205-218 (2002)

[23] Y.L. Leung, M.Y. Zhou, P.C. Wong and K.A.R. Mitchell, *Appl. Surface Sci.* **59**, 23-29 (1992)

[24] G.A. Woods, S. Haq, N.V. Richardson, S. Shaw, R. Digby and R. Raval, *Surface Sci.* **433-435**, 199-204 (1999)

[25] C.M. Bertelsen and F.J. Boerio, *Prog. Org. Coatings* **41**, 239-246 (2001)

[26] M. Kono, X. Sun, R. Li, K.C. Wong, K.A.R. Mitchell and T. Foster, *Surface Rev. Lett.* **8**, 43-50 (2001)

[27] P.R. Underhill and D.L. DuQuesnay, in: Silanes and Other Coupling Agents, Vol. 2, K.L. Mittal (Ed.), VSP, Utrecht, 2000. p. 149-158.

[28] E.W. Plueddemann, Silane Coupling Agents, Plenum Press, New York, 1982.

[29] E. Deltombe and M. Pourbaix, *Corrosion* **14**, 496-500 (1958)

[30] O. Lunder, B. Olsen and K. Nisancioglu, *Int. J. Adhesion Adhesives* **22**, 143-150 (2002)

Chapter 10

The durability of bonded aluminium joints: A comparison of AC and DC anodising pretreatments

Bernt B. Johnsen, Fabrice Lapique, Astrid Bjørgum

Int. J. Adhesion Adhesives **24**, 153-161 (2004)

Abstract

The environmental durability of anodised aluminium alloy AA6060-T6 bonded with a one-component epoxy adhesive has been investigated using the wedge test at 40°C/96% RH. DC and AC anodising in phosphoric and sulphuric acid solutions have been compared. Substrates that were AC anodised in hot phosphoric and sulphuric acid solutions performed very well, almost as good as the well-established FPL + DC-PAA pretreatment. The anodic oxide films were studied by reflection-absorption FT-IR spectroscopy. It was shown that the anodic films released water during curing of the adhesive at 180°C. The observations suggested that a transformation from the hydroxide, $Al(OH)_x$, to the oxide, Al_2O_3, state took place. Hot water sealing of the oxides produced in sulphuric acid significantly reduced the durability.

Keywords: Aluminium and alloys; Surface treatment; Infrared spectra; Wedge tests.

10.1 Introduction

Adhesives have been used for many years in aerospace applications. High durability bonded aluminium structures are obtained by using adhesives based on epoxy or phenolic resins [1]. It is well known that proper chemical pretreatment of the aluminium prior to epoxy bonding is essential for developing the bond strengths necessary for high performance aircraft applications [2]. DC anodising in phosphoric acid (DC-PAA) and chromic acid (DC-CAA) solutions are the preferred aluminium pretreatment methods for adhesive bonding in the aerospace industry. These processes typically produce a porous oxide film that exhibits good durability [2-6]. However, anodising times are quite long, making them expensive processes. There is also the problem of hexavalent chromium. Both the DC-PAA and DC-CAA processes often involve the use of hexavalent chromium. The DC-PAA substrates are normally submitted to a chromic-sulphuric acid etch prior to anodising, although ferric-sulphate processes are sometimes used instead. Hexavalent chromium is reported to be toxic [7], and environmental factors together with stricter legislation has led researchers to look for alternative, more environmentally friendly, pretreatment processes.

A cost-efficient alternative to DC anodising is AC anodising in hot acid solutions. AC anodising of aluminium has been used for many years in the coil coating industry, where anodising is performed on sheets moving at high speeds through hot acid electrolytes for periods of just few seconds. Another significant advantage of the AC process is that, apart from removal of surface grease or dirt, no degreasing or surface pretreatment prior to anodising is necessary. The aluminium substrates can be anodised as-received, since hydrogen evolution at the surface has a strong cleaning effect. These factors significantly reduce the number of process steps employed, and process times can be reduced from several minutes, typically 15-20 minutes for DC anodising, to less than a minute or only a few seconds.

Sealing of anodised surfaces in boiling water is often performed in order to improve the corrosion resistance of the surfaces, but is normally not recommended for structural

bonding. During sealing, the pores in the oxide film are filled with aluminium hydroxide as the volume expansive transformation from aluminium oxide to hydroxide takes place. The film produced on aluminium (*not* on anodised aluminium) by immersion in boiling water has been found to improve bond durability between epoxy adhesives and aluminium [8-9]. The adhesion of ethylene copolymers to aluminium pretreated by immersion in boiling water has also been examined [10-14]. The mechanisms responsible for an improvement in adhesion were suggested to be stronger acid-base interactions, increased contact surface, and mechanical keying into the porous oxide surface [11].

In this study, DC anodising has been compared with AC anodising in hot solutions. DC and AC anodising was performed on extruded profiles of aluminium alloy AA6060-T6 in both phosphoric and sulphuric acid. The effect of sealing on the surfaces anodised in sulphuric acid was also investigated. All substrates were bonded with a one-component structural epoxy adhesive, and the durability of the bonded joints was determined using a modified version of the Boeing wedge test. The ranking of bond durability found when using the Boeing wedge test has been found to correlate well with in-service experience [15]. The chemistry of the anodic films was investigated using reflection-absorption FT-IR spectroscopy.

10.2 Experimental

10.2.1 Materials

The substrate material used in this study was extruded aluminium alloy AA6060-T6, supplied by Hydro Aluminium, Tønder, Denmark. The composition of this alloy by weight is 0.46% Mg, 0.40% Si, 0.18% Fe, 0.021% Mn, 0.002% Cu, 0.015% Zn, 0.01% Ti, Al balance [16]. Extruded aluminium alloy AA7021-T1, also supplied by Hydro Aluminium, was used as reinforcement material for the wedge test specimens. The one-component structural epoxy adhesive XD4600, was delivered by Dow Automotive, Freienbach, Switzerland.

10.2.2 Surface pretreatment procedures

The AA6060-T6 aluminium substrates were anodised according to the parameters given in Table 1. The DC-PAA substrates were submitted to the Forest Product Laboratory (FPL) etch (300 g/l H_2SO_4, 45 g/l $Na_2Cr_2O_7$, 70°C, 15 min) prior to anodising. The DC-SAA substrates were alkaline etched in 10 wt% NaOH at 60°C for 50 s, then desmutted in aqueous 65% HNO_3 at room temperature for 90 s, prior to anodising. The AC-SAA and AC-PAA substrates were only acetone degreased prior to anodising. All substrates were rinsed well in running tap water, dipped in distilled water and dried at 60°C after anodising. Sealing of the DC-SAA substrates was performed for 20 min in boiling water at 100°C, while sealing of the AC-SAA substrates was performed for one min.

Table 1
Anodising parameters for pretreatment of the AA6060-T6 aluminium substrates

Type of anodising	Electro-lyte	Acid conc. (wt%)	Voltage (V)	Current density (A/dm^3)	Time	Bath temp. (°C)
DC-PAA[1]	H_3PO_4	10	10 DC		20 min	25
DC-SAA[2]	H_2SO_4	16		1.5 DC	20 min	20
AC-SAA	H_2SO_4	15		10 AC	12 sec	80
AC-PAA	H_3PO_4	10		4 AC	30 sec	50

[1]The substrates were FPL-etched prior to DC-PAA.
[2]The substrates were alkaline etched prior to DC-SAA.

10.2.3 Bond preparation and environmental testing

Wedge-style reinforced double cantilever beam (RDCB) specimens were prepared for environmental testing. Two anodised AA6060-T6 substrates with thickness 2 mm and two AA7021-T1 reinforcements with thickness 6.2 mm were bonded with XD4600 into a 'sandwich' assembly, keeping it together with paper clips during curing. Curing was performed at 180°C for 30 min, after which the assembly was cut into RDCB specimens with the geometry shown in Fig. 1. The bonding procedure has been described in greater detail elsewhere [17]. Wedges were inserted into the bondline at a constant rate of 10 mm/min, and environmental testing was performed in a climate chamber at 40°C and 96% relative humidity.

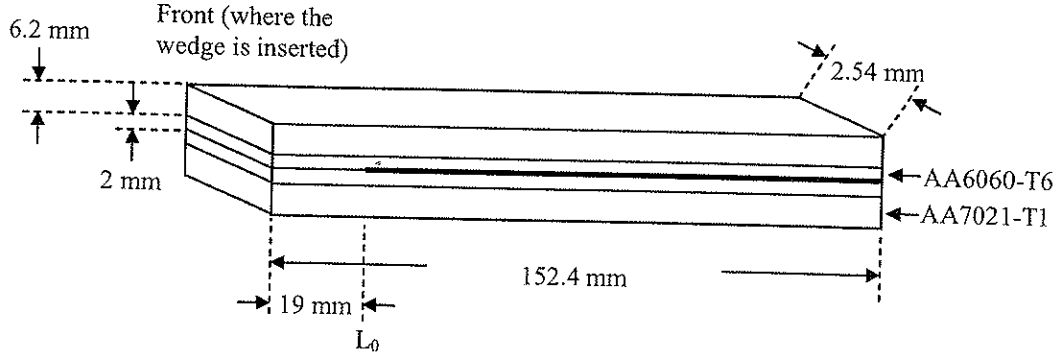

Figure 1. Schematic drawing of a RDCB specimen before insertion of the stainless steel wedge. Geometry according to ASTM D 3762-79, except for specimen thickness. Bondline thickness is 0.1 mm. Measurement of crack length starts at point L_0.

10.2.4 FT-IR spectroscopy

FT-IR spectroscopy in the reflection-absorption mode was used to investigate the anodised AA6060-T6 aluminium substrates. The analysis was performed with a Perkin Elmer Spectrum One FT-IR Spectrometer. The spectra were recorded as an average of 10 scans with a resolution of 4 cm^{-1} in the range 400-4000 cm^{-1}. The use of an external reflectance accessory enabled the infrared beam to be focused on the sample at 60° relative to the surface normal.

10.3 Results and discussion

10.3.1 Environmental durability

The crack growth of RDCB wedge test joints made of anodised AA6060-T6 aluminium substrates and XD4600 epoxy adhesive, during exposure to 40°C and 96% relative humidity, is shown in Fig. 2. The AC-SAA and AC-PAA pretreatments performed very well, almost as good as the FPL + DC-PAA pretreatment, which is widely considered to be the aluminium pretreatment process giving the most durable joints [3-4]. Excellent

durability is normally obtained on surfaces where the adhesive penetrates the pores of the oxide film and the interface between the adhesive and the oxide is extended after curing. In such cases the failure mode will be cohesive within the adhesive, as in the case of the FPL + DC-PAA pretreatment here. All the above mentioned anodising processes performed significantly better than the DC-SAA process.

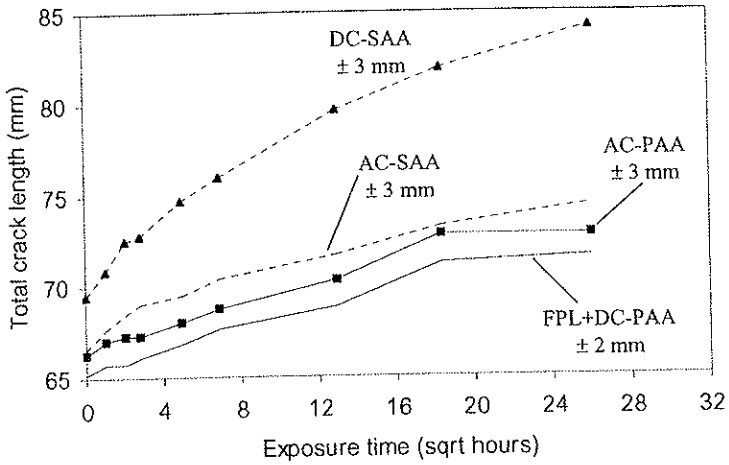

Figure 2. Total crack length as a function of exposure time for RDCB wedge test specimens made of anodised aluminium alloy AA6060-T6 bonded with XD4600 epoxy adhesive. The exposure conditions were 40°C and 96% relative humidity.

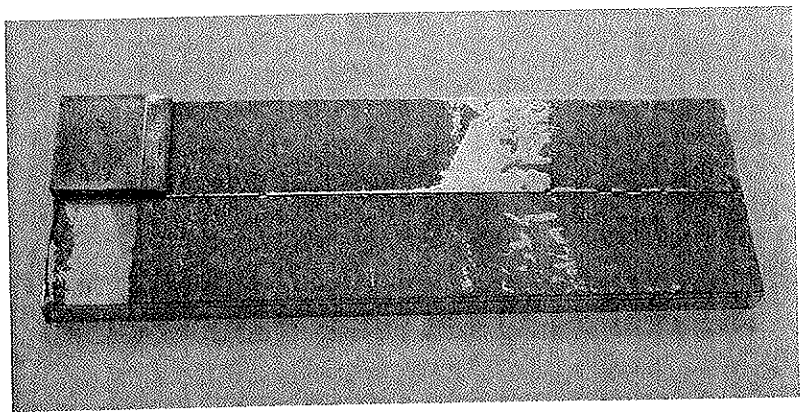

Figure 3. Picture of an opened DC-SAA wedge test joint after environmental exposure. The failure zone is the bare aluminium surface close to the middle of the specimen.

The surfaces of the opened wedge test specimens after testing can be divided into three distinct zones by visual inspection: (1) a zone where insertion of the wedge gives cohesive failure within the adhesive, (2) a zone where the crack propagates due to environmental exposure, crack propagation takes place in the aluminium/adhesive interface or cohesively within the adhesive, and (3) a zone where opening of the joints after testing gives cohesive failure. For illustration, Fig. 3 shows the appearance of a DC-SAA joint after environmental testing. Environmental degradation resulted in interfacial failure on the DC-SAA surface.

There were differences in the initial crack lengths of the bonded joints. The initial crack lengths of the DC-PAA, AC-PAA and AC-SAA substrates were shorter than that of the DC-SAA substrates. There seem to be a trend that joints with short initial cracks give better durability. Such observations have also been made earlier [17-18], but since the initial cracks are cohesive within the adhesive we are not able to explain this correlation.

The appearance of the crack growth zones of the opened wedge test specimens was investigated visually with a light microscope. The failure on the DC-PAA surface was purely cohesive, the crack propagated within the adhesive (see Fig. 4). The failure on the AC-PAA surface was very similar to that of the DC-PAA surface, although a distribution of some smaller spots of interfacial failure was observed. The failure on the AC-SAA surface was also mainly cohesive with a distribution of spots with interfacial failure. However, the number and the size of spots were higher than on the AC-PAA surface. The failure on the DC-SAA surface was purely interfacial. This means that the appearance of the failure surface after environmental exposure could be correlated with the durability of the wedge test joints. More interfacial failure resulted in lower durability.

The effect of the different anodising processes on the morphology of the oxide layer has been investigated and reported elsewhere [18-19]. It was shown that the porosity of the anodic films produced in phosphoric acid was higher compared with the films produced in sulphuric acid. A large variation in both cell and pore size was also observed. The

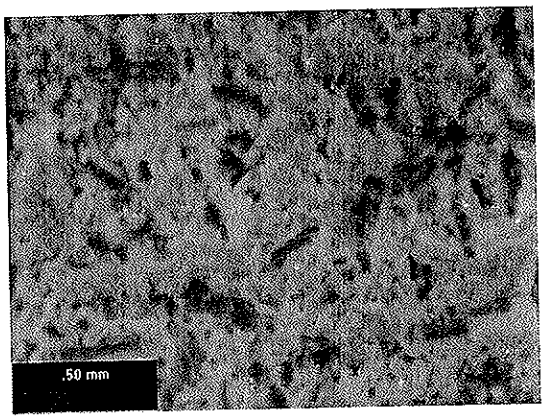

FPL + DC-PAA

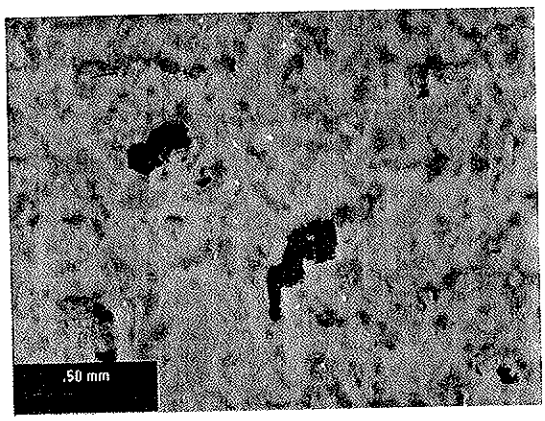

AC-PAA

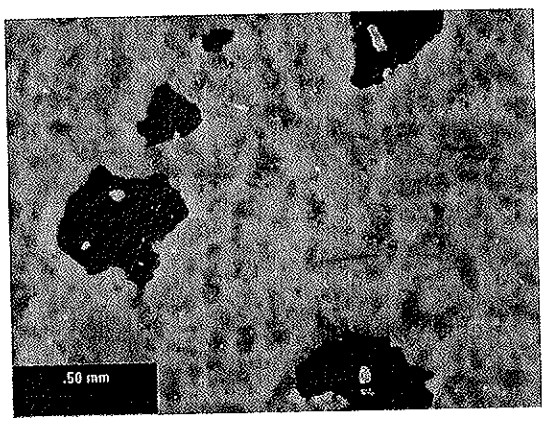

AC-SAA

Figure 4. Microscopy images of failure zones produced during environmental testing. The images of the two AC anodised surfaces represent typical areas of adhesive failure.

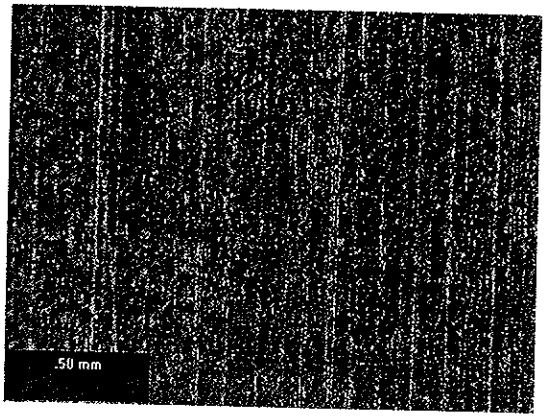

DC-SAA

Figure 4. (cont.)

films made in phosphoric acid showed a larger pore diameter and a more open cell structure. This can be important with respect to the durability of the bonded substrates. Early in the hardening process, the adhesive becomes less viscous and can then penetrate and fill the pores. The adhesive is mechanically interlocked to the oxide after curing, and the solid adhesive cannot move without plastically deforming. Adhesive penetration into oxide pores in the DC-PAA surface has been invoked as the main reason for the good durability properties of this surface in earlier studies [2,5,20]. If the adhesive is able to penetrate the pores in some of the oxides in this study, but not in others, then this can to a large extent explain the observed differences in durability. For example, Digby and Packham [20] observed that the fine pore structure of the DC-SAA surface appeared to be little penetrated by the epoxy adhesive. The surface turned out to give poor durability.

Durability investigations on similar surfaces using a two-component epoxy adhesive, performed by Bjørgum et al. [18], showed very similar results as those obtained with the one-component epoxy adhesive in this study. The ranking of durability was the same. However, some differences were observed in the failure zone in the opened wedge test specimens. On the AC-SAA substrates, purely interfacial failure was observed, as opposite to the large extent of cohesive failure occurring with the one-component

adhesive. The different behaviour of the one- and two-component adhesives can be explained in terms of viscosity. The two-component adhesive is cured at 60°C, while the one-component adhesive is cured at 180°C. The viscosity of the one-component adhesive is then possibly reduced to a level which is significantly lower than that achieved by the two-component adhesive. At this lower viscosity, the one-component adhesive can penetrate oxide pores in the AC-SAA surface, while the two-component adhesive is unable to do so. Thus, it is more likely that the one-component epoxy adhesive has penetrated the pores in the AC-SAA surface. Still, even if the two-component adhesive gave interfacial failure on the AC-SAA surface, the durability was much better than for the DC-SAA surface.

The oxide produced on aluminium by anodising in phosphoric acid contains phosphate ions, which are known to form stable oxide layers and to inhibit hydration reactions in wet environments [21-23]. On the other hand, anodic films produced in sulphuric acid contain about 15 wt% sulphate [24]. These sulphate ions are much more susceptible to the effects of water than phosphate ions, and the oxides can absorb relatively large amounts of water. This difference in susceptibility to water may have a significant effect on the long-term properties of bonded joints. Anodic films produced in sulphuric acid have the ability to absorb and desorb water, depending on the surrounding atmospheric conditions [25]. The oxide can reach an equilibrium state with a high water content when exposed to humid air. Since water has a degrading effect on adhesively bonded joints, a decrease in performance can be expected.

10.3.2 FT-IR spectroscopy

The FT-IR spectra of the oxide films on the DC-PAA, DC-SAA, AC-SAA and AC-PAA surfaces are shown in Fig. 5. The oxide film on the DC-SAA surface that was used for adhesive bonding was not possible to analyse using FT-IR spectroscopy. The applied DC-SAA process parameters results in an oxide thickness of approximately 10 μm. This proved too thick for FT-IR analysis. Therefore, a DC-SAA surface with an approximate oxide thickness of 1.0 μm was investigated instead.

The bands in the region 3460-3400 cm^{-1} are assigned to O-H stretching vibrations, the bands around 1600 cm^{-1} to physically bound water, and the bands in the region 920-850 cm^{-1} to Al-O bending vibrations. The assignments are based on refs. [26-28]. The DC-PAA oxide has an unresolved shoulder around 1060 cm^{-1} (Fig. 5A). After heat-treatment at 180°C for 30 min, as in a typical curing cycle for one-component epoxy adhesives, a band is present at 1081 cm^{-1}. This band is attributed to P-O vibrations in the phosphate ions which are incorporated in the oxide after anodic oxidation in phosphoric acid [28-29]. The oxides normally contain 6-8 wt% phosphate [24]. The P-O band at 1081 cm^{-1} appears due to the reduction of O-H bending vibrations in the same region. The intensities of the O-H stretching band at 3428 cm^{-1} and the band of physically bound water at 1591 cm^{-1} are also reduced after heat-treatment. The AC-PAA oxide also has a shoulder due to P-O vibrations around 1060 cm^{-1} which becomes better resolved after heat-treatment (Fig. 5D). However, no hydroxyl bands and very little physically bound water can be seen in the AC-PAA oxide, but a strong Al-O band is present at 883 cm^{-1}. This observation suggests that the composition is in a state of very pure alumina, Al_2O_3, with very little incorporation of hydroxide, $Al(OH)_x$.

Table 2
List of infrared frequencies

Assignment	Frequency (cm^{-1})
O-H *str*	3460-3395, 3326, 3104
H_2O *bend*	1605-1590
S-O	1152, 1136
P-O	1081
O-H *bend*	1076
Al-O *bend*	917, 895-855

The assignments are based on refs. [8,26-29].

Anodic oxide films on aluminium formed in sulphuric acid solutions are mainly composed of amorphous alumina, but also contain sulphate [27]. The FT-IR spectrum of the AC-SAA oxide is shown in Fig. 5C, and the band at 1136 cm^{-1} corresponds to S-O vibrations in the SO_4 group [27-28]. The intensity of the S-O vibrations are relatively high compared with the Al-O bending vibrations at 884 cm^{-1}, showing that the oxide contains a significant amount of sulphate. It is normally assumed that such oxides

(A) DC-PAA

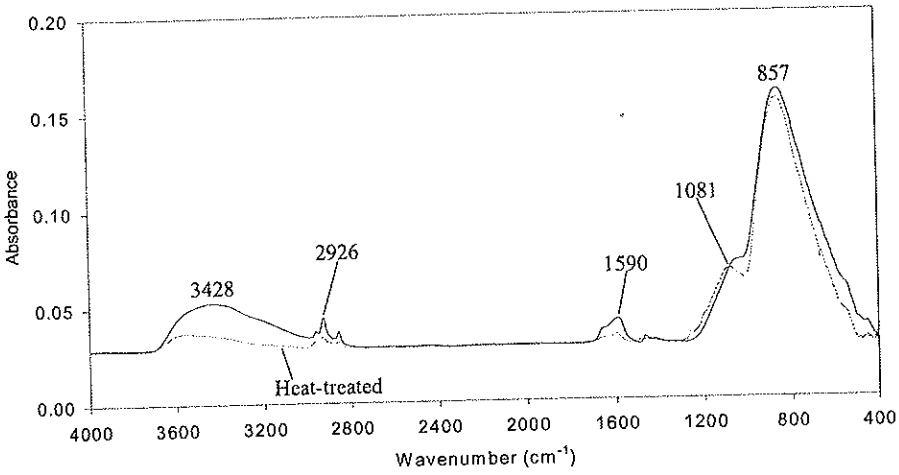

(B) DC-SAA

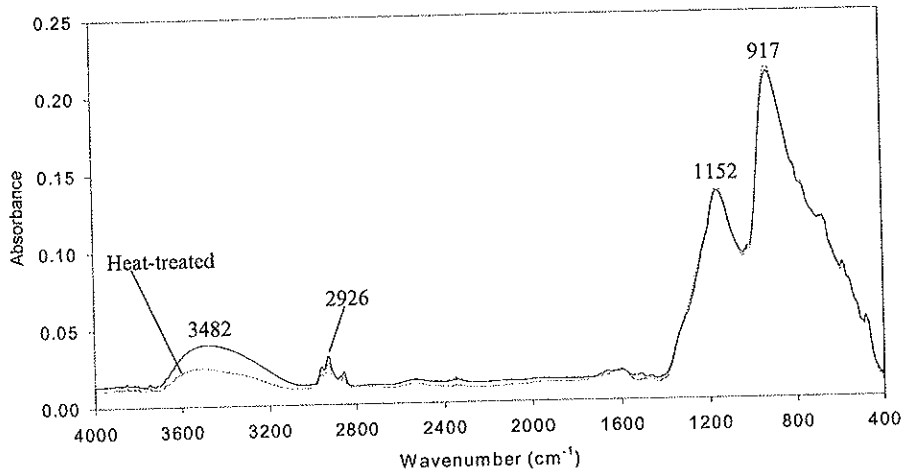

Figure 5. Reflection-absorption FT-IR spectra of oxide films before and after heat-treatment at 180°C for 30 min: (A) DC-PAA, (B) DC-SAA, (C) AC-SAA, and (D) AC-PAA.

(C) AC-SAA

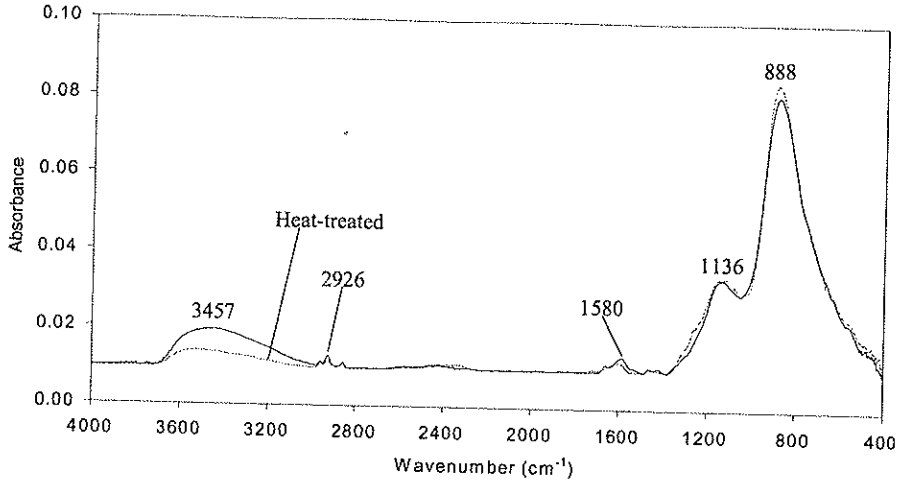

(D) AC-PAA

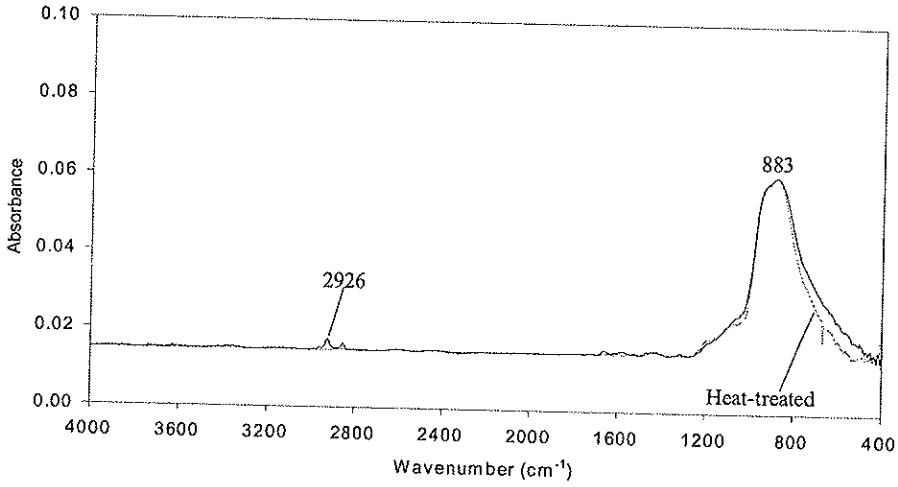

Figure 5. (cont.)

contain approximately 15 wt% sulphate [24]. Heating the AC-SAA oxide to 180°C for 30 min reduced the intensity of the O-H band at 3457 cm^{-1}, while the intensity of the Al-O band was slightly increased. The S-O band was not affected. The 1.0 μm DC-SAA oxide gave the same bands and behaved similarly during heating to 180°C as the AC-SAA oxide. However, the S-O and Al-O bands from the DC-SAA oxide are present at higher wavenumbers compared with the AC-SAA oxide, 1152 and 917 cm^{-1}, respectively. None of the anodic oxides produced in either sulphuric or phosphoric acid gave infrared spectra which are typical of pseudoboehmite.

The relative intensities of the Al-O bending modes can be correlated with the oxide thickness of the respective surfaces. The oxide thickness on the DC-SAA surface is approximately 1.0 μm, on the DC-PAA surface 0.6 μm, on the AC-SAA surface 0.2 μm, and on the AC-PAA surface 0.1 μm. As can be seen from Fig. 6, the intensity of the Al-O band is reduced with decreasing thickness of the oxide film. Based on Fig. 6, the AC-PAA oxide film seems to consist mainly of alumina, Al_2O_3. The relative intensity of the O-H stretching mode of this surface is very weak compared with the relative intensity of the Al-O bending mode. Also, the AC-SAA oxide seems to contain larger amounts of hydroxides compared with the DC-SAA and DC-PAA oxides. From

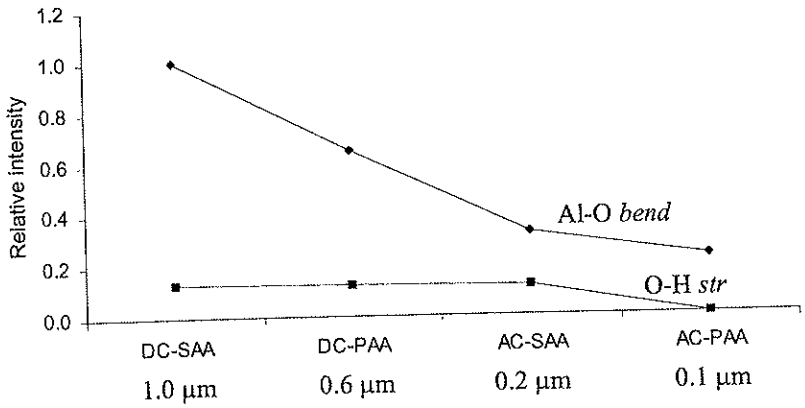

Figure 6. The relative infrared intensities of the O-H *str* and Al-O *bend* bands on anodised substrates.

the AC-SAA oxide, the relative intensity of the OH signal is higher compared with the relative intensity of the Al-O signal.

One cannot tell by the FT-IR results where the detected hydroxyls are present: on the oxide surface, in the bulk oxide, or evenly distributed between the bulk and the surface. Another uncertainty is connected to the chemical state in which the hydroxyls are present. Hydroxyls may be present both as aluminium hydroxides and as crystal water bound to sulphates. On the basis of these results it is difficult to determine to what extent the crystal water contributes to the observed trends. However, in all spectra three bands at 2959, 2926 and 2854 cm^{-1} can be seen. The band at 2926 cm^{-1} has the strongest intensity. The intensities of the bands are reduced after heat-treatment at 180°C. Also, the same bands are present in the spectrum of the boiled aluminium surface in Fig. 7. Bands in this region are normally attributed to C-H stretching vibrations, but these should not be present in the oxides. Therefore, we tentatively assign these vibrations to Al-OH stretching modes. If this is true, then much of the intensity reduction of the O-H stretching band during heating to 180°C can be attributed to the reduction of aluminium hydroxyls. In any case, it seems that heating the oxide films to 180°C significantly reduces the intensity of the O-H stretching bands, indicating that water is released and driven out of the oxides during curing of the adhesive. The effect of the release of water from the oxide film during curing will be discussed in another publication [30].

The presence of hydroxyl groups on the oxide surface may have a positive effect on adhesion. A monolayer of hydroxyl groups can increase the possibility of condensation reactions with the adhesive. On the other hand, much more than a monolayer could be considered as a hydrated layer, which is known to reduce durability. If there are more hydroxyl groups on the AC-SAA surface than on the DC-SAA surface, this may to some extent explain the difference in durability between these surfaces when bonded with the two-component epoxy adhesive investigated by Bjørgum et al. [18]. In this case both surfaces gave interfacial failure, indicating that the adhesive had not penetrated the oxide pores. If the one-component epoxy adhesive investigated in the present study can penetrate pores in the AC-SAA surface, as discussed earlier, a difference in surface hydroxyls will be of less importance.

10.3.3 Effect of sealing

Sealing of anodic oxides in boiling water is often performed in order to prevent corrosion of the surface. Sealing significantly reduced the durability of the DC-SAA and AC-SAA substrates, as can be seen from Fig. 8. The crack growth rates during the first hour(s) were very high compared with the corresponding anodised only substrates, and the crack growth of the sealed AC-SAA joints were higher than that of the sealed DC-SAA joints in the beginning of the test. However, as the test progressed, both crack growth curves seemed to stabilise at the same level. This level was much higher than what was observed for the unsealed joints. The failures in both the sealed DC-SAA and AC-SAA joints were interfacial.

The reduced durability of the anodised substrates is different from what has been observed for aluminium surfaces which were boiled only [8-9]. The immersion of aluminium in boiling water produces an oxyhydroxide film with a flake-like structure [31], and the boiling pretreatment has been found to improve bond durability between epoxy adhesives and aluminium [8-9].

During the sealing process of an anodised surface, the already existing oxide on the surface will be consumed in the formation of hydroxides. Previous investigations at our laboratories have shown that the outer oxide layer can be significantly affected by boiling in water, creating a 'fluffy' surface [32]. Failure during crack propagation then occurs in the weak, hydrated zone in the oxide surface, and not in the oxide-adhesive interface. The weak cohesive forces within the outer hydrated layer are then a probable cause of failure during environmental testing.

The oxide film produced by boiling in water has a different chemical composition than the anodic oxides (see Fig. 7). Boiling produces bands at 3326 and 3104 cm^{-1}, attributed to O-H stretching modes, and a band at 1076 cm^{-1}, attributed to the O-H bending mode. There are also unknown peaks at lower wavenumbers. It has been reported that an adherent layer of a poorly crystallised pseudoboehmite film is formed on the aluminium surface during hydration in boiling water at 100°C [12]. The chemical composition of the hydrated film can be described as an aluminium oxyhydroxide containing physically

adsorbed water, where water is bonded with strong hydrogen bridges between layers of boehmite. In this case, it seems that the oxide produced is an intermediate between boehmite and pseudoboehmite (assumption based on ref. [26]).

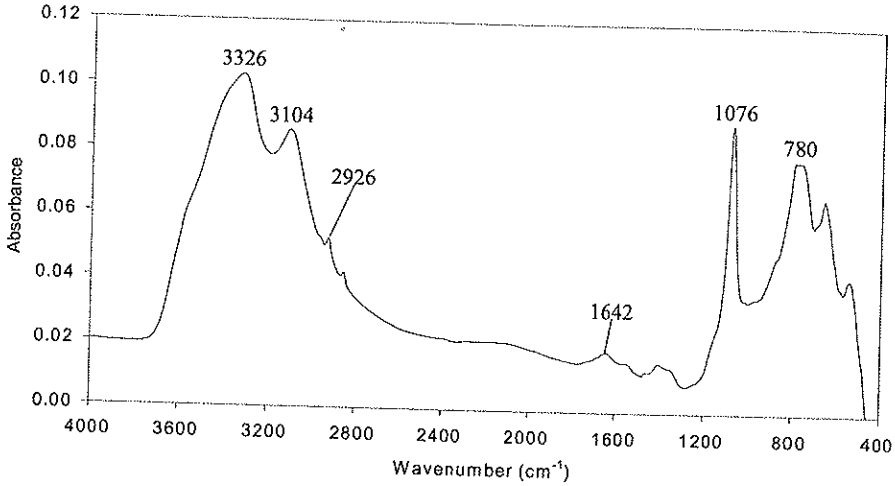

Figure 7. Reflection-absorption FT-IR spectrum of an AA6060-T6 surface that was boiled in water for 64 min.

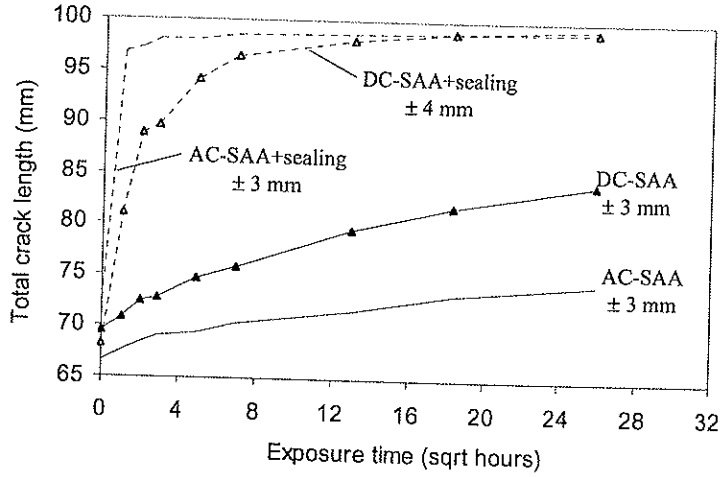

Figure 8. Total crack length as a function of exposure time for RDCB wedge test specimens made of sulphuric acid anodised aluminium alloy AA6060-T6 bonded with XD4600 epoxy adhesive: before and after sealing in boiling water. The exposure conditions were 40°C and 96% relative humidity.

Fig. 9 shows the FT-IR spectra of an AC-SAA oxide film that was boiled in water for just one min, as in the sealing process of the substrates, then heat-treated at 180°C for 30 min. Boiling resulted in an intensity increase in the O-H band at 3450 cm^{-1} and the S-O band at 1116 cm^{-1}. The intensity of the bands of physically bound water at 1603 cm^{-1} decreased. The apparent increase in the S-O band can be explained by an increase in unresolved O-H bending vibrations in the same area. Extended boiling times of the AC-SAA surface shows a further increase in the intensity of the O-H stretching modes around 3450 cm^{-1} and the O-H bending mode at 1076 cm^{-1}. Both these bands are typical bands of pseudoboehmite [26]. On the other hand, there is a decrease in the intensity of the Al-O bending vibrations at 890 cm^{-1}. These observations suggest that a transformation from the oxide towards the hydroxide state is taking place, the product possibly being pseudoboehmite:

$$Al_2O_3 + H_2O \rightarrow 2AlOOH$$

$$AlOOH + H_2O \rightarrow Al(OH)_3$$

Heat-treatment of the sealed AC-SAA oxide resulted in a decrease of the O-H and S-O bands, while the band of Al-O increased. Thus, the transformation reactions are reversed and water is released from the oxide film. We believe that the thick oxide films on the DC-SAA substrates will behave in a similar fashion as the oxide films on the AC-SAA substrates, although at a much larger scale due to the thicker oxide and the longer immersion times involved. Much more water can then be released from the sealed DC-SAA substrates during curing at 180°C.

The adhesive bondlines of the wedge test joints made of the sealed DC-SAA substrates were full of blisters, as opposite to the DC-SAA surface which only showed insignificant signs of blister formation. No blister formation was observed in the bondline for any of the other anodised joints, not even for the sealed AC-SAA joints. The formation of blisters in the bondline is connected to the desorption of water from the oxide film during the curing process at 180°C (as shown by FT-IR). Water in the

oxide films may exist in a number of forms: trapped in the oxide as a hydrate, reacted with the oxide to form a hydroxide, in the hydrated surface layers, trapped in capillaries or voids, and condensed on the surface. This water can be released during heating. The difference in blister formation between the sealed DC-SAA joints and the sealed AC-SAA joints is connected to the different oxide layer thicknesses and the different boiling times involved. The oxide thickness on the DC-SAA substrates is approximately 50 times that of the AC-SAA substrates. The boiling times are also much longer for the DC-SAA substrates. Thus, much more water may be released from the oxide films on the DC-SAA substrates.

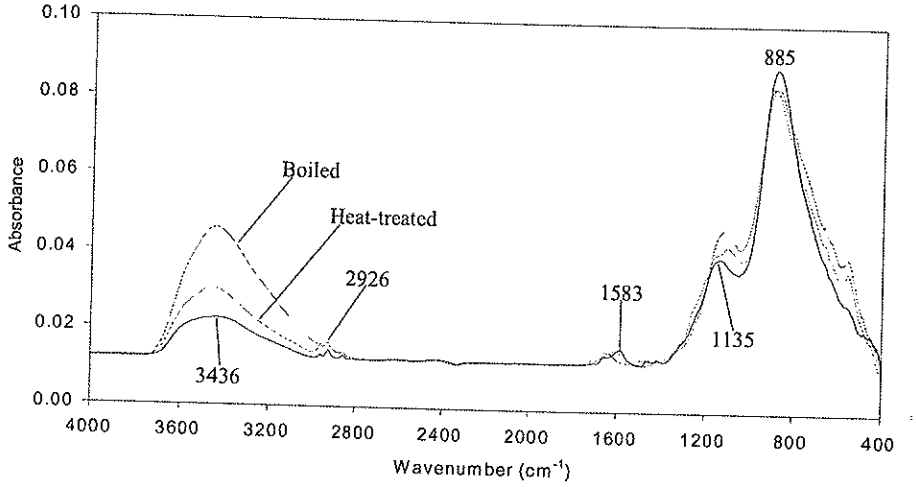

Figure 9. Reflection-absorption FT-IR spectra of an AC-SAA oxide film that was boiled in water for 1 min, then heat-treated at 180°C for 30 min.

10.4 Conclusion

The environmental durability of anodised AA6060-T6 bonded with a one-component, structural epoxy adhesive was investigated. The results showed that AC anodising in hot phosphoric and sulphuric acid solutions performed very well, almost as good as the well-established FPL + DC-PAA pretreatment. These three anodising processes performed significantly better than the DC-SAA process. FT-IR spectroscopy of the

anodic films showed that the DC-SAA and AC-SAA oxides contained significant amounts of sulphate. Sulphates can absorb relatively large amounts of water, and this can have a significant effect on the long-term properties of bonded joints.

FT-IR spectroscopy also showed that the intensity of the O-H stretching band in the oxides decreased during heat-treatment at 180°C. This observation suggested that a transformation from the hydroxide, $Al(OH)_x$, to the oxide, Al_2O_3, state took place, and that water was released and driven out of the oxides during curing of the adhesive.

Sealing of the DC-SAA and AC-SAA substrates in boiling water significantly reduced the durability. Water was released from the sealed films during curing, and this had the effect of blister formation in the wedge test joints made of sealed DC-SAA substrates.

Acknowledgements

Thanks are due to Hydro Aluminium Structures and The Research Council of Norway for financial support.

References

[1] M. Brémont, W. Brockmann, *J Adhesion* **58**, 69-99 (1996)

[2] J.D Venables, D.K McNamara, J.M. Chen, T.S. Sun and R.L. Hopping, *Appl. Surface Sci.* **3**, 88-98 (1979)

[3] G.W. Critchlow and D.M. Brewis, *Int. J. Adhesion Adhesives* **16**, 255-275 (1996)

[4] G.W. Critchlow, *Trans. IMF* **76**, B6-B10 (1998)

[5] J.D. Venables, *J. Mater. Sci.* **19**, 2431-2453 (1984)

[6] L. Kozma and I. Olefjord, *Mater. Sci. Tech.* **3**, 860-874 (1987)

[7] N.L. Rogers, in: Adhesive Bonding of Aluminum Alloys, E.W. Thrall and R.W. Shannon (Eds.), Marcel Dekker, New York, 1985. p. 41-50.

[8] A.N. Rider, *J. Adhesion Sci. Technol.* **15**, 395-422 (2001)

[9] A.N. Rider and D.R. Arnott, *Int. J. Adhesion Adhesives* **20**, 209-220 (2000)

[10] A. Strålin and T.J. Hjertberg, *J. Adhesion Sci. Technol.* **6**, 1233-1250 (1992)

[11] A. Strålin and T.J. Hjertberg, *J. Adhesion Sci. Technol.* **7**, 1211-1229 (1993)

[12] A. Strålin and T.J. Hjertberg, *J. Adhesion* **41**, 51-80 (1993)

[13] A. Strålin and T.J. Hjertberg, *Appl. Surface Sci.* **74**, 263-275 (1994)

[14] A. Strålin and T.J. Hjertberg, *J. Appl. Polym. Sci.* **49**, 511-521 (1993)

[15] J.A. Marceau, in: Adhesive Bonding of Aluminum Alloys, E.W. Thrall and R.W. Shannon (Eds.), Marcel Dekker, New York, 1985. p. 51-74.

[16] O. Lunder, B. Olsen and K. Nisancioglu, *Int. J. Adhesion Adhesives* **22**, 143-150 (2002)

[17] B.B. Johnsen, K. Olafsen, A. Stori and K. Vinje, *J. Adhesion Sci. Technol.* **16**, 931-1948 (2002)

[18] A. Bjørgum, F. Lapique, J. Walmsley and K. Redford, *Int. J. Adhesion Adhesives* **23**, 401-402 (2003)

[19] J. Walmsley, A. Bjørgum, F. Lapique, C. Marioara, S. Haarberg, B. Tanem and G. Pettersen, in: Proc. SCANDEM 2001. Stockholm, 2001.

[20] R.P. Digby and D.E. Packham, *Int. J. Adhesion Adhesives* **15**, 61-71 (1995)

[21] W.P. De Wilde, G. Van Vickenroy, L. Tirry and A.H. Cardon, *J. Adhesion Sci. Technol.* **9**, 149-158 (1995)

[22] A.N. Rider and D.R. Arnott, *Surf. Interface Anal.* **24**, 583-590 (1995)

[23] D.J. Arrowsmith, D.A. Moth and S.P. Rose, *Int. J. Adhesion Adhesives* **12**, 67-72 (1992)

[24] P.G. Sheasby and R. Pinner, The Surface Treatment and Finishing of Aluminium and its Alloys, Finishing Publications, Ltd., Stevenage, UK, 2001.

[25] T. Luksepp and K. Kristiansen. In preparation.

[26] R.S. Alwitt, in: Oxides and Oxide Films, Vol. 4, J.W. Diggle and A.K. Vijh (Eds.), Marcel Dekker, New York, 1976. p. 169-254.

[27] Y. Li, Z. Zhu, Z. Jiang and M. Yan, *Plat. Surf. Finish* **80**, 79-82 (1993)

[28] R.A. Nyquist and R.O. Kagel, Infrared Spectra of Inorganic Compounds, Academic Press, New York, 1971.

[29] C.N.R. Rao, Chemical Applications of Infrared Spectroscopy, Academic Press, New York, 1963.

[30] B.B Johnsen, F. Lapique, A. Bjørgum, J. Walmsley, B.S. Tanem and T. Luksepp, *Int. J. Adhesion Adhesives*. In press.

[31] A.J. Kinloch, Durability of Structural Adhesives, Elsevier Applied Science Publishers, London, 1983.

[32] Unpublished results.

Chapter 11

The effect of pre-bond moisture on epoxy-bonded sulphuric acid anodised aluminium

Bernt B. Johnsen, Fabrice Lapique, Astrid Bjørgum, John Walmsley, Bjørn Steinar Tanem, Tomas Luksepp

Int. J. Adhesion Adhesives **24**, 183-191 (2004)

Abstract

The adhesive bonding of sulphuric acid anodised aluminium has been investigated in wet and dry environments. Crack growth resistance was investigated using the wedge test at 40°C/96% r.h. DC-SAA joints bonded at 85% r.h. showed a significant decrease in crack growth resistance, compared with joints bonded at lower r.h. The differences were smaller between AC-SAA joints, but bonding at 85 and 11% r.h. reduced the crack growth resistance compared with 33 and 52% r.h. Significant blister formation was observed in the adhesive bondline after bonding at 85% r.h. TEM cross-sections showed that bonding at 85% r.h. also resulted in a ~200 nm wide region in the adhesive close to the oxide surface with very little thixotropic agent. This was explained by desorption of water from the oxide during curing of the adhesive.

Keywords: Epoxides; Aluminium and alloys; Surface treatment; Wedge tests; Relative humidity.

11.1 Introduction

Adhesives have been used for many years in aerospace applications. High durability bonded aluminium structures are obtained by using adhesives based on epoxy or phenolic resins [1]. It is well known that proper chemical pretreatment of the aluminium prior to epoxy bonding is essential for developing bond strengths necessary for high performance aerospace applications [2]. DC anodising in phosphoric acid (DC-PAA) or chromic acid (DC-CAA) are the preferred aluminium pretreatment methods for adhesive bonding. The processes typically produce a porous oxide film that exhibits good durability [2-6]. However, anodising times are quite long, making it an expensive process. In addition, both the DC-PAA and DC-CAA processes often involve the use of hexavalent chromium. The DC-PAA substrates are normally submitted to a chromic-sulphuric acid etch prior to anodising, although ferric-sulphate processes are sometimes used instead. Hexavalent chromium is reported to be toxic [7], and environmental factors together with stricter legislation has led researchers to look for alternative, more environmentally friendly, pretreatment processes.

A cost-efficient alternative to DC anodising is AC anodising in hot acid solutions. AC anodising of aluminium has been used for many years in the coil coating industry, where anodising is performed on sheets moving at high speeds through hot acid electrolytes for periods of just few seconds [8]. Another significant advantage of the AC process is that the requirement of degreasing and surface pretreatment prior to anodising is reduced. The aluminium substrates can be anodised as-received, since hydrogen evolution at the surface has a strong cleaning effect. These factors significantly trim down the number of process steps employed, and process times can be reduced from several minutes, typically 15-20 minutes for DC anodising, to less than a minute or only a few seconds.

Anodising of aluminium in sulphuric acid is widely used due to the visual appearance and the thick, corrosion protective films produced. However, the anodic films produced by sulphuric acid can contain significant amounts of water, depending on the

surrounding atmospheric conditions [9]. This behaviour is caused by the aluminium sulphate that is present in the oxide film after sulphuric acid anodising. One-component epoxy adhesives require high-temperature curing, and there is concern about the effect water may have on the properties close to the oxide-adhesive interface in a bonded joint. During curing of the adhesive, water will be released from the oxide as a result of the high temperatures involved [10].

In this study, the effect of water in the oxide film during adhesive bonding was investigated. Substrates that were anodised in sulphuric acid were bonded in atmospheres of different relative humidities. Both DC and AC anodising in sulphuric acid have been investigated for extruded profiles of aluminium alloy AA6060-T6. The thick oxide film (8 μm) produced by the traditional DC-SAA process, was compared with the thinner oxide film (0.2 μm) of the AC-SAA process. The anodised substrates were bonded with a one-component structural epoxy adhesive, and the crack extension of the bonded joints in humid air was determined using a modified version of the Boeing wedge test. The ranking of bond durability found when using the Boeing wedge test has been found to correlate well with in-service experience [11]. Cross-sections of the oxide-adhesive interface were investigated using transmission electron microscopy, and the chemistry of the oxides was investigated using FT-IR spectroscopy.

11.2 Experimental

11.2.1 Materials

The substrate material used in this study was extruded aluminium alloy AA6060-T6, supplied by Hydro Aluminium, Tønder, Denmark. The composition of this alloy by weight is 0.46% Mg, 0.40% Si, 0.18% Fe, 0.021% Mn, 0.002% Cu, 0.015% Zn, 0.01% Ti, Al balance [12]. Extruded aluminium alloy AA7021-T1, also supplied by Hydro Aluminium, was used as reinforcement material for the wedge test specimens. The one-component structural epoxy adhesive XD4600, was delivered by Dow Automotive, Freienbach, Switzerland.

11.2.2 Surface pretreatment procedures

The AA6060-T6 aluminium substrates were anodised according to the parameters given in Table 1. The DC-PAA substrates were submitted to the Forest Product Laboratory (FPL) etch (300 g/l H_2SO_4, 45 g/l $Na_2Cr_2O_7$, 70°C, 15 min) prior to anodising. The DC-SAA substrates (8 µm oxide thickness) were alkaline etched in 10 wt% NaOH at 60°C for 50 s, then desmutted in aqueous 65% HNO_3 at room temperature for 90 s, prior to anodising. The AC-SAA substrates (0.2 µm oxide thickness) were only acetone degreased prior to anodising. After anodising, all substrates were rinsed under running tap water, dipped in distilled water and dried at 60°C.

11.2.3 Bond preparation and environmental testing

Anodised AA6060-T6 aluminium substrates were bonded with XD4600 in environments with controlled humidity. Saturated salt solutions were used to control the relative humidity inside a sealed polyethylene glove bag, and the substrates and the adhesive were conditioned in the dry or wet environments for at least 24 h before bonding was performed inside the bag. The following salts and respectively relative humidities were employed: LiCl (11% r.h.), $MgCl_2$ (33% r.h.), $Mg(NO_3)_2$ (52% r.h.), and KCl (85% r.h.) [13]. The ambient temperature was 20°C. Bonding at 45% r.h. was performed in a laboratory atmosphere without the use of salt solutions. The relative humidity was measured using a hygrometer.

Wedge-style reinforced double cantilever beam (RDCB) specimens were prepared for environmental testing. Two anodised AA6060-T6 substrates with thickness 2 mm and two AA7021-T1 reinforcements with thickness 6.2 mm were bonded with XD4600 into a large, 110 × 175 mm, 'sandwich' assembly. The assembly was removed from the glove bag and cured at 180°C for 30 min, after which the assembly was cut into three RDCB specimens with the geometry shown in Fig. 1. The bonding procedure has been described in greater detail elsewhere [14]. Wedges were inserted into the bondline at a constant rate of 10 mm/min, and environmental testing was performed in a climate chamber at 40°C and 96 % relative humidity. The experimental matrix is shown in Table 2. Phosphoric acid anodising (DC-PAA) was used as benchmark reference.

Table 1
Anodising parameters for pretreatment of the AA6060-T6 aluminium substrates

Type of anodising	Electro-lyte	Acid conc. (wt%)	Voltage (V)	Current density (A/dm^3)	Time	Bath temp. (°C)
DC-PAA[1]	H_3PO_4	10	10 DC		20 min	25
DC-SAA[2]	H_2SO_4	16		1.5 DC	20 min	20
AC-SAA	H_2SO_4	15		10 AC	12 sec	80

[1]The substrates were FPL-etched prior to DC-PAA.
[2]The substrates were alkaline etched prior to DC-SAA.

Table 2
Experimental matrix for the determination of crack growth resistance of the anodised AA6060-T6 aluminium substrates

Pretreatment	Relative humidity (%)			
DC-PAA			45	
DC-SAA			45	85
AC-SAA	11	33	52	85

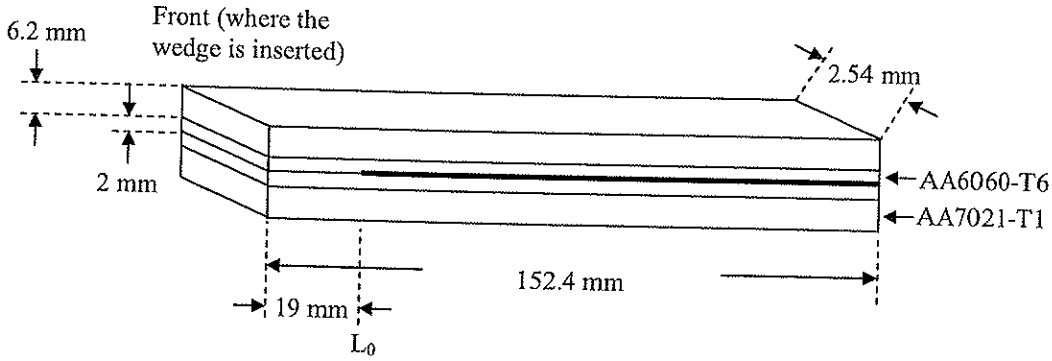

Figure 1. Schematic drawing of a RDCB specimen before insertion of the stainless steel wedge. Geometry according to ASTM D 3762-79, except for specimen thickness. Bondline thickness is 0.1 mm. Measurement of crack length starts at point L_0.

11.2.4 FT-IR spectroscopy

Two anodised AA6060-T6 aluminium substrates, one DC-SAA and one AC-SAA substrate, both with oxide thickness around 0.6 μm, where investigated with FT-IR spectroscopy in the reflection-absorption mode. The analysis was performed with a Perkin Elmer Spectrum One FT-IR Spectrometer. The spectra were recorded as an average of 10 scans with a resolution of 4 cm^{-1} in the range 400-4000 cm^{-1}. The use of an external reflectance accessory enabled the infrared beam to be focused on the samples at 60° relative to the surface normal.

11.2.5 Transmission electron microscopy (TEM)

Electron transparent foils for TEM examination were prepared by ultramicrotomy. Several foils, being ~ 75 nm in thickness, were put on Cu grids and examined in a Phillips CM 30 TEM operated at 200 keV. EDS-analysis was performed on several areas from the aluminium bulk to several tens of μm into the adhesive.

11.3 Results

11.3.1 Environmental testing

DC-SAA and AC-SAA substrates were bonded with XD4600 epoxy adhesive in atmospheres of different relative humidity. Fig. 2 displays the total crack length of the wedge test joints during exposure to 40°C and 96% r.h., crack growth takes place as a result of environmental exposure. The AC-SAA pretreatment performed very well, almost as good as the FPL + DC-PAA treatment which is widely considered to be the aluminium pretreatment process giving the most durable joints [3-4]. It is usually claimed that excellent durability is obtained on surfaces where the adhesive penetrates into pores of the oxide film and is mechanically interlocked after curing. Penetration of adhesive into pores in the oxide surface was discussed by Digby and Packham [15]. In such cases the failure mode will be cohesive within the adhesive, as in the case of the FPL + DC-PAA treatment here. The performance of the DC-SAA anodising process was inferior to that of the FPL + DC-PAA and AC-SAA pretreatments.

There were some differences in the crack growth resistance of the AC-SAA substrates bonded at different levels of relative humidity. The substrates performed in the following order from best to worse, with respect to the relative humidity at which the substrates were bonded: 33% r.h., 52% r.h., 11% r.h., and 85% r.h. (see Fig. 2). There were also some differences in the initial crack lengths of the joints. The differences in the crack growth were only minor, but a difference in crack growth resistance can still be said to exist. The forces acting at the crack tip in a joint with a short initial crack will be higher than in a joint with a long initial crack, and the 'driving' force for further crack growth during environmental exposure decreases with increasing crack length. In this case, the difference in the initial crack length of the AC-SAA substrates bonded at 85% r.h. and 33% r.h. was significant. Thus, since the tensile forces acting at the crack tip is highest in the joints with the shortest initial crack, and since the crack growth rates were approximately the same, the substrates bonded at 33% r.h. were more crack growth resistant than the 85% r.h. substrates.

As in the FPL + DC-PAA joints, the failure in the AC-SAA joints was cohesive within the adhesive. However, some localised interfacial failure was also observed: some in the 11% r.h. joints, but little in the 33, 52 and 85% r.h. joints. Another observation was that of blister formation in the adhesive bondlines with increasing levels of relative humidity. Some at 52% r.h. and significant blister formation at 85% r.h. (see Fig. 3). In the bondline of the joints bonded at 11% r.h., a different type of blister formation was observed. These blisters were not lying adjacent to the aluminium surface, but in the bulk adhesive, and they were small and spherical of nature. Hence, they were very different from the blisters observed at 52 and 85% r.h. Blister formation was also observed in the bondline of sealed DC-SAA substrates bonded with XD4600 and cured at 180°C (reported elsewhere [10]).

The difference in crack growth resistance between the DC-SAA substrates bonded in atmospheres of 85% r.h. and 45% r.h. was large. Not only was the difference in initial crack length very large, but also the crack growth rates were significantly different. The substrates bonded at 45% r.h. performed much better than the substrates bonded at 85% r.h. (see Fig. 2). The failure in the DC-SAA joints was interfacial, and there was

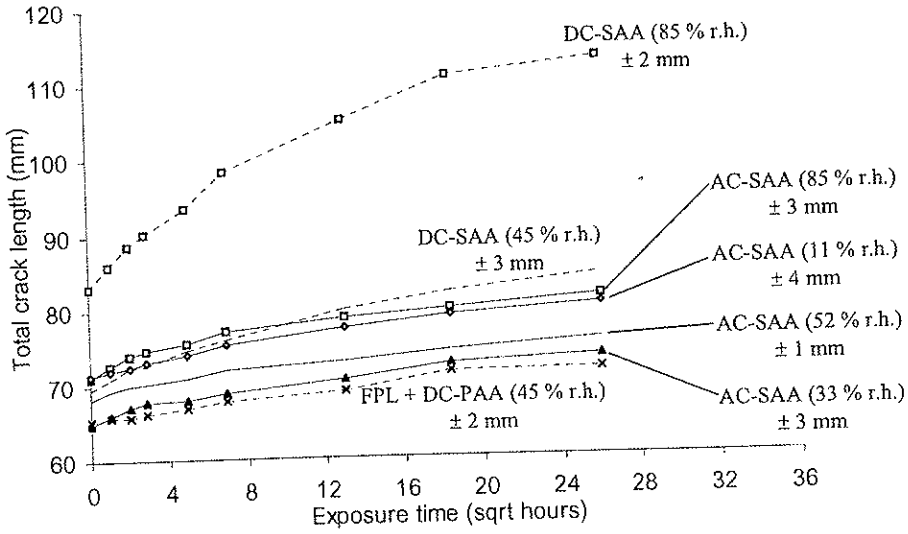

Figure 2. Total crack length as a function of exposure time for RDCB wedge test specimens made of anodised aluminium alloy AA6060-T6 and bonded with XD4600 epoxy adhesive. The exposure conditions were 40°C and 96% relative humidity.

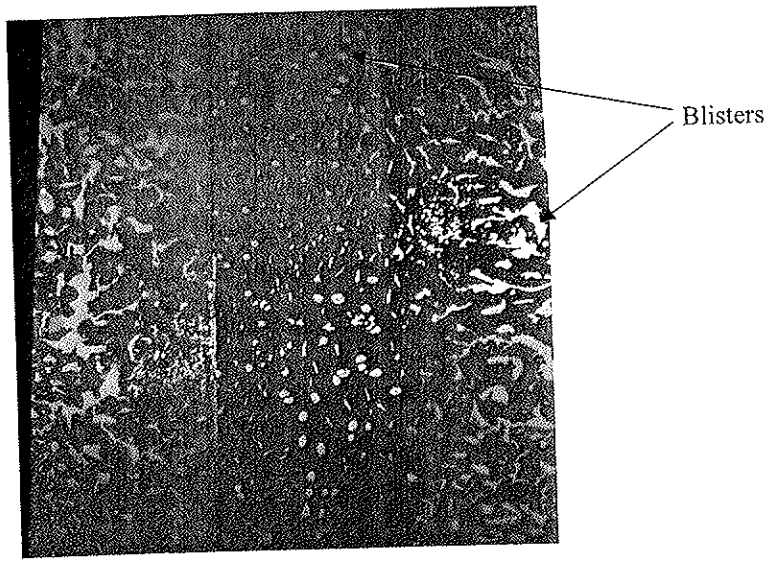

Figure 3. Picture of opened AC-SAA specimens bonded at 85% relative humidity. The pattern of the blisters indicates diffusion of water towards the edges of the bonded plate.

significant blister formation in the DC-SAA joints bonded at 85% r.h., but not at 45 % r.h.

11.3.2 FT-IR spectroscopy

FT-IR spectroscopy was performed on DC-SAA and AC-SAA substrates with an oxide thickness of 0.6 μm (not the same oxide thickness as on the substrates used for adhesive bonding) at ambient temperature and humidity. The specimens were investigated before and after heat-treatment at 180°C for 30 min, as shown in Fig. 4. The bands of O-H around 3450 cm^{-1}, S-O at 1152 cm^{-1}, and Al-O at 895 cm^{-1} for AC-SAA and at 917 cm^{-1} for DC-SAA, can be seen in the spectra. Similar oxides have been investigated and described in greater detail elsewhere [10]. The heat-treatment resulted in a marked reduction in the O-H signal around 3450 cm^{-1} in both cases. The intensity of the O-H signals after heat-treatment was about half of the initial values, possibly with a slightly higher reduction of the signal from the AC-SAA oxide. Also, the intensity of the Al-O signal from the AC-SAA oxide was slightly increased. The results indicated that a transformation from the hydroxide to the oxide state took place, and that water was released from the film. Oxide dehydration in the temperature range from 130 to 195°C has been shown earlier [16]. The AC-SAA oxide contained more hydroxyl groups than the DC-SAA oxide. The AC-SAA process is performed at a much higher temperature than the DC-SAA process, 80 and 20°C, respectively. Higher dissolution of oxide and sulphate can be expected in the hot solution, resulting in more precipitation of aluminium hydroxide in the pores of the AC-SAA oxide.

11.3.3 Transmission electron microscopy (TEM)

Cross-sections of specimens bonded at 11 and 85% relative humidity were investigated using TEM. The aim was to determine if there were any differences in the oxide-adhesive interfacial properties of the specimens. Fig. 5 shows cross-sections of the AC-SAA specimens. The presence of an oxide of about 200 nm in thickness can be seen. In the specimen bonded at 85% r.h., there seems to be a relatively structure free zone close to the oxide with an approximate width of 200 nm (indicated in the figure). Particles can be seen further out in the adhesive (indicated by arrows). These particles

are the thixotropic agent, which are included in the adhesive to control rheological properties.

(A) DC-SAA

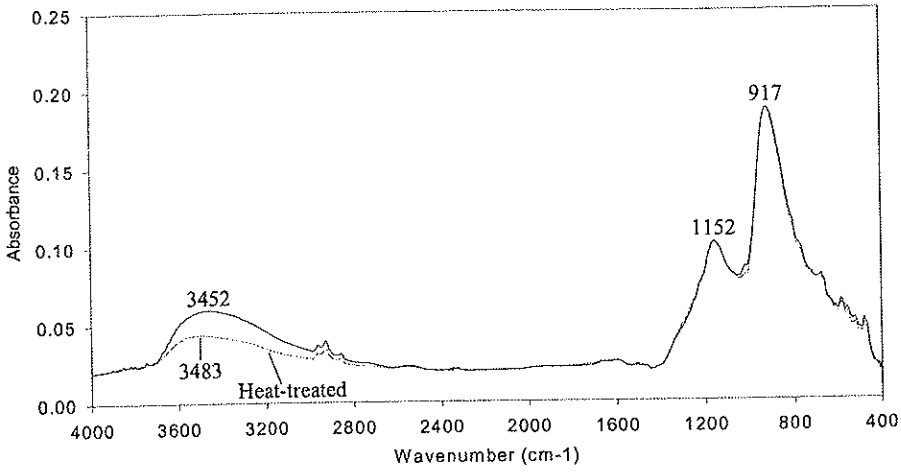

(B) AC-SAA

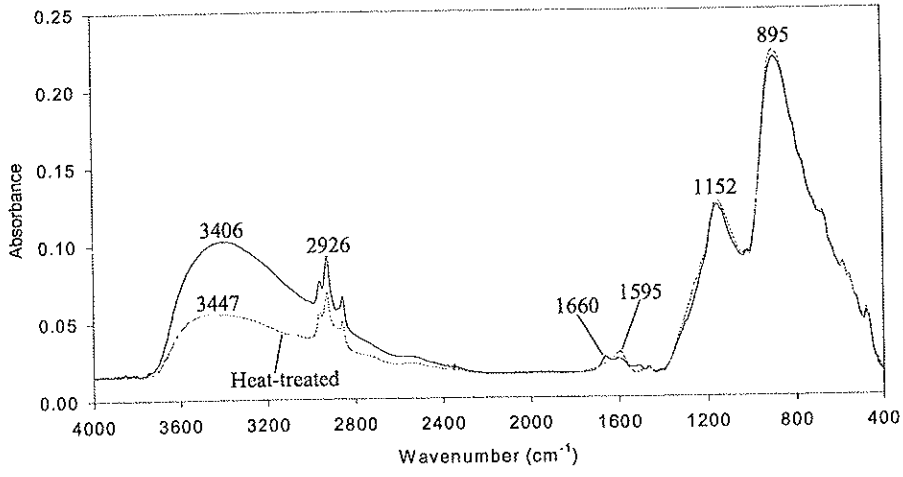

Figure 4. FT-IR spectra of (A) DC-SAA and (B) AC-SAA oxides on aluminium alloy AA6060-T6, both with thickness around 0.6 μm.

(A) AC-SAA 85% r.h.

(B) AC-SAA 11% r.h.

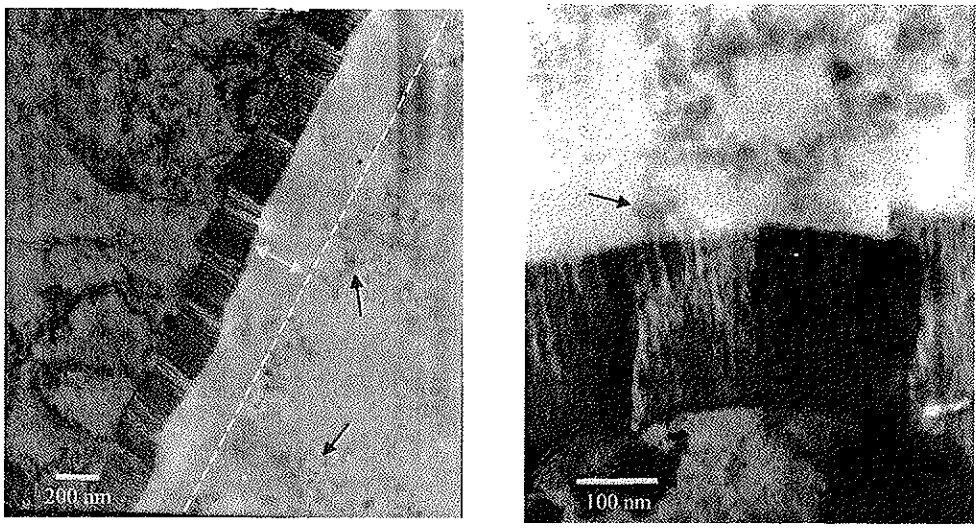

Figure 5. TEM cross-sections of AC-SAA oxides on aluminium alloy AA6060-T6 bonded with XD4600 epoxy adhesive at: (A) 85 and (B) 11% relative humidity.

(A) DC-SAA 85% r.h.

(B) DC-SAA 11% r.h.

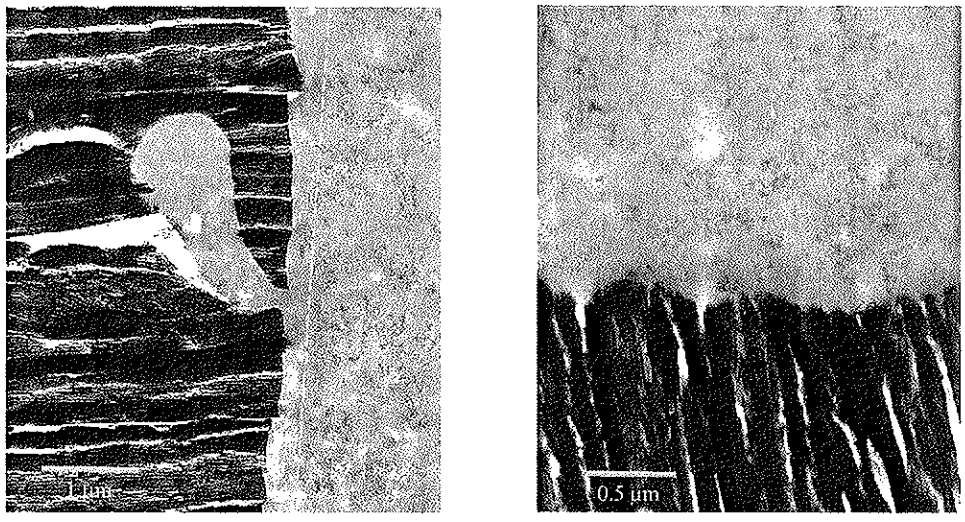

Figure 6. TEM cross-sections of DC-SAA oxides on aluminium alloy AA6060-T6 bonded with XD4600 epoxy adhesive at: (A) 85 and (B) 11% relative humidity.

The thixotropic agent consists almost exclusively of fumed silica which has been surface modified with octyl-groups to achieve a hydrophobic character. The observation of a lesser amount of silica in the structure free zone was confirmed by energy dispersive spectrometry (EDS) analysis, which showed that the amount of Si was reduced in this zone compared with further out in the adhesive. The adhesive also contains other sources of Si besides the thixotropic agent, but most of the Si detected in the adhesive is due to the thixotropic agent. Other elements found to be present in the adhesive were Al, O, C and Cl. No clear change in the intensity of these elements with distance from the oxide surface could be observed. In the AC-SAA specimen bonded at 11% r.h., the zone with reduced amount of thixotropic agent is less pronounced and some silica is also present close to the oxide (Fig. 5).

The same trends as those observed in the AC-SAA specimens were observed in the DC-SAA specimens, despite the large difference in film thickness, 0.2 and 8 μm, respectively. Fig. 6 shows that there seem to be a silica free zone close to the oxide in the specimen bonded at 85% r.h. However, this observation could not be confirmed by EDS analysis. In the DC-SAA specimen bonded at 11% r.h., there was no sign of a zone close to the oxide with a lesser amount of silica (Fig. 6).

11.4 Discussion

Water in the oxide films may exist in a number of forms: trapped in the oxide as a hydrate, reacted with the oxide to form a hydroxide, in the hydrated surface layers, trapped in capillaries or voids, and condensed on the surface. Luksepp and Kristiansen [9] have shown that anodic oxides produced in sulphuric acid can release and absorb water upon heat-treatment and exposure to humid air. Weight loss measurements revealed an incessant release of water at increasing cure temperatures. The FT-IR investigations in the present study support this observation. Luksepp and Kristiansen [9] also showed that the water content in uncured adhesive varies with the relative humidity

of ambient air. Both the anodic film and the adhesive will contain more water after exposure to air of high relative humidity.

The oxide films on aluminium produced by anodising in sulphuric acid solutions contain about 15 wt% aluminium sulphate [17]. Aluminium sulphate is very susceptible to water, and may absorb or desorb relatively large amounts of water depending on the surrounding atmospheric conditions. The aluminium sulphate to a large extent controls the amount of water present in the oxide at any time [9]. Much water is present as hydrate. Significantly more water is present in oxide films conditioned at about 35 % r.h., or more, compared with films conditioned at less than 30% r.h. at room temperature.

The susceptibility of the aluminium sulphates to water may have a significant effect on the long-term properties of anodic films produced in sulphuric acid. We have observed that storing unstressed RDCB joints made of DC-SAA substrates in a laboratory environment for 18 months, has a significant negative influence on the crack growth resistance compared with newly made joints [18]. A reasonable explanation for this behaviour is that the oxide layer absorbs water through the edges of the joints during storage, and that the absorbed water has a detrimental effect in the highly stressed wedge test.

The formation of blisters in the bondlines of the anodised substrates bonded at high relative humidity is connected to the release of water from the oxide film and the adhesive during the heat curing cycle. Table 3 shows that increasing relative humidity results in increased blister formation. In Fig. 3, a pattern of blistering can be seen on the AC-SAA substrates after conditioning and bonding at 85% r.h. At curing, the water content in the adhesive may locally reach a level beyond the point of saturation. During a short period of time, the hydrostatic pressure from water vapour will be able to crack and move gelled bulk adhesive forming blisters as seen in Fig. 3. Due to less hydrostatic pressure there are larger blisters closer to the edges of the 'curing sandwich assembly'. The water release occurring during the setting of the adhesive will be most damaging.

Table 3
The correlation between bondline blister formation and initial crack length

Specimen	Area of blisters in bondline (%)	Initial crack length (mm)
AC-SAA, 11% r.h.	-	71.2
AC-SAA, 33% r.h.	-	64.8
AC-SAA, 52% r.h.	1-2	68.3
AC-SAA, 85% r.h.	5-13	71.0
DC-SAA, 45% r.h.	-	69.5
DC-SAA, 85% r.h.	11-22	83.0

Fondeur and Koenig [18] showed with nuclear magnetic resonance imaging that the curing of epoxy adhesive is somewhat delayed close to the anodised surface compared to the bulk of the adhesive. This behaviour has been confirmed on DC-SAA samples. Lap shear specimens have been removed at different times from an oven, followed by immediate cooling in liquid nitrogen and breaking the specimens apart. The viscous layer exists for about 2 min [9]. The lack of thixotropic agent in the interphase region seen with TEM, propose a more distinct difference in rheological behaviour.

The blister formation was more pronounced in the DC-SAA joints than in the AC-SAA joints. This can be related to the different thickness of the oxide films on the respective surfaces. DC-SAA anodising produces an oxide film with an approximate thickness of 8 μm, while the thickness of the AC-SAA oxide is approximately 0.2 μm. Thus, the DC-SAA oxide can absorb more water, which can be released from the oxide during the curing process.

With respect to Table 3, it seems that blister formation in the bondline has effect on the bond strength. The initial crack length can be regarded as a measure of bond strength. Table 3 shows that increasing area of blister formation, that is, the area which not has been bonded can be correlated with the initial crack length of the joints. The exception is the AC-SAA substrates bonded at 11% r.h. After curing in dry environment, the T_g of the adhesive will be higher, and the adhesive will be more brittle. This can contribute to longer crack growth during insertion of the wedges. There may also be subtle changes

in the adhesive curing in dry environment. At curing, the adhesive will shrink, and if contraction is constrained, residual stresses are likely to be present, reducing the capacity of mechanical load. The observed formation of voids different from the blistering discussed before could suggest cavities due to shrinkage early in the curing cycle, i.e., at the setting of the adhesive.

As can be seen in Fig. 3 of the AC-SAA substrates bonded at 85% r.h., the blister formation was more pronounced at the edges of the bonded plate (around 13% blister area) as compared with the middle of the plate (around 5% blister area). The initial crack lengths of the specimens cut from the respective areas showed that the initial crack length of the 13% area was up to 73.0 mm, while that of the 5% area was down to 67.5 mm. The latter specimen also gave less crack growth. Similar trends were observed for the DC-SAA substrates bonded at 85% r.h., but the crack growth was the same for all specimens. Hence, blister formation in the bondline seems to have a weakening effect on the bond strength. A high degree of blister formation would reduce the contact area between the adhesive and the surface, as well as reduce the strength of the adhesive bondline.

It can be argued that the observed differences in crack growth resistance are the result of blister formation. More blister formation results in a smaller bonded area, thus, the contact area between the oxide and the adhesive is smaller. In addition, blisters may allow humidity faster access into the joint, also in front of the crack tip. The altered layer due to the reduced amount of thixotropic agent could also be a weak boundary layer. A material full of blisters will likely not fail in this layer, whereas the crack likely will start in the adhesive bulk after each passed blister. In the case of interfacial failure for the AC-SAA substrates bonded at 11% r.h. a homogenous joint may fail at the weakest path, which probably is close to the interface despite the lack of the altered layer. This could be attributed to the effects described above or less good adhesion.

In discussions of wedge test results it is normally referred to the 'durability' of the bonded joints or the bonded surfaces. However, with blister formation playing an important role with respect to crack growth in this study the expression would be

misleading. The expression 'crack growth resistance', on the other hand, gives information of the behaviour of the bonded joints during environmental exposure without necessarily taking into account the durability of the surface.

The water content in the oxide during adhesive bonding has effect on the structure of the adhesive close to the oxide surface, as shown by TEM in Figs. 5 and 6. The dehydration of the oxide during heating to 180°C at curing seems to have effect on the hydrophobic thixotropic agent which is evicted from the oxide surface due to desorbing water. This was observed at 85% r.h., but not at 11% r.h. It was expected that a larger amount of water in the thicker DC-SAA oxide would have a more pronounced effect on the structure of the adhesive close to the oxide surface compared with the AC-SAA oxide. However, there did not seem to be a significant difference in the thickness of the structure free zones of these surfaces, both being around 200 nm wide. It is possible that the diffusion distance of the thixotropic agent is limited by the curing of the adhesive. When the adhesive cures, the mobility of particles in the adhesive is reduced. On both surfaces, the particles may be driven a certain distance into the bulk adhesive before the curing process stops this migration. Thus, any subsequent desorption of water from the oxide will not have effect on the structure of the adhesive close to the oxide.

There were defects in the DC-SAA oxide, into which the low viscous adhesive could penetrate during curing. An inclusion of adhesive in the oxide is shown in Fig. 5A. An interesting observation is that no thixotropic agent seems to be present in the inclusion. Hence, no thixotropic agent has approached the oxide surface when the adhesive became less viscous during the curing stage. The thixotropic agent has probably been 'pushed away' by water desorbing from the oxide, or not taken into the surface area during the initial heating stage.

No indications of adhesive penetration into the oxide pores could be seen in any of the specimens investigated. However, for these thin oxides it is probably impossible to detect this without using more sophisticated TEM-techniques. Hence, it can not be said whether oxide penetration has occurred or not.

11.5 Conclusion

Pre-bond humidity was shown to have effect on the crack growth resistance of joints made of sulphuric acid anodised AA6060-T6 substrates bonded with a one-component epoxy adhesive cured at 180°C. The difference was significant for DC-SAA substrates bonded in dry and wet environments. A wet environment of 85% r.h. gave a large decrease in crack growth resistance. The differences were smaller between AC-SAA substrates. The crack growth resistance of these substrates almost approached the crack growth resistance of the well-established FPL + DC-PAA pretreatment. However, adhesive bonding in very wet (85% r.h.) and very dry (11% r.h.) environments resulted in reduced crack growth resistance. In joints bonded at 85% r.h., significant blister formation in the adhesive bondline was observed. The blister formation is connected to the release of water from the conditioned adhesive and oxide films during curing of the adhesive.

TEM cross-sections of specimens bonded in wet and dry environments showed differences in the oxide-adhesive interphase. Close to the oxide bonded at 85% r.h., a relatively structure free zone with very little thixotropic agent was observed. The range of this zone was about 200 nm. No such zone was observed in specimens bonded at 11% r.h. The thixotropic agent is hydrophobic of nature. It may then be evicted from the oxide surface when water is desorbed from the oxide during curing of the adhesive.

Acknowledgements

Thanks are due to Hydro Aluminium Structures and The Research Council of Norway for financial support.

References

[1] M. Brémont and W. Brockmann, *J. Adhesion* **58**, 69-99 (1996)

[2] J.D. Venables, D.K. McNamara, J.M. Chen, T.S. Sun and R.L. Hopping, *Appl. Surface Sci.* **3**, 88-98 (1979)

[3] G.W. Critchlow and D.M. Brewis, *Int. J. Adhesion Adhesives* **16**, 255-275 (1996)

[4] G.W. Critchlow, *Trans. IMF* **76**, B6-B10 (1998)

[5] J.D. Venables, *J. Mater. Sci.* **19**, 2431-2453 (1984)

[6] L. Kozma and I. Olefjord, *Mater. Sci. Tech.* **3**, 860-874 (1987)

[7] N.L. Rogers, in: Adhesive Bonding of Aluminum Alloys, E.W. Thrall and R.W. Shannon (Eds.), Marcel Dekker, New York, 1985. p. 41-50.

[8] J. Ball, P.K.F. Limbach and J.D.B. Sharman, in: Proc. 1st ASST. Antwerp, 1997.

[9] T. Luksepp and K. Kristiansen. In preparation.

[10] B.B. Johnsen, F. Lapique and A. Bjørgum, *Int. J. Adhesion Adhesives* **24**, 153-161 (2004)

[11] J.A. Marceau, in: Adhesive Bonding of Aluminum Alloys, E.W. Thrall and R.W. Shannon (Eds.), Marcel Dekker, New York, 1985. p. 51-74.

[12] O. Lunder, B. Olsen and K. Nisancioglu, *Int. J. Adhesion Adhesives* **22**, 143-150 (2002)

[13] CRC Handbook of Chemistry and Physics, 78th Ed. (Eds. DR Lide and HPR Fredrikse), CRC Press, New York, 1997.

[14] B.B. Johnsen, K. Olafsen, A. Stori and K. Vinje, *J. Adhesion Sci. Technol.* **16**, 1931-1948 (2002)

[15] R.P. Digby and D.E. Packham, *Int. J. Adhesion Adhesives* **15**, 61-71 (1995)

[16] R.S. Alwitt, in: Oxides and Oxide Films, Vol. 4, J.W. Diggle and A.K. Vijh (Eds.), Marcel Dekker, New York, 1976. p. 169-254.

[17] The Surface Treatment and Finishing of Aluminium and its Alloys, 6th Ed., P.G. Sheasby and R. Pinner (Eds.), Finishing Publications, Ltd., Stevenage, UK, 2001.

[18] Unpublished results.

[19] F. Fondeur and J.L. Koenig, *J. Adhesion* **43**, 289-308 (1993)

Chapter 12
Conclusions

Concluding remarks for silanisation of pretreated aluminium alloy AA6060-T6 with a 1 wt% aqueous solutions of GPS. Adhesive bonding was performed with XD4600 one-component epoxy adhesive:

- The durability of grit-blasted, alkaline etched and abraded surfaces are significantly improved after treatment with GPS. The grit-blasting + GPS pretreatment process results in very good durability, significantly better than the chromic-sulphuric acid FPL-etch. The ranking between the pretreatments is the same before and after treatment with GPS.

- Surface topography and surface contamination are important with respect to durability. Increased surface roughness improves the durability, while increased surface contamination reduces the durability.

- GPS films treated with amines strongly indicate a chemical reaction, as observed in the intensity reduction of the epoxy band at 910 cm^{-1} using FT-IR spectroscopy. The amines also catalyse the condensation of SiOH groups, and a higher degree of SiOSi crosslink density is observed in the siloxane films. Treatment with DICY also shows a band at 2190 cm^{-1}, which is assigned to the formation of a covalent bond between the curing agent and the epoxy ring of GPS.

- Chemical reaction between the silane and the adhesive is not necessary for improved durability, as shown by both reactive and unreactive silanes. The hydrophobicity of the bonded surface is also an important factor. It is believed that a hydrophobic surface to some extent can prevent water from entering the aluminium-adhesive interface.

- Desmutting in concentrated nitric acid significantly decreases the durability of alkaline etched surfaces. Desmutting removes a 'smut' layer rich in magnesium oxide, which is expected to improve the stability of the surface.

- GPS films on alkaline etched AA6060-T6 behave different in acidic, neutral and alkaline environments. In acidic (pH 4) and neutral (pH 7) environments the silane is desorbed from the surface, but the silane film is stable in alkaline environment (pH 8).

- The durability of similar surfaces is significantly reduced in highly acidic environment (pH 2). In the pH range from 4 to 11, somewhat higher durability is observed in alkaline environments. The observed trends are connected to rehydrolysis of the siloxane network in acidic environments and better stability of the aluminium surface in alkaline environments.

Concluding remarks for anodising of pretreated aluminium alloy AA6060-T6. Adhesive bonding with XD4600 one-component epoxy adhesive:

- Anodising in hot phosphoric acid (AC-PAA) and sulphuric acid (AC-SAA) solutions gives very good durability, almost as good as the well-established FPL + DC-PAA pretreatment. DC anodising in sulphuric acid (DC-SAA) performs inferior.

- FT-IR spectroscopy of the anodic films showed that the DC-SAA and AC-SAA oxides contain significant amounts of aluminium sulphate. Sulphates can absorb relatively large amounts of water, which can have a significant effect on the long-term properties of bonded joints.

- The intensity of the O-H stretching band in the oxides decrease during heat-treatment at 180°C. The observation suggests that a transformation from the hydroxide, $Al(OH)_x$, to the oxide, Al_2O_3, state takes place. Water is released and

driven out of the oxides during curing of the adhesive. The amount of water released depends on the thickness of the oxide and the environment in which the oxide was bonded.

- Sealing of DC-SAA and AC-SAA substrates in boiling water significantly reduces the durability.

- Pre-bond humidity has effect on the durability of DC-SAA and AC-SAA substrates. The difference is significant for DC-SAA substrates bonded in dry and wet environments. Bonding in 85% r.h. decreases durability compared with 45% r.h. Significant blister formation is observed in the adhesive bondline at 85% r.h.

- The effects of pre-bond humidity are smaller for AC-SAA substrates. However, adhesive bonding in very wet (85% r.h.) and very dry (11% r.h.) environments results in reduced durability compared with 33 and 52% r.h.

- In AC-SAA and DC-SAA specimens bonded at 85% r.h., a zone with very little thixotropic agent is formed close to the oxide surface. The zone extends about 200 nm into the adhesive. No such zone is observed in specimens bonded at 11% r.h. The thixotropic agent is hydrophobic of nature, and may be 'driven away' from the oxide surface when water is desorbed from the oxide during curing of the adhesive.

Suggestions for further work:

The general theory is that silanes improve the adhesion between aluminium surfaces and epoxy adhesives through the formation of a crosslinked 'bridge' between the surface and adhesive. However, it seems that covalent bonding is not necessary for good adhesion to silane treated aluminium surfaces - surface hydrophobicity also plays an important role. A more hydrophobic surface could prevent water from entering the aluminium-adhesive interface, thereby reducing the degrading effect of water. The

effect of surface hydrophobicity, and other mechanisms, should be more thoroughly investigated. This can be done using silanes that are unreactive towards the adhesive.

The composition of the adhesive close to the aluminium oxide surface is different from the composition of the bulk adhesive. A compositional gradient has been reported in the literature, and in Chapter 11 it is shown that less thixotropic agent is present close to the oxide surface in DC-SAA and AC-SAA specimens bonded with XD4600 at high relative humidity. The difference in composition and/or lack of thixotropic agent will result in differences in mechanical properties. This effect should be investigated in more detail. Perhaps these effects will result in a weak boundary layer close to the oxide surface.

Storage at ambient has a negative effect on the properties of bonded DC-SAA joints. The explanation of this observation is probably absorption of water in the DC-SAA oxide. However, the degradation mechanisms are not fully understood and should be more thoroughly investigated. A comparison with AC-SAA, AC-PAA and DC-PAA oxides should be made to ascertain the role of the aluminium sulphate.

Appendix

Total crack length of RDCB wedge test joints tested at 60°C/100% RH. Comparison of the grit-blasting + GPS pretreatment discussed in Chapter 6 and the FPL+PAA pretreatment. Testing of the FPL+PAA pretreatment was performed after publication of the paper.

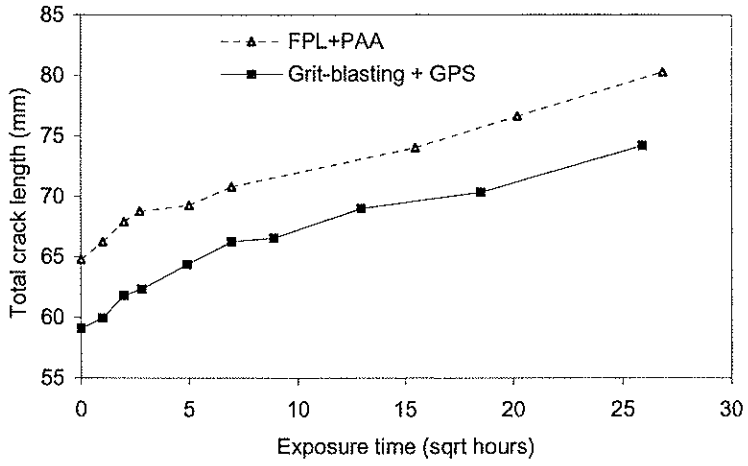

As can be seen from the figure, the grit-blasting + GPS pretreatment results in better durability than the FPL+PAA pretreatment.